NASA/CR—2004-213199/VOL5 (Corrected Copy)

Numerical, Analytical, Experimental Study of Fluid Dynamic Forces in Seals

Volume 5—Description of Seal Dynamics Code DYSEAL and Labyrinth Seals Code KTK

Wilbur Shapiro
Mechanical Technology, Inc., Latham, New York

Raymond Chupp, Glenn Holle, and Thomas Scott
Allison Engine Company, Indianapolis, Indiana

October 2004

The NASA STI Program Office . . . in Profile

Since its founding, NASA has been dedicated to the advancement of aeronautics and space science. The NASA Scientific and Technical Information (STI) Program Office plays a key part in helping NASA maintain this important role.

The NASA STI Program Office is operated by Langley Research Center, the Lead Center for NASA's scientific and technical information. The NASA STI Program Office provides access to the NASA STI Database, the largest collection of aeronautical and space science STI in the world. The Program Office is also NASA's institutional mechanism for disseminating the results of its research and development activities. These results are published by NASA in the NASA STI Report Series, which includes the following report types:

- TECHNICAL PUBLICATION. Reports of completed research or a major significant phase of research that present the results of NASA programs and include extensive data or theoretical analysis. Includes compilations of significant scientific and technical data and information deemed to be of continuing reference value. NASA's counterpart of peer-reviewed formal professional papers but has less stringent limitations on manuscript length and extent of graphic presentations.

- TECHNICAL MEMORANDUM. Scientific and technical findings that are preliminary or of specialized interest, e.g., quick release reports, working papers, and bibliographies that contain minimal annotation. Does not contain extensive analysis.

- CONTRACTOR REPORT. Scientific and technical findings by NASA-sponsored contractors and grantees.

- CONFERENCE PUBLICATION. Collected papers from scientific and technical conferences, symposia, seminars, or other meetings sponsored or cosponsored by NASA.

- SPECIAL PUBLICATION. Scientific, technical, or historical information from NASA programs, projects, and missions, often concerned with subjects having substantial public interest.

- TECHNICAL TRANSLATION. English-language translations of foreign scientific and technical material pertinent to NASA's mission.

Specialized services that complement the STI Program Office's diverse offerings include creating custom thesauri, building customized databases, organizing and publishing research results . . . even providing videos.

For more information about the NASA STI Program Office, see the following:

- Access the NASA STI Program Home Page at ***http://www.sti.nasa.gov***

- E-mail your question via the Internet to help@sti.nasa.gov

- Fax your question to the NASA Access Help Desk at 301–621–0134

- Telephone the NASA Access Help Desk at 301–621–0390

- Write to:
  NASA Access Help Desk
  NASA Center for AeroSpace Information
  7121 Standard Drive
  Hanover, MD 21076

NASA/CR—2004-213199/VOL5 (Corrected Copy)

Numerical, Analytical, Experimental Study of Fluid Dynamic Forces in Seals

Volume 5—Description of Seal Dynamics Code DYSEAL and Labyrinth Seals Code KTK

Wilbur Shapiro
Mechanical Technology, Inc., Latham, New York

Raymond Chupp, Glenn Holle, and Thomas Scott
Allison Engine Company, Indianapolis, Indiana

Prepared under Contract NAS3–25644

National Aeronautics and
Space Administration

Glenn Research Center

October 2004

Document Change History

This corrected copy replaces copies printed October 2004. It contains the following changes on the cover, title page, and Report Documentation Page:

The spelling of the second author's last name has been changed from Chubb to Chupp.
The spelling of the third author's first name has been changed from Glen to Glenn.
The spelling of Allision Engine Company has been changed to Allison Engine Company.

Available from

NASA Center for Aerospace Information
7121 Standard Drive
Hanover, MD 21076

National Technical Information Service
5285 Port Royal Road
Springfield, VA 22100

Available electronically at http://gltrs.grc.nasa.gov

FOREWORD

The Computational Fluid Dynamics (CFD) computer codes and Knowledge-Based System (KBS) were generated under NASA contract NAS3-25644 originating from the Office of Advanced Concepts and Technology and administered through NASA-Lewis Research Center. The support of the Program Manager, Anita Liang, and the advice and direction of the Technical Monitor, Robert Hendricks, are gratefully appreciated. Major contributors to code development were:

- Dr. Bharat Aggarwal: KBS and OS/2 PC conversion of labyrinth seal code KTK
- Dr. Antonio Artiles: cylindrical and face seal codes ICYL and IFACE
- Dr. Mahesh Athavale and Dr. Andrzej Przekwas: CFD code SCISEAL
- Mr. Wilbur Shapiro: gas cylindrical and face seal codes GCYLT, GFACE, and seal dynamics code DYSEAL
- Dr. Jed Walowit: spiral groove gas and liquid cylindrical and face seal codes SPIRALG and SPIRALI.

The labyrinth seal code, KTK, was developed by Allison Gas Turbine Division of General Motors Corporation for the Aero Propulsion Laboratory, Air Force Wright Aeronautical Laboratories, Wright-Patterson Air Force Base, Ohio. It is included as part of the CFD industrial codes package by the permission of the Air Force.

TABLE OF CONTENTS

TABLE OF CONTENTS (Continued)

LIST OF FIGURES

LIST OF FIGURES (Continued)

LIST OF TABLES

NOMENCLATURE

A	=	cross-sectional area ($in.^2$)
A_t	=	flow area between seal knives and land, seal throat ($in.^2$)
CL	=	clearance between seal knives and land (in.)
DTC	=	distance to contact: axial clearance between knife and land, undefined for constant height straight-through seals (in.)
f ( )	=	function of the variables ( )
f	=	Fanning friction factor
g_c	=	standard gravitational acceleration mass conversion factor ($lb_m ft/lb_b$)
H	=	seal height (in.)
H	=	hydraulic diameter, $H = \frac{4A}{P}$ (in.)
K_c	=	contraction coefficient
K_e	=	expansion coefficient
K_f	=	wall friction loss coefficient
KH	=	knife height (in.)
KN	=	number of knives
KP	=	knife pitch (in.)
KR	=	knife tip radius (in.)
KT	=	knife tip thickness (in.)
K_{vf}	=	Venturi-friction coefficient
K_β	=	knife taper angle (degree)
K_θ	=	knife slant angle (degree)
L	=	length of seal (in.)
LTSD	=	leakage flow direction from large-to-small seal diameter
M	=	mach number
P	=	wetted perimeter of duct (in.)
P_s	=	local static pressure (psia)
P_D	=	seal plenum downstream pressure (psia)
P_R	=	seal pressure ratio, P_U/P_D
P_t	=	local total pressure (psia)

NOMENCLATURE (continued)

P_U, P_l = seal plenum upstream pressure (psia)

r = P_D/P_U

R = gas constant $\left(\frac{lb_f\ ft}{lb_m\ °R}\right)$

Re = streamwise Reynolds number, $\frac{\rho VH}{\mu}$

SH = step height (in.)

STLD = leakage flow direction form the small-to-large seal diameter

T = local total temperature (°F)

T_U = seal upstream plenum temperature (°R)

V = leakage gas velocity (ft/sec)

w = seal airflow rate (lb_m/sec)

XMUL = area correction factor for clearance above a knife downstream of a step

$\propto$ = jet expansion angle (degree)

Υ = ratio of specific heats

δ = jet expansion height (in.)

ε = land surface roughness (μin.)

μ = fluid dynamic viscosity $\left(\frac{lb_m}{ft\ sec}\right)$

π = conventional transcendental number, ratio of circular circumference to diameter

ρ = density $\left(\frac{lb_m}{ft^3}\right)$

ϕ = $\frac{w\sqrt{T_U}}{P_U A_t}$ airflow parameter $\left(\frac{lb_m\ °R^{1/2}}{lb_f\ sec}\right)$

1.0 INTRODUCTION

NASA's advanced engine programs are aimed at progressively higher efficiencies, greater reliability, and longer life. Recent studies have indicated that significant engine performance advantages can be achieved by employing advanced seals [1]*, and dramatic life extensions can also be achieved. Advanced seals are not only required to control leakage, but are necessary to control lubricant and coolant flow, prevent entrance of contamination, inhibit the mixture of incompatible fluids, and assist in the control of rotor response.

Recognizing the importance and need of advanced seals, NASA, in 1990, embarked on a five-year program (Contract NAS3-25644) to provide the U.S. aerospace industry with computer codes that would facilitate configuration selection and the design and application of advanced seals.

The program included four principal activities:

1. Development of a scientific code called SCISEAL, which is a Computational Fluid Dynamics (CFD) code capable of producing full three-dimensional flow field information for a variety of cylindrical configurations. The code is used to enhance understanding of flow phenomena and mechanisms, to predict performance of complex situations, and to furnish accuracy standards for the industrial codes. The SCISEAL code also has the unique capability to produce stiffness and damping coefficients that are necessary for rotordynamic computations.
2. Generation of industrial codes for expeditious analysis, design, and optimization of turbomachinery seals. The industrial codes consist of a series of separate stand-alone codes that were integrated by a Knowledge-Based System (KBS).
3. Production of a KBS that couples the industrial codes with a user friendly Graphical User Interface (GUI) that can in the future be integrated with an expert system to assist in seal selection and data interpretation and provide design guidance.
4. Technology transfer via four multiday workshops at NASA facilities where the results of the program were presented and information exchanged among suppliers and users of advanced seals. A Peer Panel also met at the workshops to provide guidance and suggestions to the program.

This final report has been divided into separate volumes, as follows:

Volume 1: Executive Summary and Description of Knowledge-Based System
Volume 2: Description of Gas Seal Codes GCYLT and GFACE
Volume 3: Description of Spiral-Groove Codes SPIRALG and SPIRALI
Volume 4: Description of Incompressible Seal Codes ICYL and IFACE
Volume 5: Description of Seal Dynamics Code DYSEAL and Labyrinth Seal Code KTK
Volume 6: Description of Scientific CFD Code SCISEAL.

* Numbers in brackets designate references presented in Section 7.0.

This volume describes two codes: DYSEAL and KTK. The code DYSEAL determines the response of face and cylindrical seals to shaft excursions. The code KTK is a labyrinth code that was obtained from the Air Force and produces leakage information for straight and stepped labyrinth seals and includes routines for geometric optimization. References 2 and 3 provide the details of the code implementation. Reference 3 is an edited version of Volume IV of report AFWAL-TR-85-2103 prepared by Allison Engine Company for the U.S. Air Force.

1.1 Code DYSEAL (Dynamic Response of Seals)

Dynamic response of seal rings to rotor motions is an important consideration in seal design. For contact seals, dynamic motions can impose significant increases in interfacial forces, resulting in high wear and reduction in useful life. For fluid film seals, the rotor excursions are generally greater than the film thickness, and if the seal ring does not track, contact and failure may occur. The computer code DYSEAL can determine the tracking capability of fluid film seals and can be used for parametric geometric variations to find acceptable configurations.

The type of seals that can be analyzed are depicted in Figures 1 through 3. Figure 1 shows a stationary seal ring and a rotating mating ring. The secondary seal is a piston ring with radial pressure loading on the OD. The shaft or rotor can be given five degrees of freedom, consisting of three translations (x, y, and z) and two rotations about the x and y axes, respectively. The seal ring response is also in five degrees of freedom. The interface is represented by cross coupled stiffness and damping coefficients that are obtained from other codes. The effects of Coulomb friction of the secondary seals on seal ring response are included. Figure 2 shows an inverted configuration with the initial radial pressure on the piston ring on its ID. This inside configuration results in less pressure loading on the ring because the ID area is less than the OD area. The reduced loading also reduces the secondary seal ring friction that may retard tracking. In addition to piston ring secondary seals, an O-ring secondary can also be applied.

Figure 3 shows a floating ring seal that can also be analyzed by the code. This configuration permits two degrees of freedom for both the shaft and ring, and is intended to determine seal ring response to an orbiting shaft. The secondary seal occurs between the ring and the wall and x-y Coulomb friction at that location is accounted for.

The method of computation is a forward integration in time that provides absolute motions in all degrees of freedom. The reason that this approach was chosen was because of complications caused by Coulomb friction. At every time step, friction has to be evaluated to determine if motions continue or are halted.

1.2 Code KTK

The computer code KTK calculates the leakage and pressure distribution through labyrinth seals based on a detailed knife-to-knife (KTK) analysis. Input data are required to describe in detail the seal geometry and the environmental conditions affecting the leakage. Output is provided in the form of leakage flow and flow resistance characteristics, i.e., flow factor versus pressure ratio. In addition, an

optimization feature is included which permits the user to identify global geometric constraints and allows the code to identify an optimum seal configuration based on minimum leakage.

This volume describes the fundamental theory of the design model, features of the design model computer program KTK, and resulting output data. Appendix A includes sample output data.

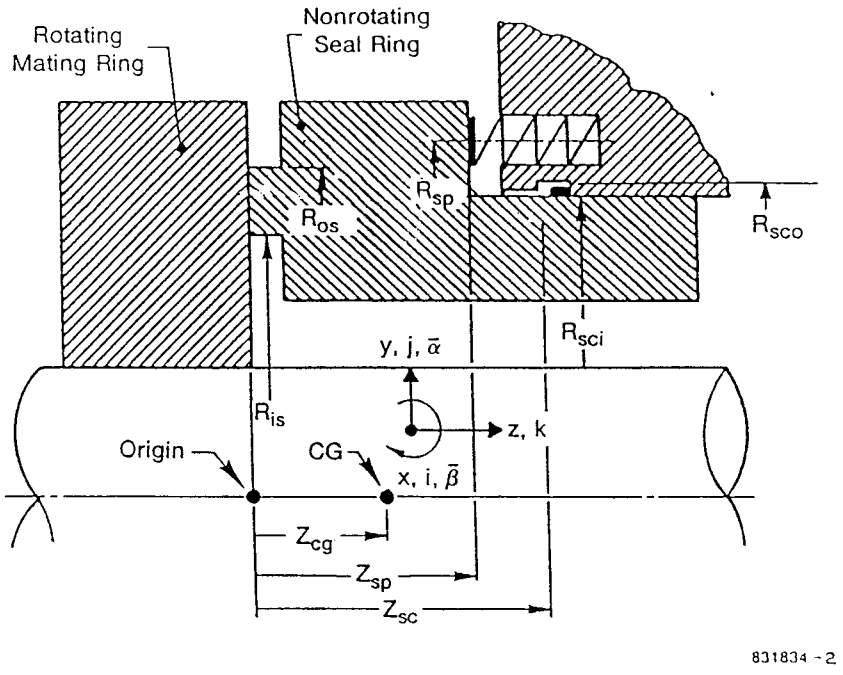

Figure 1. Fluid Film Face Seal Parameters

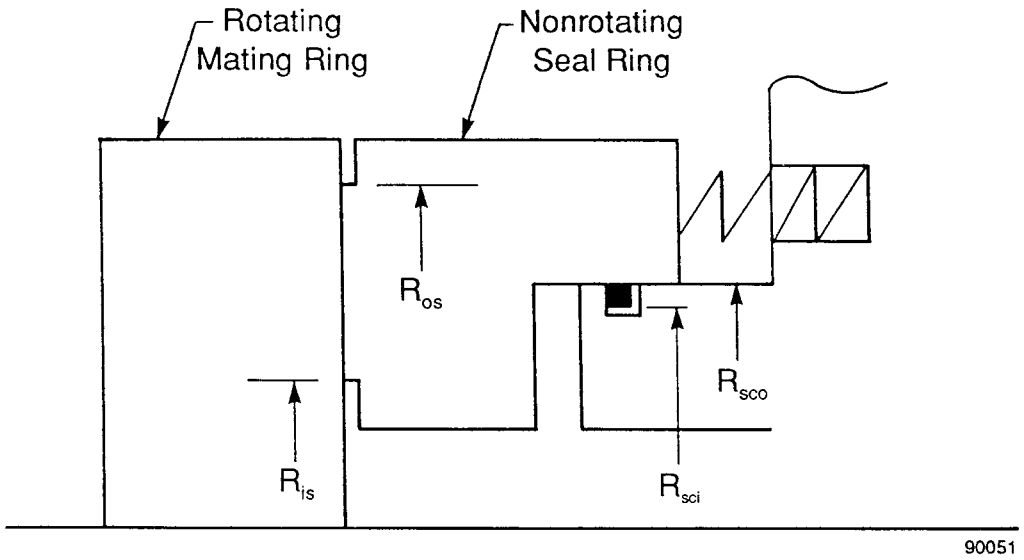

Figure 2. Face Seal Configuration (Piston Ring on ID of Seal Ring)

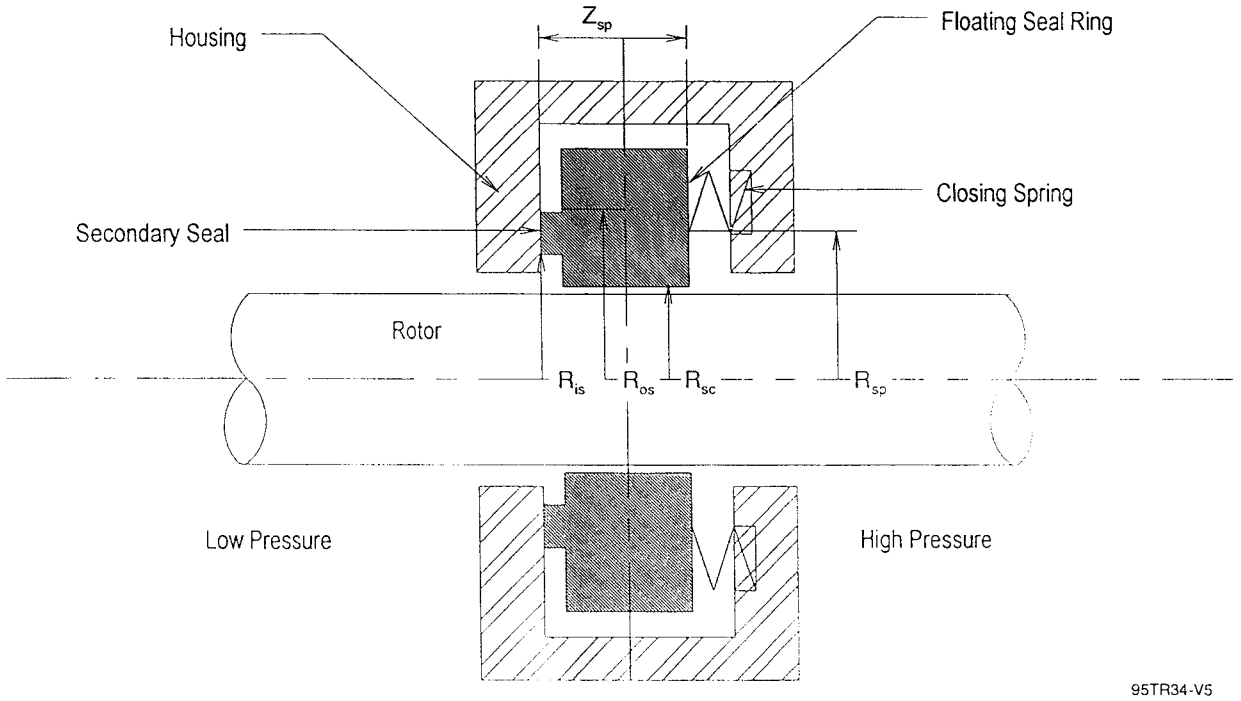

Figure 3. Floating Ring Seal

2.0 THEORETICAL DEVELOPMENT OF CODE DYSEAL

The code determines the response of the seal ring in five degrees of freedom to shaft vibrations in as many as five degrees of freedom. These degrees of freedom are:

1. x_s = seal ring displacement in x direction.
2. y_s = seal ring displacement in y direction.
3. z_s = seal ring displacement in z direction.
4. β_s = seal ring rotation about x-x axis.
5. α_s = seal ring rotation about y-y axis.

Note that throughout this report, seal motions are subscripted with an s and shaft motions are nonsubscripted. Unit vectors are $\hat{i}$, $\hat{j}$, and $\hat{k}$ in the x, y, and z directions, respectively. Coulomb friction is accounted for in both the secondary seal and the interface.

2.1 Equations of Motion

Considering small motions, the following equations apply:

$$\sum \vec{F}_x = m\ddot{x}_s \tag{2.1}$$

$$\sum \vec{F}_y = m\ddot{y}_s \tag{2.2}$$

$$\sum \vec{F}_z = m\ddot{z}_s \tag{2.3}$$

$$\sum \vec{M}_x = I_t\ddot{\beta}_s \tag{2.4}$$

$$\sum \vec{M}_y = I_t\ddot{\alpha}_s \tag{2.5}$$

where m = mass of seal ring and I_t = transverse moment of inertia of seal ring.

2.2 Development of Newmarks' Method

The solution to the equations of motion are obtained by the use of Newmarks' method or the average acceleration method [4]. The velocity $\dot{U}_{i+1}$ at a time station, i+1 is approximated as

$$\dot{U}_{i+1} = \dot{U}_i + \left(\frac{\ddot{U}_i + \ddot{U}_{i+1}}{2}\right)\Delta t \tag{2.6}$$

Similarly,

$$U_{i+1} = U_i + \left(\frac{\dot{U}_i + \dot{U}_{i+1}}{2}\right)\Delta t \tag{2.7}$$

If the value of $\dot{U}_{i+1}$ from Equation (2.7) is substituted into Equation (2.6), the following equation results:

$$U_{i+1} = U_i + \dot{U}_i \Delta t + \left(\frac{\ddot{U}_i + \ddot{U}_{i+1}}{4} \right) \Delta t^2 \tag{2.8}$$

but

$$\ddot{U}_{i+1} = M^{-1} \left\{ F_{i+1} - K U_{i+1} - D \dot{U}_{i+1} \right\} \tag{2.9}$$

where M = mass matrix; F = unbalanced force vector; K = stiffness matrix; and D = damping matrix.

Substituting Equation (2.9) into (2.8) produces:

$$U_{i+1} \left(\frac{4}{\Delta t^2} + K M^{-1} \right) = \frac{4}{\Delta t^2} U_i + \frac{4}{\Delta t} \dot{U}_i + \ddot{U}_i + M^{-1} F_{i+1} - D M^{-1} \dot{U}_{i+1} \tag{2.10}$$

Now from Equation (2.7),

$$\dot{U}_{i+1} = \frac{2U_{i+1}}{\Delta t} - \frac{2U_i}{\Delta t} - \dot{U}_i \tag{2.11}$$

Substituting Equation (2.11) into (2.10) and multiplying by M produces:

$$\left(\frac{4M}{\Delta t^2} + K + \frac{2D}{\Delta t} \right) U_{i+1} = F_{i+1} + \left(\frac{4M}{\Delta t^2} + \frac{2D}{\Delta t} \right) U_i + \left(\frac{4M}{\Delta t} + D \right) \dot{U}_i + M \ddot{U}_i \tag{2.12}$$

Thus, an expression has been derived that relates the displacement at the new time step to displacements, velocities, and accelerations at the prior time step.

Once U_{i+1} is obtained, $\dot{U}_{i+1}$ and $\ddot{U}_{i+1}$ are obtained from Equations (2.7) and (2.6), respectively.

$$\dot{U}_{i+1} = \frac{2}{\Delta t} \left[U_{i+1} - U_i \right] - \dot{U}_i \tag{2.13}$$

From Equation (2.6),

$$\ddot{U}_{i+1} = \frac{2}{\Delta t} \left[\dot{U}_{i+1} - \dot{U}_i \right] - \ddot{U}_i \tag{2.14}$$

Substituting Equation (2.13) into (2.14) gives:

$$\ddot{U}_{i+1} = \frac{4}{\Delta t^2}(U_{i+1} - U_i) - \frac{4}{\Delta t}\dot{U}_i - \ddot{U}_i \tag{2.15}$$

Thus, displacements, velocities, and accelerations are determined from the results of previous time steps. Initially, these quantities equal zero ultimately.

2.3 Solution Process

Figure 4 is a flow diagram of the program logic. The program computes the mass and inertia properties of the seal ring and the location of the center of gravity. After computing all constants and matrix elements that are independent of time, the program enters the time step loop. Shaft motions are incremented first. Using updated shaft motions, the secondary seal friction is determined. This includes friction magnitudes and direction in the x_s, y_s, z_s, β_s, and α_s directions as well as the friction components that go into the stiffness and damping matrices and force vector.

The force vector, F, is next updated because, as indicated in using Newmarks method, the most recent force vector, F_{i+1}, is required. Then, Newmarks method is applied and the new seal displacements, velocities, and accelerations are determined. Subsequent to the calculations, adjustments are made to these variables because of friction resistance. The following paragraphs describe the development of the theory for the individual steps in the solution process, as outlined in Figure 4.

2.4 Initialization

Displacements, velocities, and acceleration are initialized prior to entering the time step loop. Initial displacements correspond to the shaft displacements at the first time step, so that the seal ring and shaft are in correspondence. Initial values of velocities and acceleration are nulled.

2.5 Mass Matrix

The code develops the mass and inertia properties from a series of connected ring elements. Up to 20 elements can be inputted with individual OD, ID, length, and density. From this input, the code determines the location of the center of gravity (CG), the mass, and the polar and transverse moments of inertia of the seal ring. Computed values are included in program output.

2.6 Computation of Constants

The closing area is the unbalanced hydraulic closing area that varies for the type of seal being analyzed. For a piston ring seal (Figure 1), the closing area is:

$$A_{CL} = \pi\left(R_{os}^2 - R_{sci}^2\right) \tag{2.16}$$

If an inside ring is employed (see Figure 2), then

$$A_{CL} = \pi\left(R_{os}^2 - R_{sco}^2\right) \tag{2.17}$$

For an O-ring secondary seal, there is no distinction between the inside and outside radii and the closing area is given by:

$$A_{CL} = \pi\left(R_{os}^2 - R_{sc}^2\right) \tag{2.18}$$

The same expression applies for a ring seal except that R_{sc} is taken as the inside radius of the seal.

The interface area is the mating area and is given (for all seals) by:

$$A_{IF} = \pi\left(R_{os}^2 - R_{is}^2\right) \tag{2.19}$$

Another area of interest is the difference between the interface and closing areas. The absolute difference between the interface and closing areas is:

$$A_{CLL} = \left|A_{CL} - A_{IF}\right| \tag{2.20}$$

For a face seal, the hydraulic closing force is:

$$F_{HCL} = P_H A_{CL} + P_L A_{CLL} \tag{2.21}$$

where P_H = high pressure and P_L = low pressure.

For ring seals,

$$F_{HCL} = P_H A_{CL} - P_L A_{CLL} \tag{2.22}$$

The code computes the spring preload by summing the preload from the individual springs. For a piston ring, there will be initial preloads from the installation spring stiffness and from pressure

on the ring circumference and on the ring face. The secondary seal preload per unit length for a ring pressurized on its OD is:

$$P_{re\ell} = P_H \frac{R_o w}{R_i} + (P_{e\ell})_i \tag{2.23}$$

where $P_{re\ell}$ = preload per unit of circumference; R_o = outside radius of the piston ring; R_i = inside radius of the piston ring; w = the width of the piston ring; and $(P_{re\ell})_i$ = installed preload per unit of circumference.

The total preload is:

$$P_r = 2\pi R_i P_{re\ell} \tag{2.24}$$

For an inside ring, R_L and R_o are reversed in computing $P_{re\ell}$.

For an O-ring seal, the preload per unit of circumference is an input quantity and the preload is given by Equation (2.24).

The face seal axial forces are a function of preload and the coefficient of friction, such that

$$F_{fz} = P_r \times \nu \tag{2.25}$$

where F_{fz} = secondary seal friction in the axial direction and ν = coefficient of friction.

The initial interface preload includes components from closing pressure and spring load and is equal to:

$$F_{IF} = F_{HCL} + F_{SP} \tag{2.26}$$

where F_{IF} = initial interface load and F_{SP} = initial spring closing load.

The code computes the initial axial position of the seal ring accounting for secondary seal ring friction. For face seals, the equilibrium fluid film interface force is an input quantity. The procedure is to balance the closing loads by the fluid film load using the axial stiffness of the fluid film to determine position iterations. Figure 5 shows the algorithms used.

For a ring seal, the fluid film stiffness is replaced by the structural stiffness of the seal ring. Often, a soft material such as carbon is used for the seal ring and its initial compression and face load are of interest. The ring seal stiffness is approximated by:

$$K_{zz} = A_{IF} E / L$$

where A_{IF} = interface area; E = elastic modulus of the seal ring; and L = seal ring length.

2.7 Stiffness and Damping Outside of the Time Step Loop

There are stiffness and damping quantities that are invariant and can be matrixed outside of the time step loop.

2.7.1 Fluid Film Stiffness and Damping

The fluid film interfaces are represented by cross coupled stiffness and damping coefficients that are obtained from other codes. For face seals, the fluid film has three degrees of freedom (z, β, α) and the stiffness and damping quantities occupy the lower right portion of the 5 × 5 stiffness and damping matrix. The ring seal fluid film has two degrees of freedom (x and y) and the stiffness and damping values occupy the upper left portion of the matrices. Tables 1 and 2 show the locations of the stiffness and damping quantities.

2.7.2 Spring Stiffnesses

The total spring force is (see Figure 6):

$$\overline{F}_{sp} = k_{sp} \sum_{i=1}^{Nsp} \delta_{sp}^{i} \tag{2.27}$$

where $\overline{F}_{sp}$ = total spring force; k_{sp} = spring stiffness; δ_{sp}^{i} = displacement of ith spring; and N_{sp} = number of springs. (Note: the spring preload does not enter into the equations of motion since it is equilibrated by initial conditions.) The displacement of the ith spring is:

$$\delta_{sp}^{i} = \left(\overline{\delta}_{cg} + \overline{\phi}_{s} \times \overline{r}_{sp}^{i}\right) \cdot \hat{k} \tag{2.28}$$

where

$$\overline{\delta}_{cg} = \text{displacement of cg} = \begin{Bmatrix} x_s \\ y_s \\ z_s \end{Bmatrix}$$

$$\overline{\phi}_{s} = \text{rotation of seal ring about axis through cg} = \begin{Bmatrix} \beta \\ \alpha \\ o \end{Bmatrix}$$

$$\overline{r}_{sp}^{i} = \text{vector from cg to ith spring} = \begin{Bmatrix} R_{sp} \cos\theta^{i} \\ R_{sp} \sin\theta^{i} \\ z_{sp} \end{Bmatrix}$$

Table 1. Stiffness Coefficients

F \ Δ	X	Y	Z	β	α
F_x	K_{xx}	K_{yy}			
F_y	K_{yx}	K_{yy}			
F_z			K_{zz}	$K_{z\beta}$	$K_{z\alpha}$
M_x			$K_{\beta z}$	$K_{\beta\beta}$	$K_{\beta\alpha}$
M_y			$K_{\alpha z}$	$K_{\alpha\beta}$	$K_{\alpha\alpha}$

Ring Seals

Face Seals

95TR34-V5

Table 2. Damping Coefficients

F \ Δ	X	Y	Z	β	α
F_x	D_{xx}	D_{yy}			
F_y	D_{yx}	D_{yy}			
F_z			D_{zz}	$D_{z\beta}$	$D_{z\alpha}$
M_x			$D_{\beta z}$	$D_{\beta\beta}$	$D_{\beta\alpha}$
M_y			$D_{\alpha z}$	$D_{\alpha\beta}$	$D_{\alpha\alpha}$

Ring Seals

Face Seals

95TR34-V5

The moments of the spring forces about the center of gravity are:

$$\overline{M}_{sp} = \sum_{i=1}^{N_{sp}} \overline{r}_{sp}^{i} \times \overline{F}_{sp}^{i} = \begin{Bmatrix} M_{xx} \\ M_{yy} \\ o \end{Bmatrix} \tag{2.29}$$

The axial stiffness of the spring is:

$$N_{sp} \cdot k_{sp} \tag{2.30}$$

Rotational stiffness can be obtained explicitly.

$$K_{sp}^{i,j} = \frac{M_{sp}^{i,j}(j+\delta_j) - M_{sp}^{i,j}(j)}{\Delta j} \tag{2.31}$$

where i = moment axis and j = displacement.

For a single spring, the rotational spring constant is:

$$K_{spt} = \frac{k_{sp} R_{sp}^2}{2} \tag{2.32}$$

The program numerically computes the spring stiffnesses and then adds them to the stiffness matrix for Newmarks computations.

Stiffness and damping are also computed for the O-ring secondary seals, and is presented in Section 2.14 along with the discussion of O-ring friction, which is a parameter whose direction varies with time.

2.8 Shaft Increments

Shaft motions are incremented inside the time step loop according to the following equations:

$$x = x_o \cos \omega_x t \tag{2.33}$$
$$y = y_o \sin \omega_y t \tag{2.34}$$
$$z = z_o \sin \omega_z t \tag{2.35}$$
$$\beta = \beta_o \cos \omega_\beta t \tag{2.36}$$
$$\alpha = \alpha_o \sin \omega_\alpha t \tag{2.37}$$

where x = shaft displacement in x direction; y = shaft displacement in y direction; z = shaft displacement in z direction; β = shaft rotation about x axis; and α = shaft rotation about y axis.

To simulate circular orbits, x and y are 90° out of phase. The amplitudes x_o, y_o, etc., are input quantities and can be arbitrary to simulate elliptical shaft orbits. Also, the frequencies of vibration, ω_x, ω_y, etc., are input quantities and can be varied arbitrarily at the discretion of the user. Velocities and accelerations are computed by taking derivatives in the usual manner.

2.9 Updating [K] and [D]

For a ring seal, the fluid film stiffness and damping are constant quantities but their components in x and y vary with the position of the shaft, and thus they must be updated inside of the time step loop. Basically, the input values of K_{xx}, K_{xy}, etc., are values that are parallel and normal to the eccentricity vector. Referring to Figure 7, the position of the eccentricity vector varies as the shaft orbits. As shown in Figure 7, the eccentricity is along the x′ axis. Then, for the primed axes,

$$F' = -K'\delta' - D'\dot{\delta}' \tag{2.38}$$

where

$$F' = \begin{Bmatrix} F'_x \\ F'_y \end{Bmatrix}$$

and

$$K' = \begin{bmatrix} K'_{xx} & K'_{xy} \\ K'_{yx} & K'_{yy} \end{bmatrix}$$

which are input quantities

$$\delta' = \begin{Bmatrix} \delta'_x \\ \delta'_y \end{Bmatrix}$$

$$\dot{\delta}' = \begin{Bmatrix} \dot{\delta}'_x \\ \dot{\delta}'_y \end{Bmatrix}$$

$$D' = \begin{bmatrix} D'_{xx} & D'_{yx} \\ D'_{yx} & D'_{yy} \end{bmatrix}$$

The forces along x′, y′ must be transposed along x and y

$$F = AF' \tag{2.39}$$

where

$$F = \begin{Bmatrix} F_x \\ F_y \end{Bmatrix}$$

$$A = \begin{bmatrix} \cos\theta & -\sin\theta \\ \sin\theta & \cos\theta \end{bmatrix}$$

Substituting Equation (2.38) into (2.39), we obtain

$$F = A\left[-k'\delta' - D'\dot{\delta}'\right] \tag{2.40}$$

but $\delta' = A^T\delta$ and $\dot{\delta} = A^T\dot{\delta}$. Therefore,

$$F = -AK'A^T\delta - AD'A^T\dot{\delta} \tag{2.41}$$

but, F also equals

$$F = -K\delta - D\dot{\delta} \tag{2.42}$$

where

$$K = \begin{bmatrix} K_{xx} & K_{xy} \\ K_{yx} & K_{yy} \end{bmatrix}$$

$$D = \begin{bmatrix} D_{xx} & D_{xy} \\ D_{yx} & D_{yy} \end{bmatrix}$$

Therefore, comparing Equations (2.41) and (2.42)

$$K = AK'A^T \text{ and } D = AD'A^T \tag{2.43}$$

The code determines the position of the eccentricity vector by calculating the position of the minimum film thickness. The stiffness and damping transformations are appropriately added to the stiffness and damping matrices for NEWMARK computations.

2.10 Viscous Shear Forces and Moments

For face seals, viscous shear forces are produced at the interface. These forces are

$$F = \frac{-\mu A V}{h} \tag{2.44}$$

$$F = \begin{Bmatrix} F_x \\ F_y \end{Bmatrix} \tag{2.45}$$

$$V = \begin{Bmatrix} V_x \\ V_y \end{Bmatrix} \tag{2.46}$$

where

A = interface area
V = seal ring velocity in x-y plane
h = film thickness
μ = absolute viscosity

The coefficients $\mu A/h$ are included in the damping matrix.

2.11 Applied Forces

The computation of applied forces and moments are necessary for subsequent friction computations. The applied force vector includes all forces and moments excluding equilibrium and friction forces and moments.

For ring seals,

$$F_a = -K(\delta_s - \delta) - D(\dot{\delta}_s - \dot{\delta}) \tag{2.47}$$

where:

$$F_a = \text{applied force vector} = \begin{Bmatrix} F_{ax} \\ F_{ay} \end{Bmatrix}$$

$$K = \text{film stiffness matrix} = \begin{bmatrix} K_{xx} & K_{xy} \\ K_{yx} & K_{yy} \end{bmatrix}$$

$$D = \text{film damping matrix} = \begin{bmatrix} D_{xx} & D_{xy} \\ D_{yx} & D_{yy} \end{bmatrix}$$

$$\delta_s = \text{seal ring displacement} = \begin{Bmatrix} \delta_{sx} \\ \delta_{sy} \end{Bmatrix}$$

$$\delta = \text{shaft displacement} = \begin{Bmatrix} \delta_x \\ \delta_y \end{Bmatrix}$$

Similarly, $\dot{\delta}_s$ and $\dot{\delta}$ are seal ring and shaft velocity vectors, respectively.

For face seals, the matrix formulation is:

$$F_a = -K\delta_r - D\dot{\delta}_r \tag{2.48}$$

where:

$$F_a = \text{applied force vector} = \begin{Bmatrix} F_{ax} \\ F_{ay} \\ F_{az} \\ M_{ax} \\ M_{ay} \end{Bmatrix}$$

$$\delta_r = \text{relative displacement vector} = \begin{Bmatrix} x_s \\ y_s \\ z_s - z \\ \beta_s - \beta \\ \alpha_s - \alpha \end{Bmatrix}$$

$$\dot{\delta}_r = \text{relative velocity vector} = \begin{Bmatrix} \dot{x}_s \\ \dot{y}_s \\ \dot{z}_s - \dot{z} \\ \dot{\beta}_s - \beta \\ \dot{\alpha}_s - \dot{\alpha} \end{Bmatrix}$$

The forces from x and y displacements occur between the secondary seal and housing and are not relative with respect to the shaft.

Subscript, s, refers to the seal ring. Displacements without subscripts refer to the shaft motions. The elements of the stiffness and damping matrices are:

$K_{11} = -K_x^{sc}$ = O-ring stiffness in x direction

$K_{22} = -K_y^{sc}$ = O-ring stiffness in y direction

$K_{33} = -K_z^{sp} + K_{zz}$ = spring stiffness + fluid film stiffness in z direction

$K_{34} = K_{z\beta}$ = cross coupled film stiffness

$K_{35} = K_{z\alpha}$ = cross coupled film stiffness

$K_{43} = K_{\beta z}$ = cross coupled film stiffness

$K_{44} = -K_\beta^{sp} + K_{\beta\beta}$ = spring rotational stiffness + film stiffness about x axis

$K_{45} = K_{\beta\alpha}$ = cross coupled film stiffness

$K_{53} = K_{\alpha z}$ = cross coupled film stiffness

$K_{54} = K_{\alpha\beta}$ = cross coupled film stiffness

$K_{55} = -K_\alpha^{sp} + K_{\alpha\alpha}$ = spring rotational stiffness about y axis + film rotational stiffness.

The damping matrix includes the viscous shear damping:

$D_{11} = D_{SH} - D_{xx}^{sc}$ = shear damping coefficient + O-ring damping in x direction

$D_{15} = -D_{SH} z_{cg}$ = shear damping coefficient × axial distance to cg

$D_{22} = D_{SH} - D_{yy}^{sc}$ = shear damping coefficient + O-ring damping in y direction

$D_{25} = D_{SH} z_{cg}$ = shear damping coefficient × axial distance to cg

$D_{33} = D_{zz}$ = film damping coefficient

$D_{34} = D_{z\beta}$ = cross coupled film damping coefficient

$D_{35} = D_{z\alpha}$ = cross coupled film damping coefficient

$D_{z42} = D_{SH} z_{cg}$ = shear damping coefficient × axial distance to cg

$D_{43} = D_{\beta z}$ = cross coupled film damping coefficient

$D_{44} = D_{\beta\beta} + D_{SH} z_{cg}^2$ = film damping coefficient + shear damping coefficient × the square of the cg distance

$D_{45} = D_{\beta\beta} + D_{SH} z_{cg}^2$ = film damping coefficient + shear damping coefficient × the square of the cg distance

$D_{51} = -D_{SH} z_{cg}$ = shear damping coefficient × the distance to the cg

$D_{53} = D_{\alpha z}$ = cross coupled film damping coefficient

$D_{54} = D_{\alpha\beta}$ = cross coupled film damping coefficient

$D_{55} = D_{\alpha\alpha} + D_{SH} z_{cg}^2$ = cross coupled film damping + shear damping coefficient × the square of the cg distance.

2.12 Piston Ring Secondary Seal Friction Forces and Moments

2.12.1 Friction Forces and Moments from the Radial Surface of the Piston Ring

The piston ring moves with the shaft in x and y, and can also hold back the shaft from moving (see Figure 8). Surface 2 of the piston ring is the radial face, and Surface 1 is the interior cylindrical surface. The velocity of Surface 2 is:

$$\begin{aligned}\overline{V}_{sc2} &= \dot{x}_s\hat{i} + \dot{y}_s\hat{j} + \overline{\omega}_s \times \bar{r}_2 \\ \overline{\omega}_s &= \dot{\beta}_s\hat{i} + \dot{\alpha}_s\hat{j}\end{aligned} \tag{2.49}$$

$$\bar{r}_2 = z_1\hat{k} + r_f\cos\theta\hat{i} + r_f\sin\theta\hat{j} \tag{2.50}$$

$$\overline{\omega}_s \times \bar{r}_2 = -\dot{\beta}_s z_1\hat{j} + \dot{\beta}_s r_f\sin\theta\hat{k} + \dot{\alpha}_s z_1\hat{i} - \dot{\alpha}_s r_f\cos\theta\hat{k} \tag{2.51}$$

It is assumed that there is zero k velocity of the piston ring. Therefore:

$$\overline{V}_{sc2} = (\dot{x}_s + \dot{\alpha}_s z_1)\hat{i} + (\dot{y}_s - \dot{\beta}_s z_1)\hat{j} = \overline{V}\hat{i}_{sc2x} + V\hat{j}_{sc2y} \tag{2.52}$$

The direction of the friction force is opposite to that of the velocity

$$\overline{F}_{sc2} = \text{friction force} = -p_o A_p \nu \frac{\overline{V}_{sc2}}{|V_{sc2}|} \tag{2.53}$$

where:

p_o = applied pressure on piston ring
A_p = unbalanced contact area of piston ring
ν = coefficient of friction

and

$$F_{sc2x} = -p_o A_p \nu \text{ (sign Vsczx)} \tag{2.54}$$
$$F_{sc2y} = -p_o A_p \nu \text{ (sign Vsczy)} \tag{2.55}$$

The moment about the CG from the face friction force is:

$$\begin{aligned}\overline{M}_2 &= \bar{r}_2 \times \overline{F}_{sc2} = \left(z_1\hat{k} + r_f\cos\theta\hat{i} + r_f\sin\theta\hat{j}\right) \times \left(F_{sc2x}\hat{i} + F_{sc2y}\hat{j}\right) \\ &= z_1 F_{sc2x}\hat{j} - z_1 F_{sc2y}\hat{i} + \text{k components that are neglected.}\end{aligned} \tag{2.56}$$

where F_{sc2x} and F_{sc2y} are defined above.

The friction forces and moments are subsequently added to the force vector in the Newmark formulations.

2.13 Friction Forces From the ID of the Piston Ring

At the ID piston ring interface, there is only velocity in the z direction, which equals the relative velocity of the seal ring in the z direction. The major contribution to the normal force at the ID is the pressure that p_o applies to the OD. The following equation results for the load per unit length at the ID of the piston ring.

$$P_{e\ell} = \frac{p_o R_{sco} w}{R_{sci}} + P'_{e\ell} \tag{2.57}$$

where:

$P_{e\ell}$ = preload per unit length of ID of piston ring
p_o = pressure on OD of piston ring
R_{sco} = outside radius of piston ring
R_{sci} = inside radius of piston ring
w = width of contact surface at ID
$P'_{e\ell}$ = initial or installed preload per unit length

The direction of the friction force is opposite the direction of the axial velocity, $\overline{V}_z$. If $\overline{V}_z = 0$, the direction of the friction force is opposite the direction of the applied force in the z direction, $\overline{F}_{az}$. Therefore,

$$F_f = -2\pi v R_{sci} P_{e\ell} (\text{sign } \overline{V}_z \text{ or sign } \overline{F}_{az}) \tag{2.58}$$

2.14 O-Ring Secondary Seal Stiffness and Friction Forces and Moments

An O-ring secondary seal contributes stiffness and damping and friction forces and moments. Explicit analysis was conducted to determine these contributions. The O-ring is divided into 72 segments of 5 degrees each. The displacement of the ℓth segment is:

$$\overline{\delta}^{\ell} = \overline{u} + \overline{\phi} \times \overline{r}^{\ell}_{se} \tag{2.59}$$

where:

$$\overline{\delta}^{\ell} = \begin{Bmatrix} \overline{\delta}^{\ell}_x \\ \delta^{\ell}_y \\ \delta^{\ell}_z \end{Bmatrix}, \quad \overline{u} = \begin{Bmatrix} u_1 \\ u_2 \\ 0 \end{Bmatrix}, \quad \phi = \begin{Bmatrix} \beta_s \\ \alpha_s \\ 0 \end{Bmatrix}, \quad r^{\ell}_{sc} = \begin{Bmatrix} R_{sc} \cos\theta^{\ell} \\ R_{sc} \sin\theta^{\ell} \\ z_{sc} - u(3) \end{Bmatrix}$$

The normal vector at θ^ℓ is $\hat{n}^\ell$ (Figure 9), where

$$\hat{n}^\ell = \cos\theta^\ell \hat{i} + \sin\theta^\ell \hat{j} \tag{2.60}$$

$$\bar{\delta}^\ell \cdot \hat{n}^\ell = \delta_n^\ell \tag{2.61}$$

where δ_n^ℓ = normal displacement at θ^ℓ. Similarly, the velocity of the seal ring at the ℓth segment is:

$$\dot{\bar{\delta}}^\ell = \dot{\bar{u}} + \dot{\bar{\phi}} \times \bar{r}_{sc}^\ell \tag{2.62}$$

where

$$\dot{\bar{u}} = \begin{Bmatrix} \dot{u}_1 \\ \dot{u}_2 \\ 0 \end{Bmatrix}, \quad \dot{\bar{\phi}} = \begin{Bmatrix} \dot{\beta}_s \\ \dot{\alpha}_s \\ 0 \end{Bmatrix}$$

and

$$\dot{\delta}_n^\ell = \dot{\delta}^\ell \cdot \hat{n}^\ell \tag{2.63}$$

The normal force at the ℓth segment on the seal ring is:

$$F_n^\ell = -k_{e\ell}\delta_n^\ell R_{sc} d\theta^\ell - D_{e\ell}\dot{\delta}_n^\ell R_{sc} d\theta^\ell - Pr_{e\ell} \cdot R_{sc} d\theta^\ell \tag{2.64}$$

where:

$k_{e\ell}$ = O-ring stiffness per unit length
$D_{e\ell}$ = O-ring damping per unit length
$Pr_{e\ell}$ = O-ring preload per unit length
F_n^ℓ = normal O-ring force at θ^ℓ

and

$$F_x^\ell = F_n^\ell \cos\theta^\ell \tag{2.65}$$

$$F_y^\ell = F_n^\ell \sin\theta^\ell \tag{2.66}$$

$$F_x = \sum_{\ell=1}^{72} F_x^\ell \tag{2.67}$$

$$F_y = \sum_{\ell=1}^{72} F_y^\ell \tag{2.68}$$

where:

F_x^ℓ = x force at θ^ℓ
F_y^ℓ = y force at θ^ℓ
F_x = total O-ring x force
F_y = total O-ring y force

The O-ring moment is:

$$\overline{M}^\ell = \overline{r}_{se}^\ell \times \overline{F}_n^\ell \tag{2.69}$$

and

$$\overline{M}^\ell = \begin{Bmatrix} M_x^\ell \\ M_y^\ell \\ M_z^\ell \end{Bmatrix}$$

where:

$\overline{M}^\ell$ = moment due to the normal force at θ^ℓ

and

$$M_x = \sum_{\ell=1}^{72} M_x^\ell, \qquad M_y = \sum_{\ell=1}^{72} M_y^\ell \tag{2.70}$$

The stiffness of the O-ring is:

$$K_{ij} = \frac{F_i(\delta_j)}{\delta_j} \tag{2.71}$$

where:

K_{ij} = ith stiffness in the i direction due to a j displacement
δ_j = displacement in j direction.

These stiffnesses are determined from a zero displacement position and are constant values. They are added to the stiffness matrix that is used in the NEWMARK computations. Similarly,

$$D_{ij} = \frac{F_i(\delta_j)}{\dot{\delta}_j} \tag{2.72}$$

where:

D_{ij} = damping in i direction due to a j velocity.

The O-ring friction imposes additional forces and moments on the seal ring. The friction forces are always along the z axis and direction is always opposite the velocity vector. The relative velocity at sector ℓ is:

$$\overline{V}_z^{\ell} = \left(\overline{\dot{u}}^{\ell} + \overline{\dot{\phi}} \times \overline{r}_{se}^{\ell}\right) \cdot \hat{k} \tag{2.73}$$

Then the friction force at the ℓth segment is:

$$F_f^{\ell} = \nu F_n^{\ell}\left(-\text{sign} V_z^{\ell}\right) \tag{2.74}$$

where ν = the coefficient of friction. The total friction force is:

$$F_f = \sum_{\ell=1}^{72} F_f^{\ell} \tag{2.75}$$

The moment due to the friction force is:

$$\overline{M}_f = \sum_{\ell=1}^{72} \left(\overline{r}_{sc}^{\ell} \times \overline{F}_f^{\ell}\right) \tag{2.76}$$

$$\overline{F}_f = \begin{Bmatrix} 0 \\ 0 \\ F_f \end{Bmatrix}, \quad \overline{M}_f = \begin{Bmatrix} M_x \\ M_y \\ 0 \end{Bmatrix} \tag{2.77}$$

These forces and moments are added to the force vector used in the NEWMARK computations.

2.15 Computation of the Force Vector

The force vector contains all terms that are not directly multiplied by the seal ring displacements, velocities, or accelerations.

$$m\ddot{x}_s + kx_s + D\dot{x}_s = F \tag{2.78}$$

where:

m = mass matrix
k = stiffness matrix
D = damping matrix
F = force vector
$x_s, \dot{x}_s, \ddot{x}_s$ = seal ring displacement, velocity, and acceleration vectors

The terms of the force vector, F, contain stiffness and damping multiplied by shaft displacements and velocities plus friction restraint force:

$$F = kx + D\dot{x} + F_f$$

where

F_f = friction vector
K = fluid film stiffness matrix
D = fluid film damping matrix plus viscous shear damping terms
F_f = friction restraint forces in all degrees of freedom

2.16 Friction Restraint

After the displacements, velocities, and accelerations are updated, it is necessary to determine whether friction should have halted the motion. When determining friction restraint, it is important to realize that total forces and velocities are applied, and considering components alone can be misleading. For example, a body moving in a plane will not be restrained in a component direction as long as the total applied force exceeds the total friction force even though a component friction force can exceed a component applied force. For purposes of illustration, a piston ring secondary seal will be discussed. Referring back, Figure 8 showed the piston ring model.

Wall friction on the piston ring will restrain lateral (x and y) and angular (α and β) motions of the seal ring. The ID friction of the piston ring will restrain axial motions of the seal ring. Consider a velocity versus time plot, as shown on Figure 10.

There are three regions of accountability:

1. When accelerating, F_f and F_a are opposite $|F_f| < |F_a|$
   - F_f = friction force
   - F_a = applied force.
2. When decelerating, F_f and F_a are of the same sign; a finite velocity implies $|F_f| < |F_a|$.
3. If the velocity changes sign between successive time steps, then somewhere between motion has stopped and cannot restart until $|F_a| > |F_f|$. Thus, there is a discontinuity in the velocity curve. If we followed the normal procedure without taking into account the finite stopping time, the velocity would be repositioned to point B in Figure 10 instead of point A.

At the piston ring wall, the velocities of the ring in the x and y directions are:

$$V_x = \dot{x} + \dot{\alpha} z_1 \tag{2.79}$$

$$V_y = \dot{y} - \beta z_1 \tag{2.80}$$

and the total velocity is:

$$V_T = \sqrt{V_x^2 + V_y^2} \tag{2.81}$$

where:

V_x = x component of velocity of piston ring
V_y = y component of velocity of piston ring
$\dot{x}$ = x component of velocity of seal ring at CG
$\dot{y}$ = y component of velocity of seal ring at CG
α = rotational velocity about y axis
β = rotational velocity about x axis
z_1 = axial distance from CG to piston ring wall

The forces that would move the piston ring along the wall (x-y plane) come from both the lateral applied forces at the CG and the total applied moments about the CG.

$$F_{axt} = F_{ax} + M_{yy} / z_1 \tag{2.82}$$

$$F_{ayt} = F_{ay} - M_{xx} / z_1 \tag{2.83}$$

where:

F_{ax} = x component of applied force at CG
F_{ay} = y component of applied force at CG
M_{yy} = applied moment about y axis
M_{xx} = applied moment about x axis
F_{axt} = total x component of applied force at ring wall
F_{ayt} = total y component of applied force at ring wall

The total applied force at the ring wall is F_a, defined as:

$$F_a = \sqrt{F_{axt}^2 + F_{ayt}^2} \tag{2.84}$$

Other parameters include:

$$V_{xy} = \sqrt{\dot{x}^2 + \dot{y}^2} \tag{2.85}$$

where V_{xy} = total translatory velocity at CG.

$$F_{axy} = \sqrt{F_{ax}^2 + F_{ay}^2} \tag{2.86}$$

where F_{axy} = total translatory applied force at CG. The friction force at the wall is defined as:

$$F_f = \sqrt{F_{fx}^2 + F_{fy}^2} \tag{2.87}$$

where:

F_f = total friction force
F_{fx} = friction force in x direction
F_{xy} = friction force in y direction.

With these terms and definitions, a flow chart of the friction wall restraining algorithm is indicated on Figure 11. Note that even though friction may not restrain piston ring motion, a check has to be made on x and y motions at the CG. This is because the piston ring can move due to angular rotations about the CG without x, y translations of the CG.

A similar routine has been established for restraint in the z direction. Since this is a single-degree-of-freedom motion, it is a much simpler algorithm than for the coupled x, y and angular modes.

2.17 Minimum Film Thickness

At each time step, the minimum film thickness is computed to determine if a negative film occurs. If so, the computations are halted and the seal is considered failed.

Face Seal. Because of angular rotations, the minimum film thickness is computed at the outside radius of the fluid-film interface. The film thickness varies around the circumference of the seal and is thus a function of theta. In computing the film thickness, the circumference is subdivided into 72 increments, and the film thickness determined at each incremental intersection.

$$H_p = H_o + \Delta Z + \bar{\phi} \times \bar{r}_p \cdot \hat{k} \tag{2.88}$$

where:

H_o = equilibrium film thickness
ΔZ = difference between seal ring and shaft displacement
$\bar{\phi}$ = rotation vector
$\bar{r}_p$ = position vector from center of gravity to point p

For a face seal with a stationary (nonrotating) seal ring,

$$H = H_o + (Z_s - Z) + \left[\left((\beta_s - \beta)\hat{i} + (\alpha_s - \alpha)\hat{j}\right) \times \left(-z_{cg}\hat{k} + R_o \cos\theta_p \hat{i} + R_o \sin\theta_p \hat{j}\right)\right] \cdot \hat{k}$$

$$H = H_o + (Z_s - Z) + \left[(\beta_s - \beta)R_o \sin\theta_p - (\alpha_s - \alpha)R_o \cos\theta_p\right] \tag{2.89}$$

Ring Seal Clearance. Ring seal parameters are shown on Figure 12. Ring seals are limited to two degrees of freedom, x and y. Since both the shaft and ring can move, the film thickness is a function of relative displacements between them. The equations are as follows:

$$\begin{aligned}\overline{\xi}_r &= \overline{\xi}_s - \overline{\xi} \\ \overline{\phi}_r &= \overline{\phi}_s - \phi \\ H &= C + \overline{\xi}_r \cdot \hat{n}\end{aligned} \tag{2.90}$$

where:

$\overline{\xi}_s$ = displacement vector of seal ring
$\overline{\xi}$ = displacement vector of shaft
$\overline{\xi}_r$ = relative displacement

and

$$\overline{\xi}_s = x_s\hat{i} + y_s\hat{j}; \quad \xi = x\hat{i} + y\hat{j}$$

$$\overline{\xi}_r = (x_s - x)\hat{i} + (y_s - y)\hat{j} \tag{2.91}$$

$$\hat{n} = \cos\theta\hat{i} + \sin\theta\hat{j} \tag{2.92}$$

$$\overline{\xi}_r \cdot \hat{n} = (x_s - x)\cos\theta + (y_s - y)\sin\theta \tag{2.93}$$

$$H = C + (x_s - x)\cos\theta + (y_s - y)\sin\theta = C + (x_s - x)\cos\theta + (y_s - y)\sin\theta \tag{2.94}$$

where:

z = longest distance from CG to end of seal.

2.18 Units

The units for the English and metric systems are as follows:

English

- Length: in.
- Density: lb/in.^{3}
- E: lb/in.^{2}
- Stiffness: lb/in., lb/rad, in.-lb/rad
- Damping: lb-sec/in., lb-sec/rad, in.-lb-sec/rad
- Rotational speed and frequency: rad/sec

- Viscosity: lb-sec/in.^{2} (reyns)
- Pressure: lb/in.^{2}
- Force: lb
- Film thickness: in.

Metric

- Length: meters
- Density: kg/m^3
- E: N/m^2
- Stiffness: N/m, N/rad, N-m/rad
- Damping: N-s/m, N-s/rad, m-N-s/rad
- Rotational speed and frequency: rad/s
- Viscosity: Pa-s = N-s/m^2
- Pressure: Pa = N/m^2
- Force: N
- Film thickness: microns

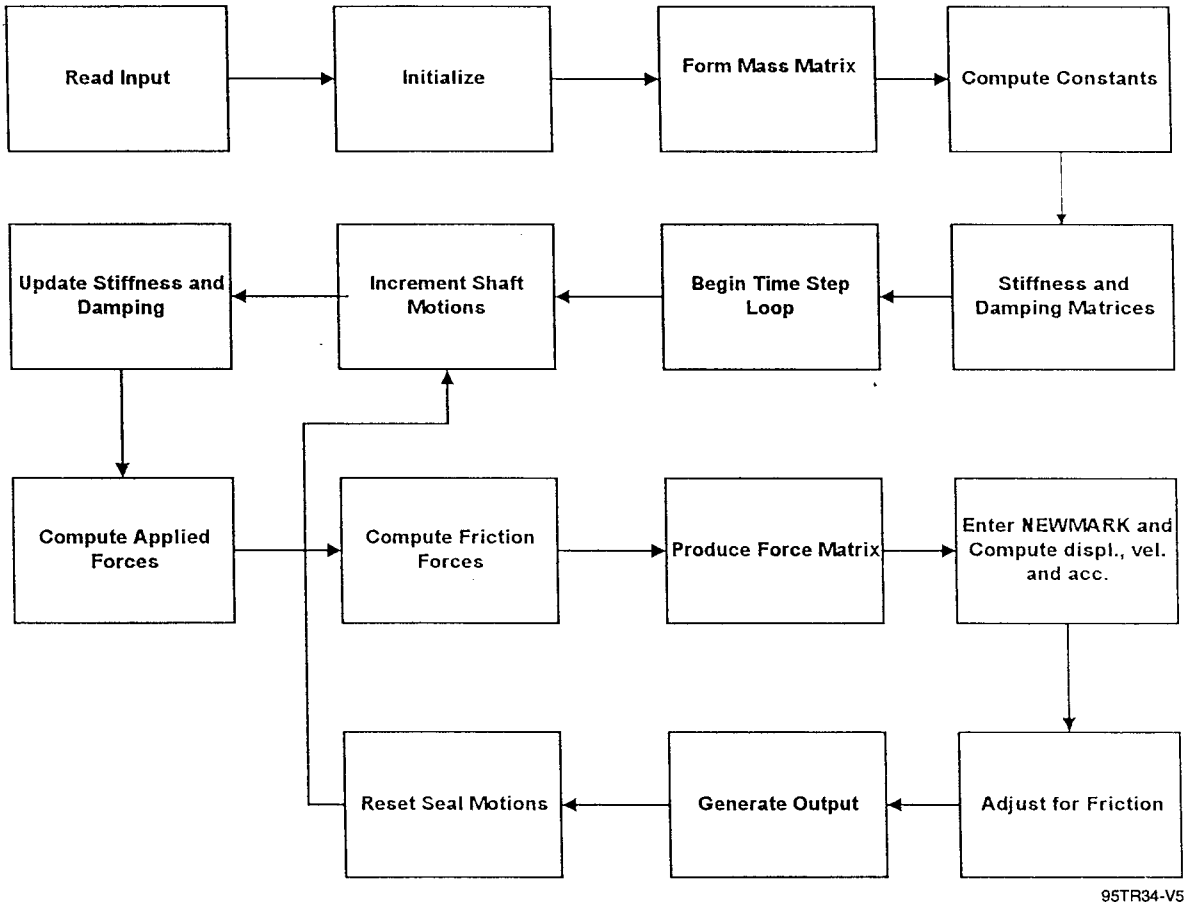

Figure 4. Program Flow Chart

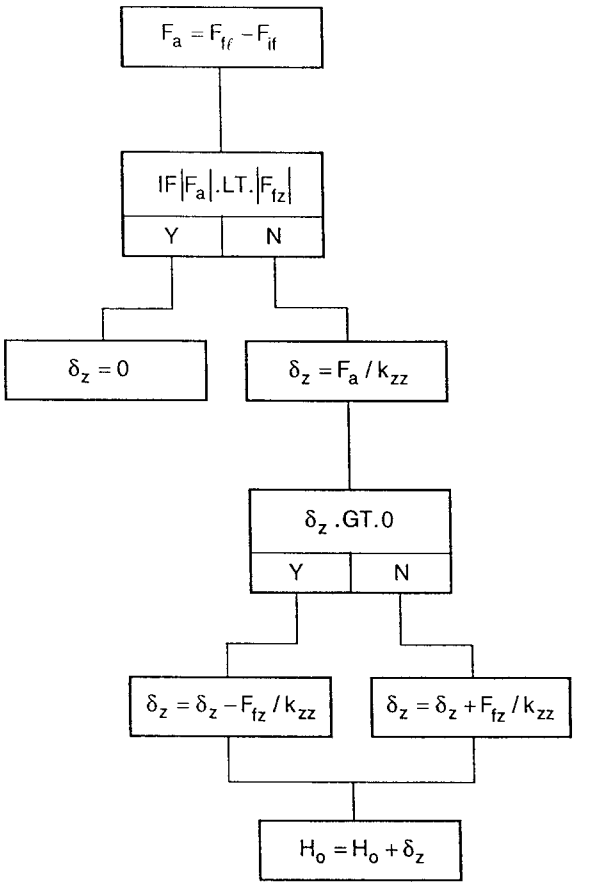

F_a = Axial force
$F_{f\ell}$ = Fluid film force
F_{fz} = Axial friction force
δ_z = Axial seal ring displacement
k_{zz} = Fluid film axial stiffness coefficient

Figure 5. Initial Equilibrium Algorithm

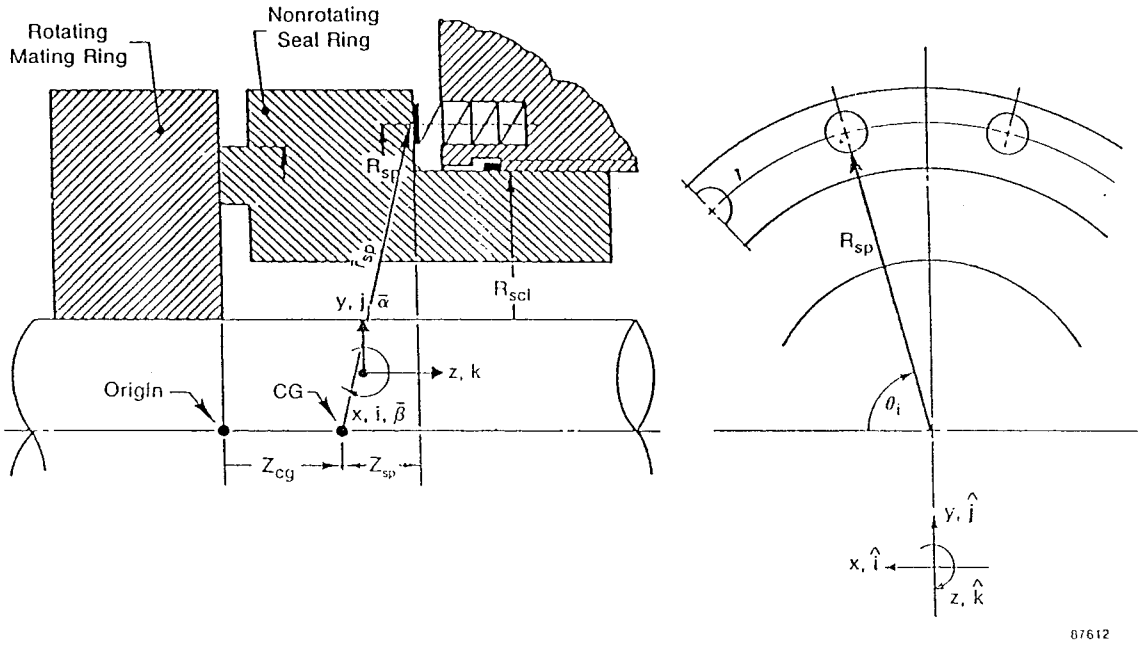

Figure 6. Spring Forces and Moments

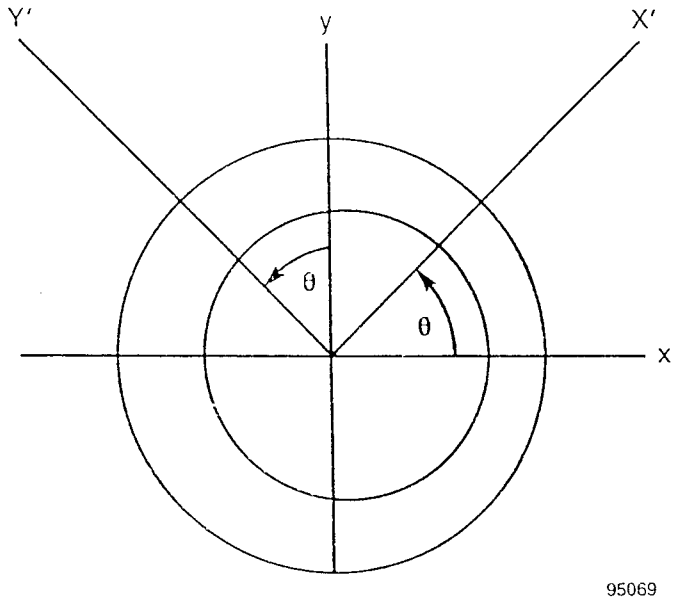

Figure 7. Ring Seal Transformations

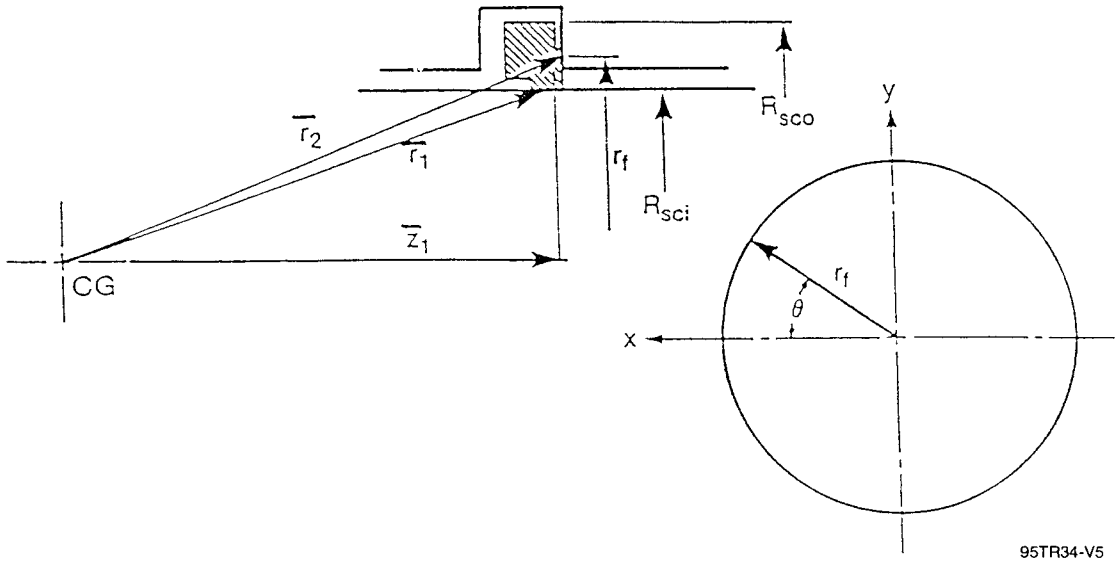

Figure 8. Piston Ring Forces and Moments

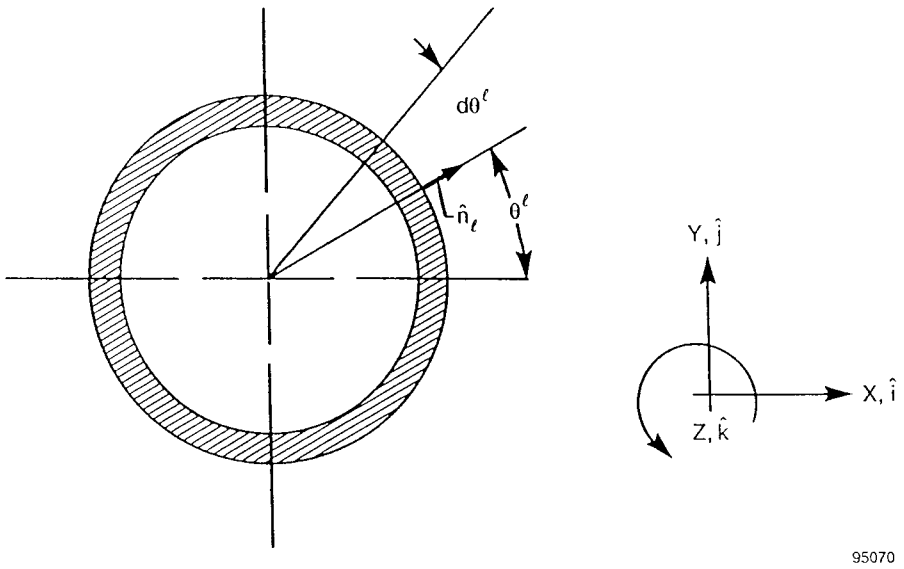

Figure 9. O-Ring Parameters

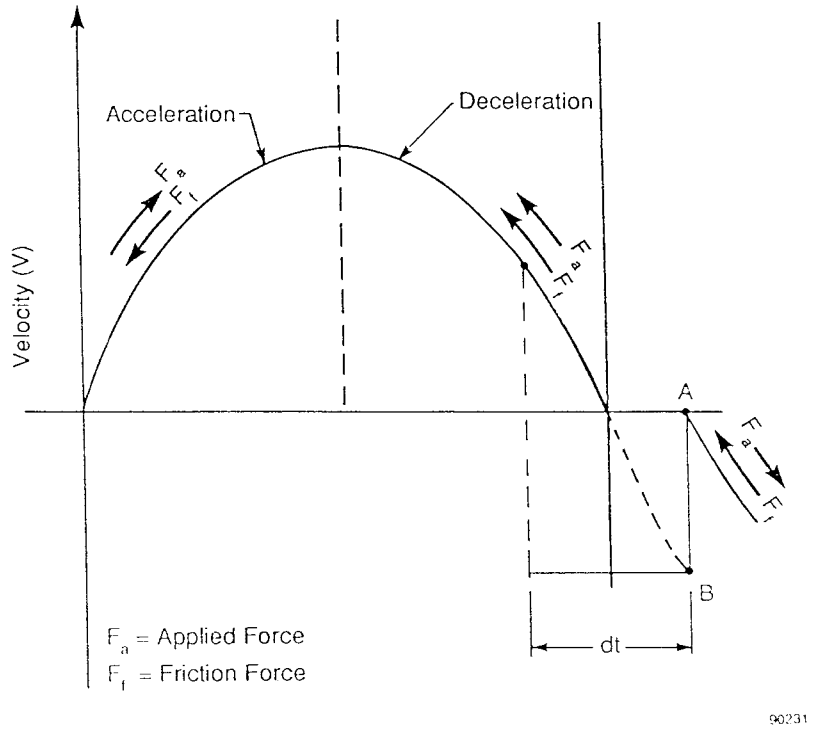

Figure 10. Velocity versus Time Including Friction Restraint

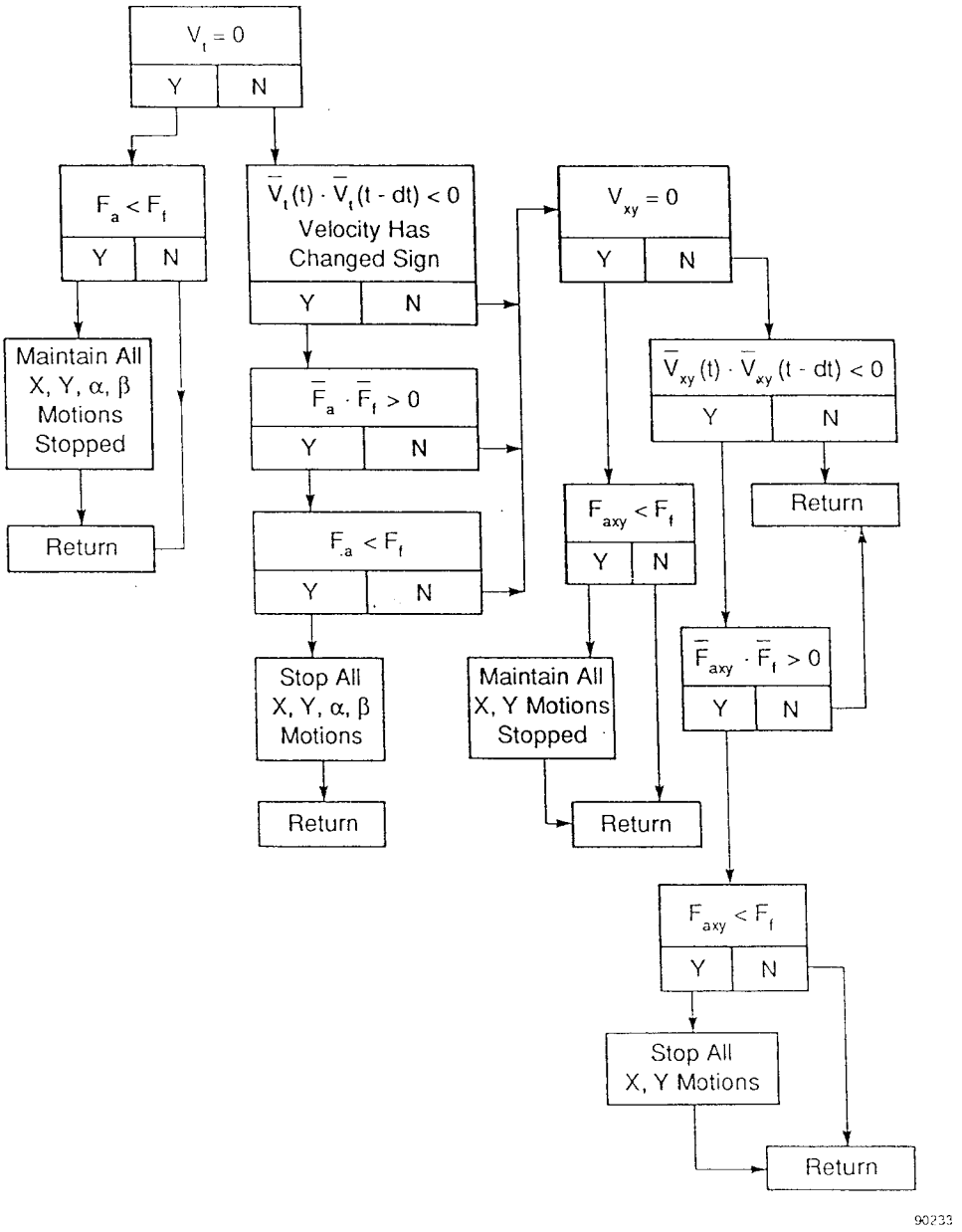

Figure 11. Flow Chart of Piston Ring Wall Friction Restraining Algorithm

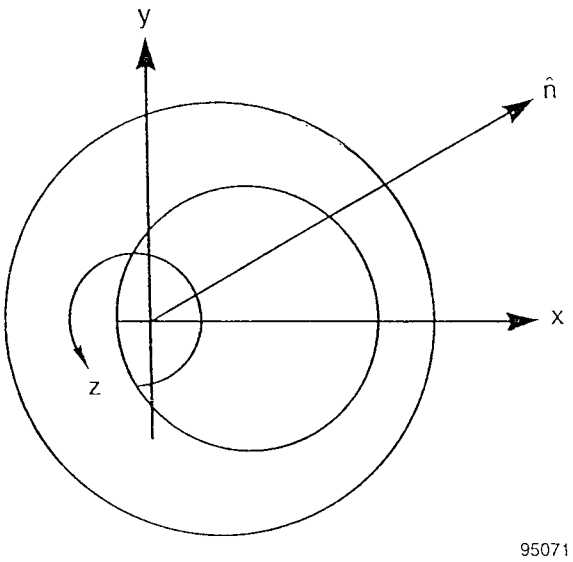

Figure 12. Ring Seal Clearance

3.0 SAMPLE PROBLEMS FOR CODE DYSEAL

The sample problems included in this section are intended to demonstrate program usage and do not necessarily represent seal designs. Face seal samples are included in this section. Ring seal sample problems are demonstrated in the verification section where output was compared against published data.

3.1 Sample Problem 1: Piston Ring Face Seal Input

The sample problem analyzes the 50-mm spiral-groove seal described in Reference 5. Key geometrical parameters are shown in Figure 13. The seal ring was partitioned into three elements. The first element was the seal ring face. The inside radius of the seal ring face was taken as the same as that of the other two elements, since the actual length of the inside radius of the face is very thin (~0.20 in.). Input is shown in Figure 14. Spring and damping coefficients were taken from the work reported upon in Reference 5. The shaft displacements were 0.0005 in. and rotations were 0.0005 radians, respectively.

Plotted output is shown in Figures 15 through 26. In some cases, multiple plots were employed, such as in Figure 15, which shows the x displacement of the seal ring, XS, and the x displacement of the shaft, X. The shaft displacements are sinusoidal patterns, while the seal ring displacements are the generally lower amplitude and more irregular response, due to secondary seal friction.

3.2 Sample Problem 2: Continuation

Sample Problem 2 is a continuation of Sample Problem 1, for another 5 revolutions or 500 time steps. Continuous variables are obtained from the printed output of Sample Problem No. 1. One plot of minimum film thickness was made and is shown in Figure 27.

3.3 Sample Problem 3: O-Ring Secondary Seal

The O-ring secondary seal introduces several new variables. These include:

- **Secondary Seal Stiffness Per Unit Length** which is available from O-ring catalogs. Figure 28 shows percent compression versus load per lineal inch of seal for various O-ring cross sections and durometer. This figure was extracted from a Parker O-ring catalog. Percent compression is obtained by calculating the squeeze of the ring divided by the cross sectional width of the ring. This information is also obtainable from the catalog. The load per lineal inch divided by the squeeze gives the stiffness per unit length.

- **Secondary Seal Damping Per Unit Length.** Information is not available from O-ring catalogs. Elastomers are light damping devices, and a reasonable number is 1/(RSC π).
- **Secondary Seal Preload Per Unit Length.** Generally equal to secondary seal stiffness per unit length, spring stiffness per unit length.
- **Radius to Secondary Seal.**

The input for this case is shown in Figure 29.

Figure 30 shows the x displacement of the seal ring versus shaft revolutions. The displacement is very small - on the order of 20×10^{-6} milli-radians. Similar results apply to the y motions shown on Figure 31. The only exciting forces in these modes is viscous shear between the mating ring and seal ring, which is a small value. Figure 32 shows the axial displacement of both the runner and seal ring. The seal ring response is in phase and slightly magnified above the excitation. Rotations about the x-x and y-y axes are shown in Figures 33 and 34, respectively. The minimum film thickness as a function of shaft revolutions is indicated in Figure 35. Axial and rotational friction are shown in Figures 36 through 38.

3.4 Ring Seal Sample Problems and Verification

For purposes of sample problems and verification, the ring seals described by Kirk in Reference 6 were analyzed. Kirk used a time transient scheme that varied the fluid film forces at each time step using short bearing theory. That differs from the approximate analysis used in DYSEAL in which the fluid film is represented by constant but rotating cross coupled stiffness and damping coefficients. Kirk also assumed a rotor modal mass supported on springs and dashpots and determined the response of the modal mass. In DYSEAL, rotor motions are prescribed.

The first case, as represented by Figure 39 (Kirk, Figure 7), included the following parameters:

- Speed = 1780 rpm
- Axial interface force = 20.9 lb
- Ring mass = 2.13 lb
- Clearance = 0.003 in.
- Length = 0.904 in.
- Viscosity = 0.8125×10^{-7} lb-sec/in.^{2}
- Friction coefficient = 0.150
- P_{high} = 72 psig
- P_{low} = 60 psig
- Shaft radius = 2.090 in.
- Rotor excursion = 0.0024 in.

The film stiffness and damping coefficients were obtained from external codes at an eccentricity ratio of 0.5. The eccentricity was chosen on the basis of load capacity to overcome the friction forces of the secondary seal. The cross coupled coefficients are indicated on the input file, Figure 40. A model was configured that simulated the mass of the ring and provided identical wall interface and friction forces. The given rotor orbit was circular at an eccentricity ratio of 0.8, or a finite value of 0.0024 in. This corresponds to the shaft eccentricity prescribed by Kirk. The given rotor circular orbit is indicated in Figure 41. Orbital response of the seal ring is shown in Figure 42. There is a significant amount of orbit overlapping and the orbit is confined to the 0.0024-in. stimulus from the shaft. As shown at the bottom of Kirk's Figure 7, the orbit does overlap in a similar manner. Figure 43 shows the seal ring displacement as a function of shaft revolutions. Note that there is a strong half frequency component because of the strong cross coupling influence of the stiffness coefficients. The subsynchronous component further explains the orbital loops. Figure 44 shows the y displacement as a function of shaft revolutions. The minimum film thickness is indicated in Figure 45. From Kirk's Figure 7, the seal is tracking the rotor at approximately 0.5 eccentricity or with a minimum film of 1.5 mil. From Figure 45, the median of the film variation is approximately 1.5 mil. Figures 46 and 47 show the friction forces in the x and y direction, respectively. The comparative results are excellent, especially considering the differences in problem solution methods.

A similar analysis was conducted for Kirk's Figure 8 problem (see Figure 48). This seal was identical to Kirk's Figure 7 problem except that the length of the seal was reduced from 0.904 to 0.600 in. This required the development of a new set of stiffness and damping coefficients. The input for this case is shown in Figure 49. The seal ring orbital response is shown in Figure 50. It is a complex pattern of interior looping. The minimum film thickness predicted by DYSEAL is shown in Figure 51. Kirk indicates the seal ring tracks at an eccentricity of 0.75 or at a minimum film thickness of 0.75 mils, which is verified on Figure 51. The minimum film thickness on Figure 51, however, is diminishing with revolutions and may eventually fail. Examination of Kirk's orbital plots reveal that the orbit is continuing to expand after the three revolutions that Kirk examined, and the orbit is not confined. If Kirk increased the number of revolutions, he may have come to the same conclusion as DYSEAL - that this ring may eventually fail by contact.

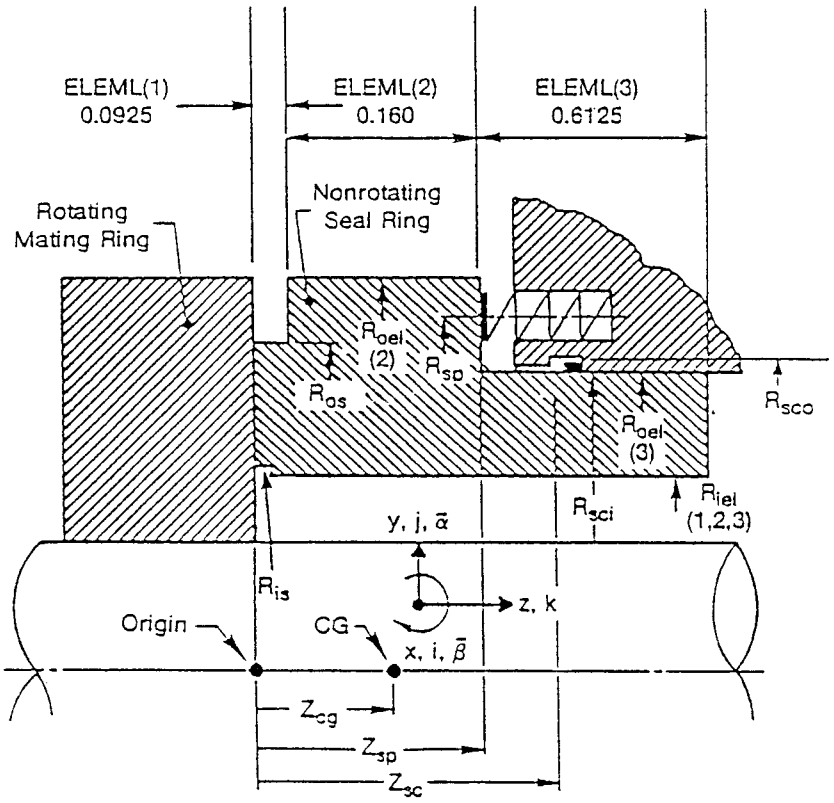

R_{os} = 1.58 in.	R_{oel} (1) = R_{os} = 1.58 in.	Z_{sp} = 0.2525 in.
R_{is} = 1.24 in.	R_{oel} (2) = 1.78 in.	Z_{sc} = 0.7120 in.
R_{sp} = 1.563 in.	R_{oel} (3) = 1.22 in.	
R_{sci} = 1.22 in.	R_{iel} (1, 2, 3) = 1.025 in.	
R_{sco} = 1.40 in.		

95TR34-V5

Figure 13. Geometry for Sample Problem 1

```
SAMPLE1
DYSEAL SAMPLE INPUT
*
HELP
*GEOMETRY
PISTON
ZSCO          0.712
ROS           1.58
RIS           1.24
RSCI          1.22
RSCO          1.40
RSP           1.5625
NELM          3
ZSPO          0.2525
THETO         0.0
DTHET         .5236
RIEL(20)       1.025  1.025  1.025
ROEL(20)       1.580  1.780  1.220
ELEML(20)      .0925  .1600  .6125
DENS(20)       .250   .250   .250
ZL(20)         0.0 .0925  .2525
APR           .536
WPR           .025
*SPRING AND DAMPING
SPPRE         .150
NOSP          12
SKZZ          421000.
SKZA          0.0
SKZB          0.0
SKBZ          0.0
SKBB          361239.
*SKBA         0.0
*SKAZ         0.0
*SKAB         0.0
SKAA          361239.
DZZ             0.0
DZB             0.0
DZA             0.0
DBZ             0.0
DBB             0.0
DBA             0.0
DAZ             0.0
DAB             0.0
DAA             0.0
SPRST           5.050
HO            .00117
FFL           2375.0
*OPERATING CONDITIONS
OMEGA         7330.
POO           750.
PID           0.0
COFSC            .2
VISC          1.7E-08
DT          8.571876E-06
NTS           1000
NT            1
*INITIAL CONDITIONS
XO                .0005
YO                .0005
ZO                .0005
AO                .0005
BO                .0005
OMEGAX        7330.
OMEGAY        7330.
OMEGAZ        7330.
TINIT           0.0
```



```
OMEGAB        7330.
OMEGAA        7330.
END
```

95TR34-V5

Figure 14. Sample Problem 1 Input

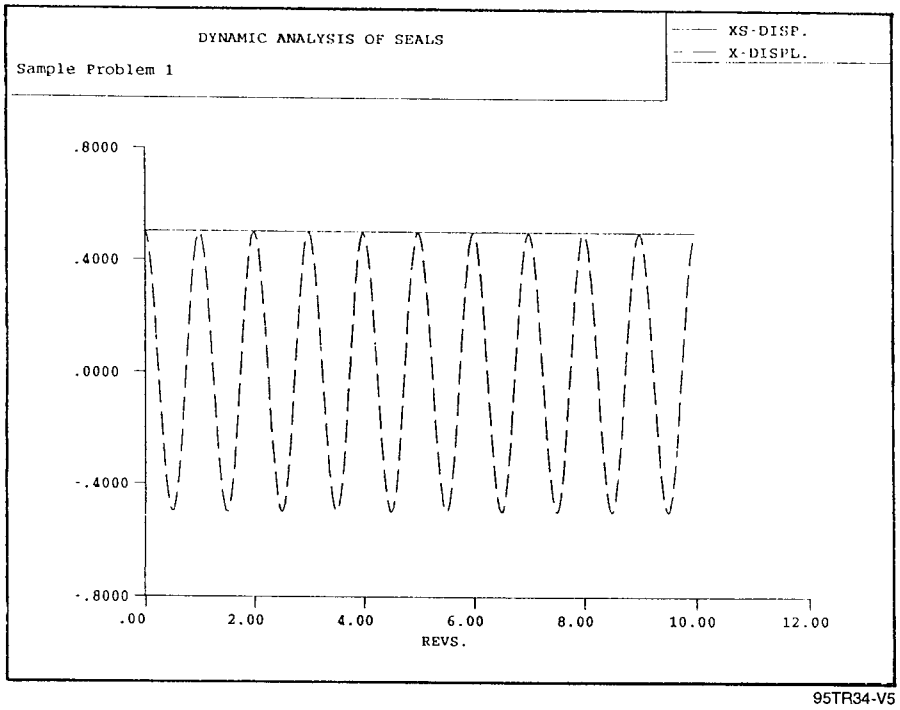

Figure 15. x Displacement versus Shaft Revolutions

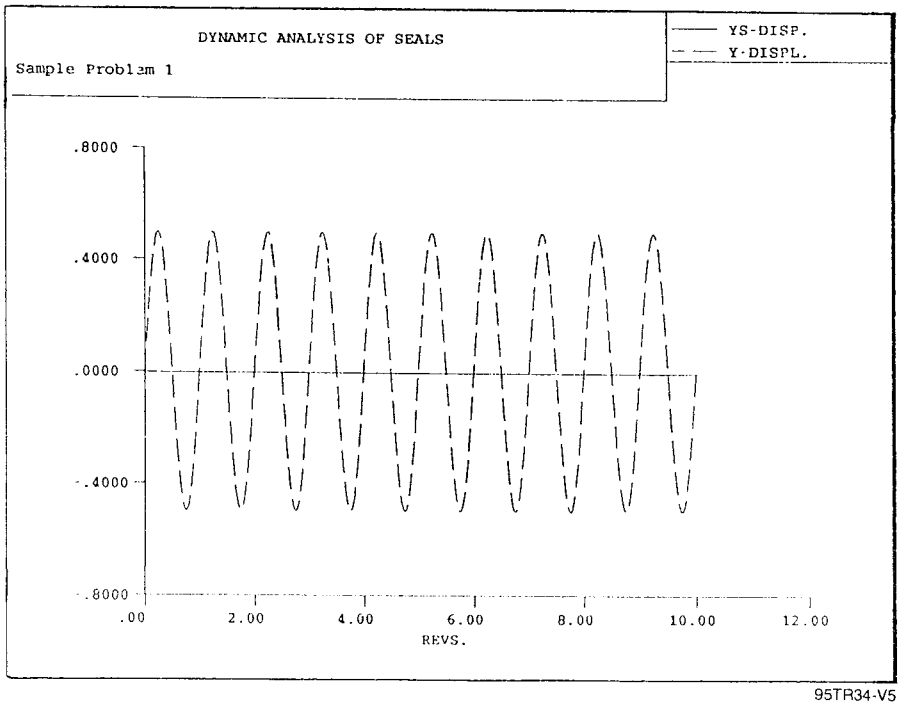

Figure 16. y Displacement versus Shaft Revolutions

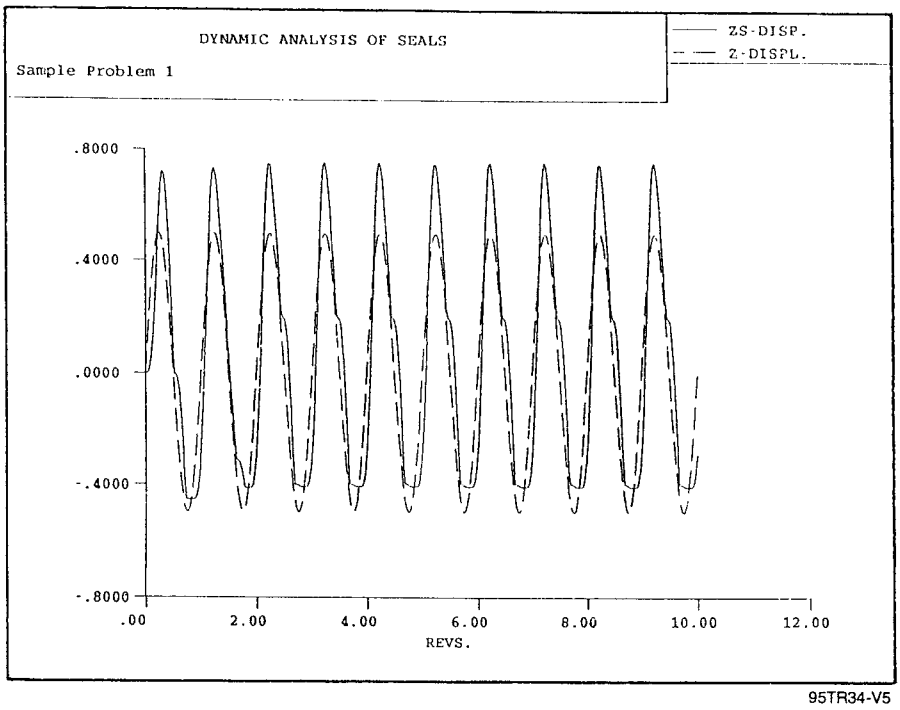

Figure 17. z Displacement versus Shaft Revolutions

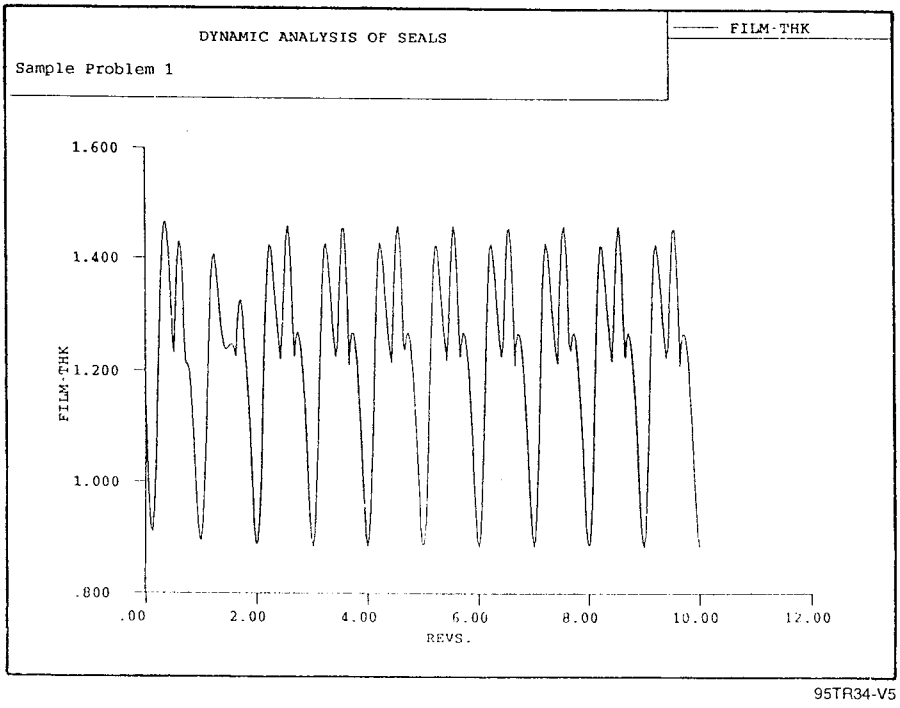

Figure 18. Film Thickness versus Shaft Revolutions

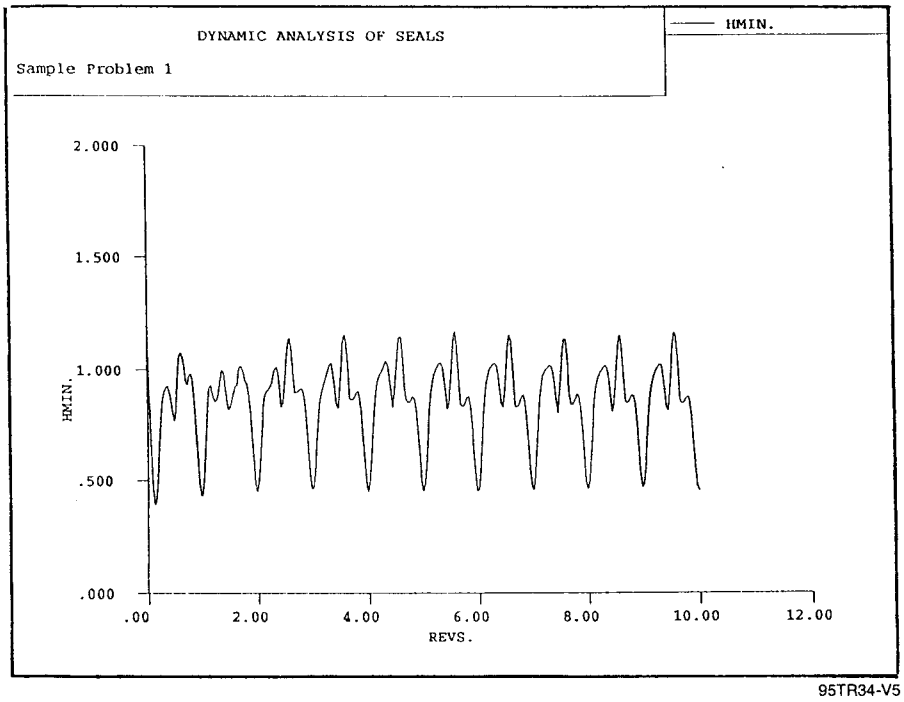

Figure 19. Minimum Film Thickness versus Shaft Revolutions

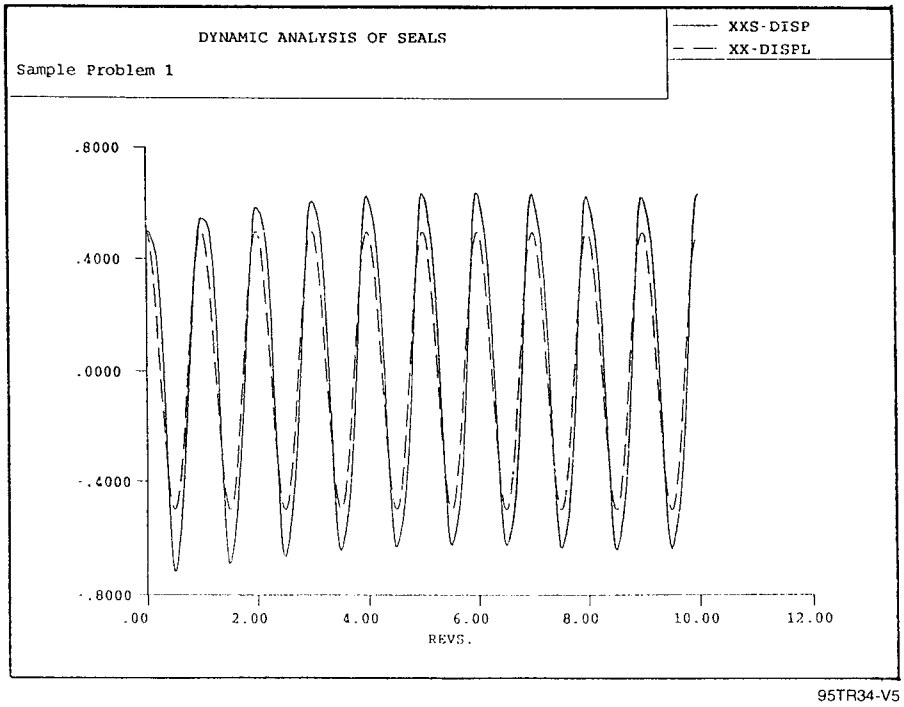

Figure 20. Rotational Displacement About x Axis versus Shaft Revolutions

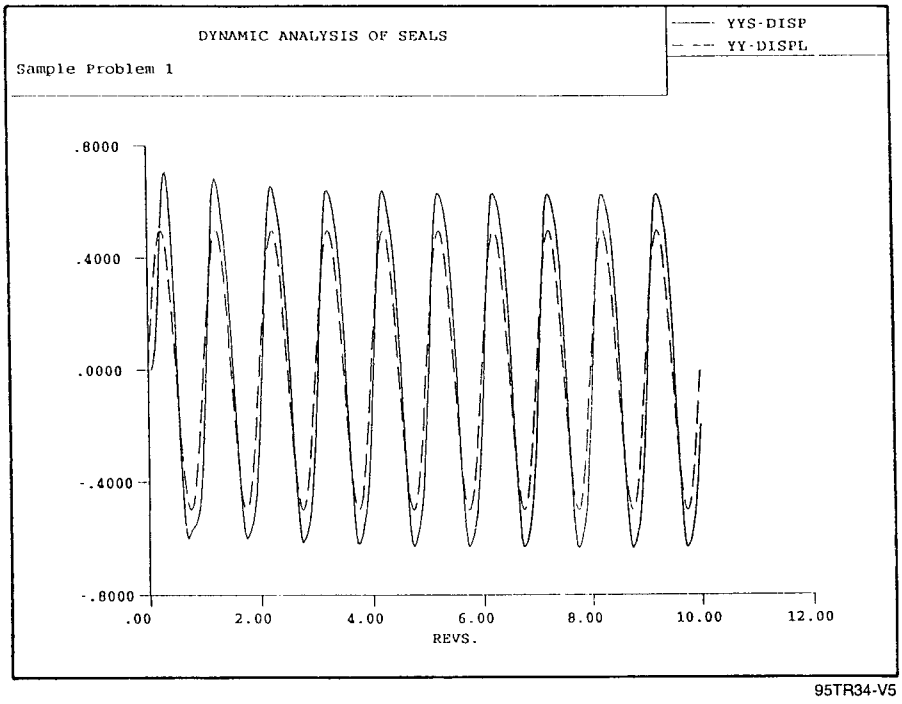

Figure 21. Rotational Displacement About y Axis versus Shaft Revolutions

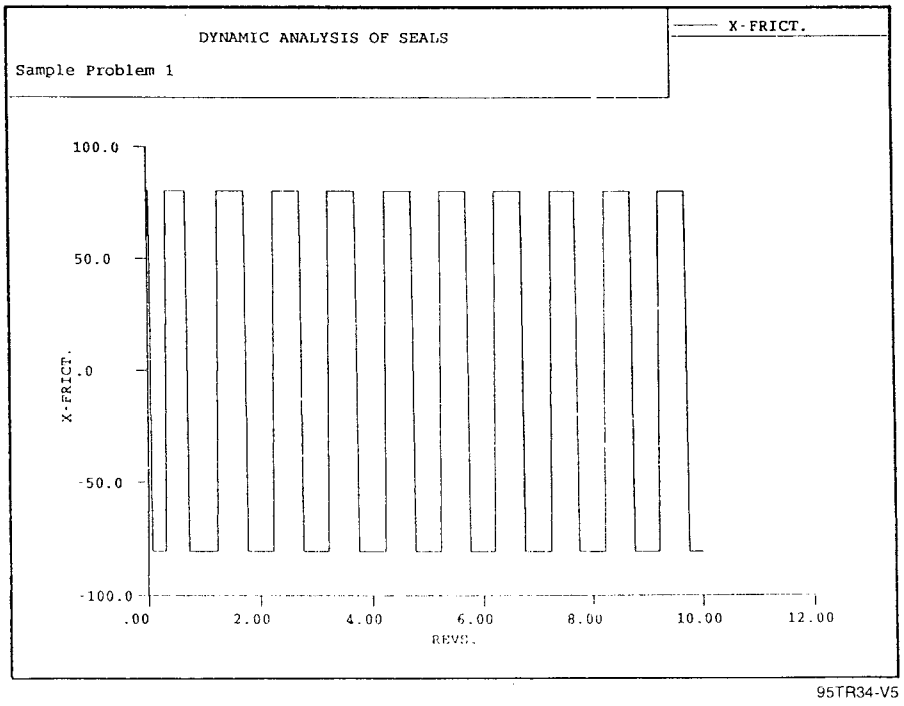

Figure 22. x Friction versus Shaft Revolutions

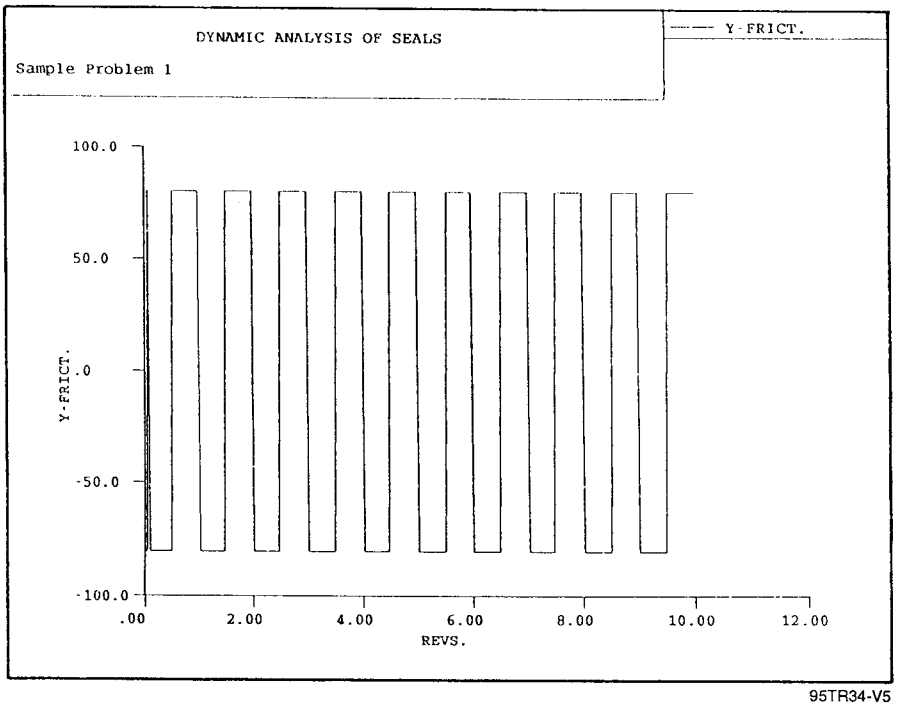

Figure 23. y Friction versus Shaft Revolutions

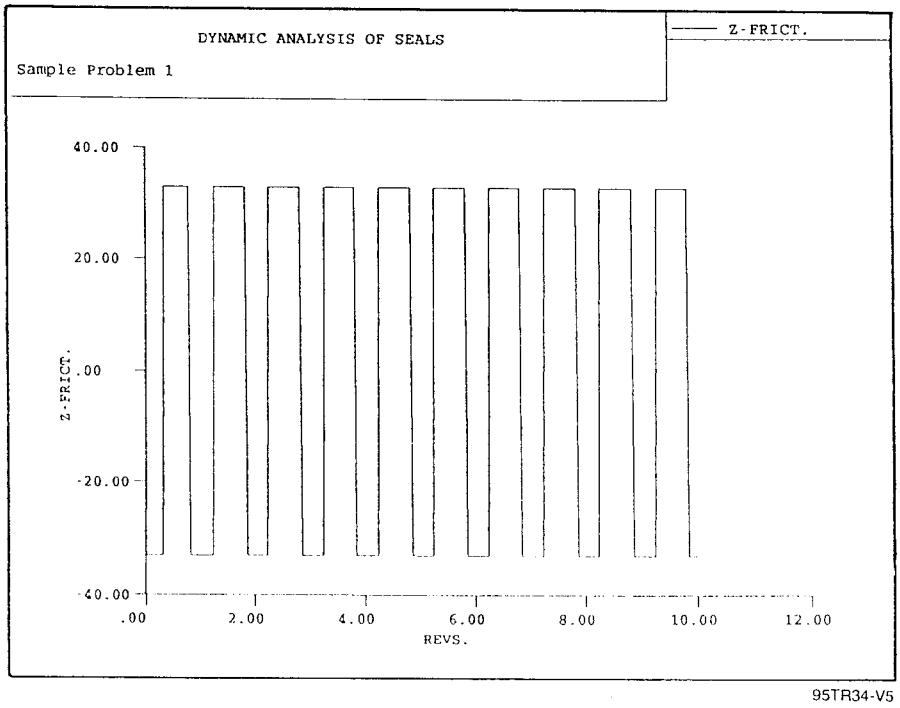

Figure 24. z Friction versus Shaft Revolutions

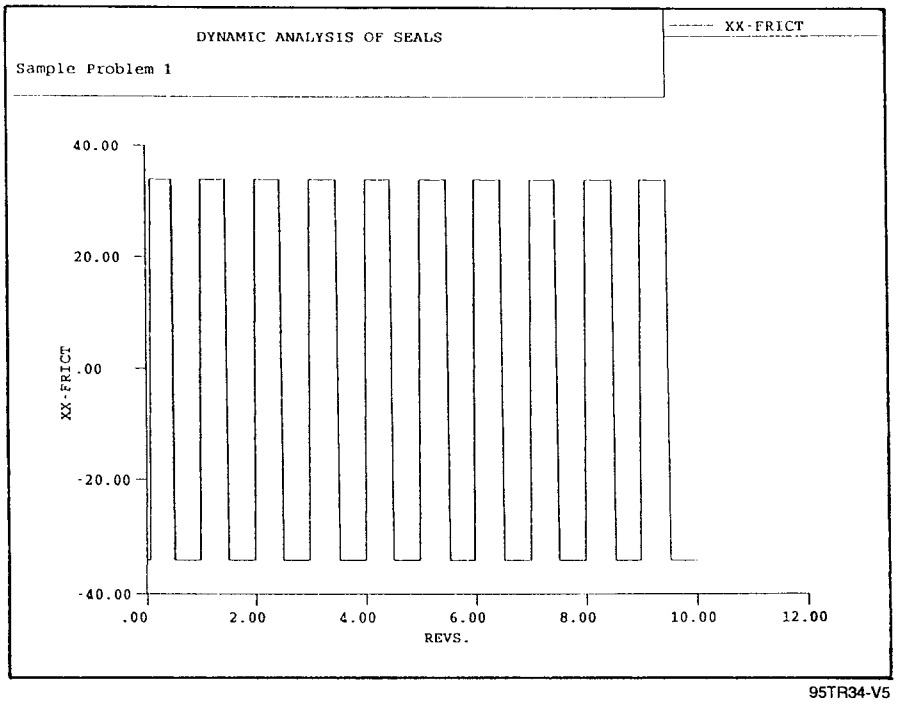

Figure 25. Friction Moment About x Axis versus Shaft Revolutions

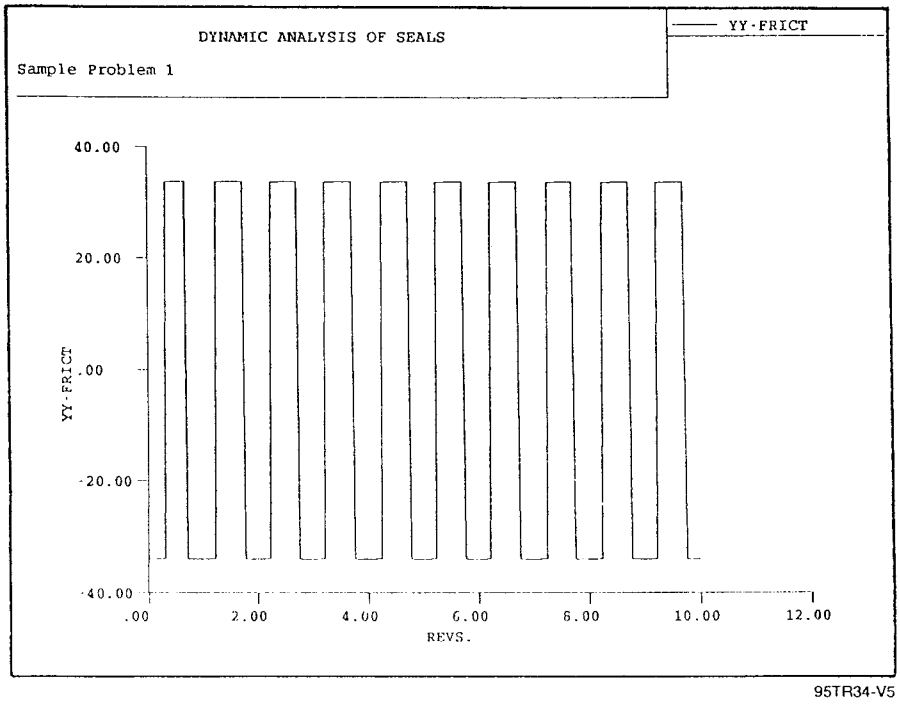

Figure 26. Friction Moment About y Axis versus Shaft Revolutions

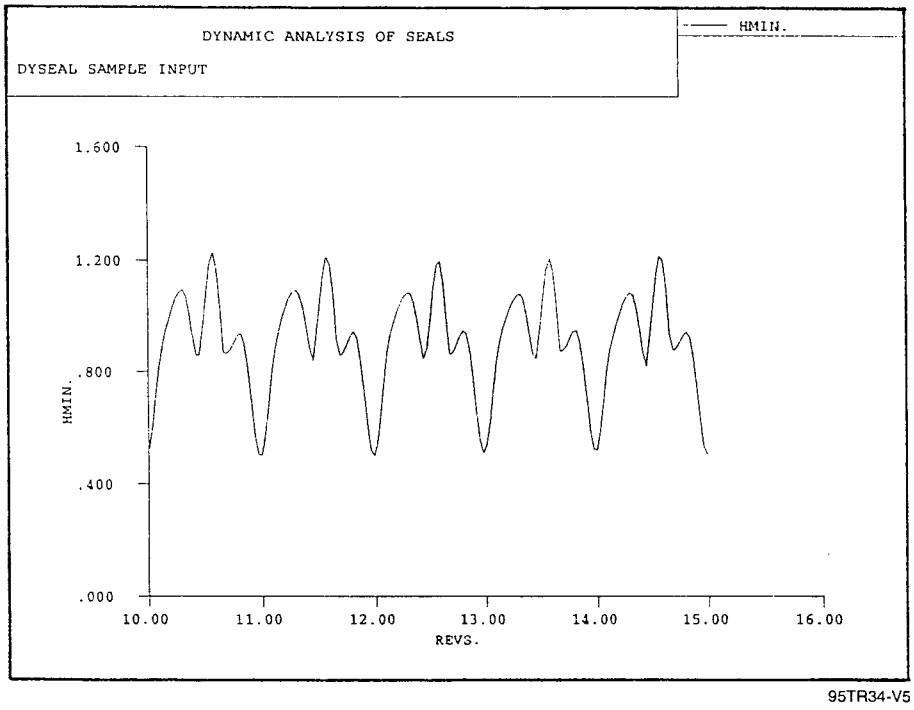

Figure 27. Sample Problem 2 Minimum Film Thickness versus Shaft Revolutions

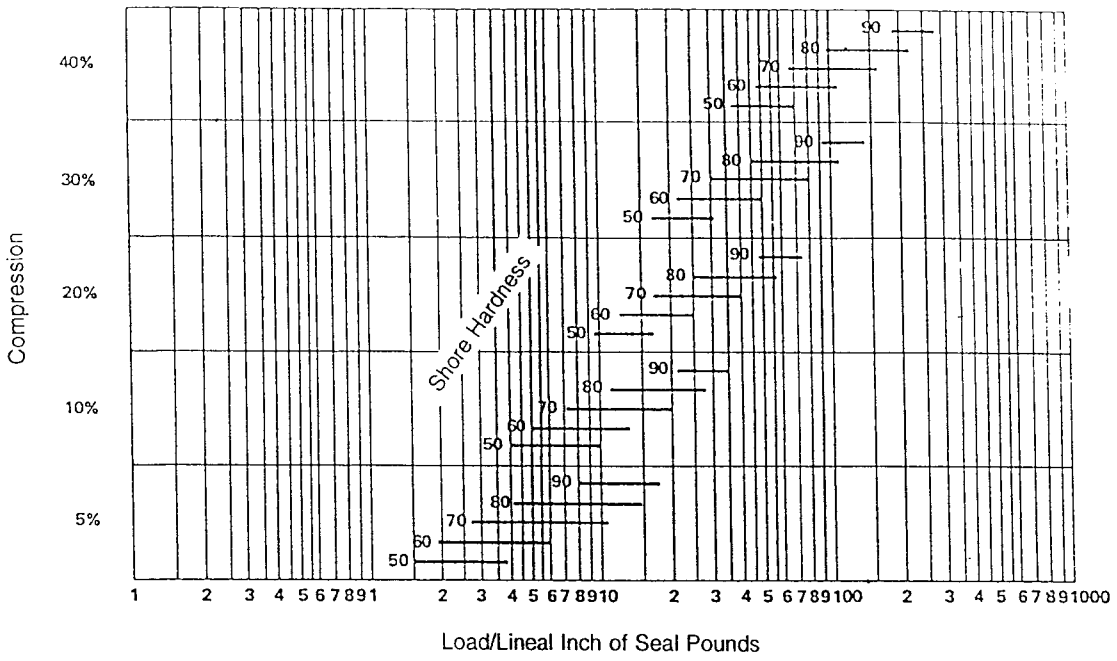

a) **0.210-in. Cross Section**

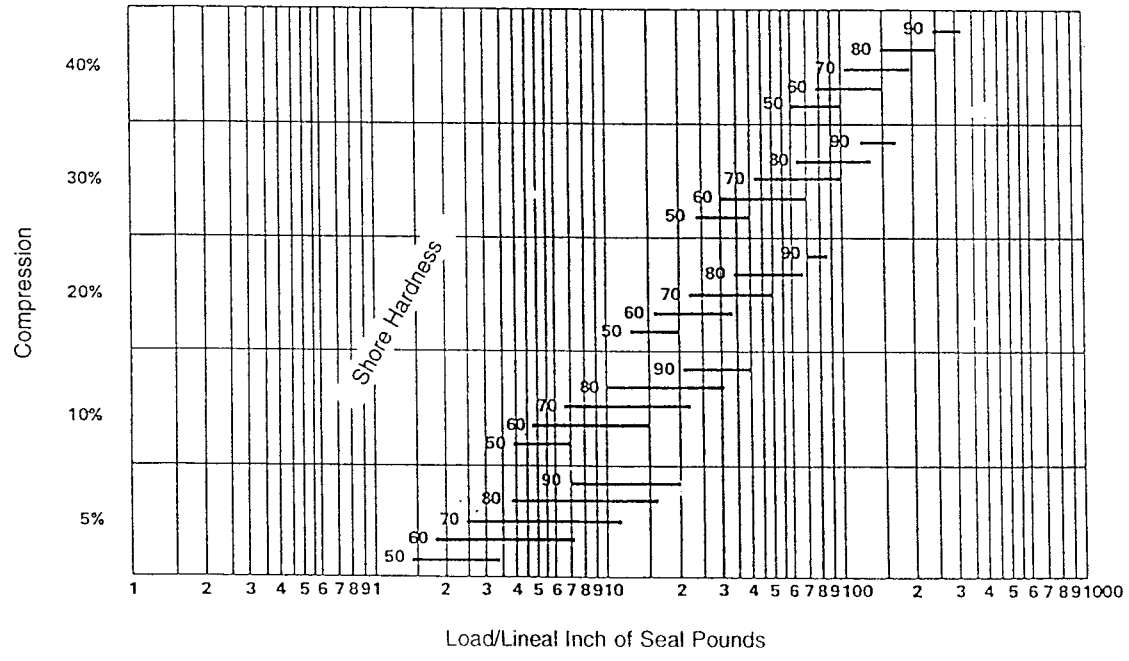

b) **0.275-in. Cross Section**

95TR34-V5

Figure 28. Typical O-Ring Data for Computing Stiffness and Preload Per Unit Length

03/29/1995 23:54 Filename: ORING.INP Page 1

```
ORING
DYSEAL O-RING SAMPLE PROBLEM
*
HELP
*GEOMETRY
ORING
ZSCO          0.712
ROS           1.58
RIS           1.24
RSC           1.31
RSP           1.5625
NELM          3
ZSPO          0.2525
THETO         0.0
DTHET         .5236
RIEL(20)       1.025  1.025  1.025
ROEL(20)       1.580  1.780  1.220
ELEML(20)      .0925  .1600  .6125
DENS(20)       .250   .250   .250
ZL(20)        0.0 .0925  .2525
*SPRING AND DAMPING
SPPRE         .150
NOSP          12
SKZZ          421000.
SKZA          0.0
SKZB          0.0
SKBZ          0.0
SKBB          361239.
*SKBA         0.0
*SKAZ         0.0
*SKAB         0.0
SKAA          361239.
DZZ             0.0
DZB             0.0
DZA             0.0
DBZ             0.0
DBB             0.0
DBA             0.0
DAZ             0.0
DAB             0.0
DAA             0.0
SPRST         5.050
SKEL          10.
SCPREL        10.
DEL           0.243
HO            .00117
FFL           2375.0
*OPERATING CONDITIONS
OMEGA         7330.
POO           750.
PID           0.0
COFSC            .2
VISC          1.7E-08
DT          8.571876E-06
NTS           1000
NT               1
*INITIAL CONDITIONS
XO                .0005
YO                .0005
ZO                .0005
AO                .0005
BO                .0005
OMEGAX        7330.
OMEGAY        7330.
OMEGAZ        7330.
TINIT            0.0
```

03/29/1995 23:54 Filename: ORING.INP Page 2

```
OMEGAB        7330.
OMEGAA        7330.
END
```

95TR34-V5

Figure 29. O-Ring Sample Problem Input

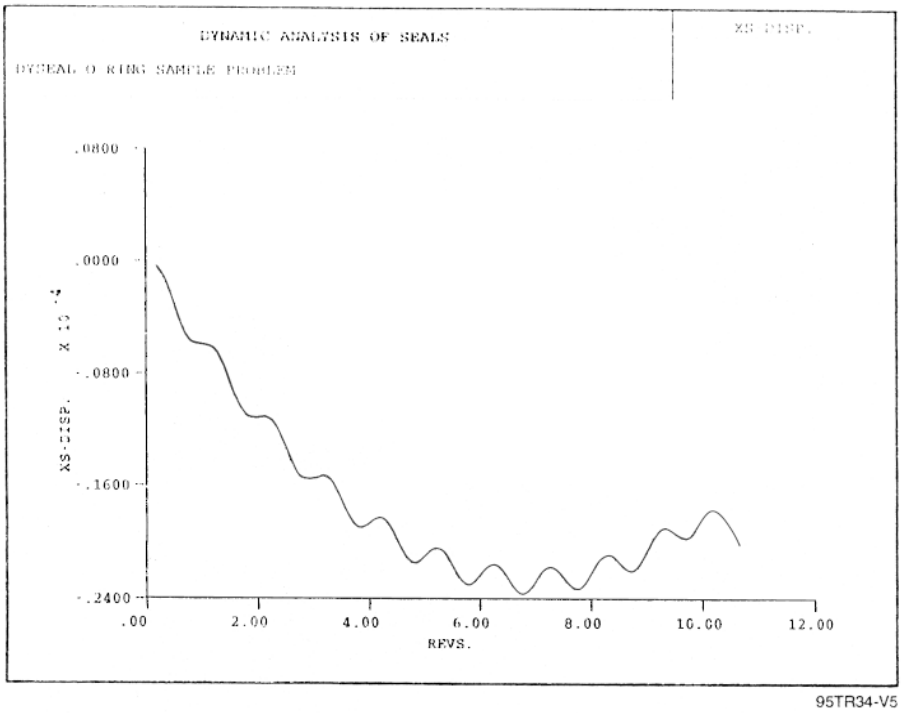

Figure 30. O-Ring Sample Problem x Displacement versus Shaft Revolutions

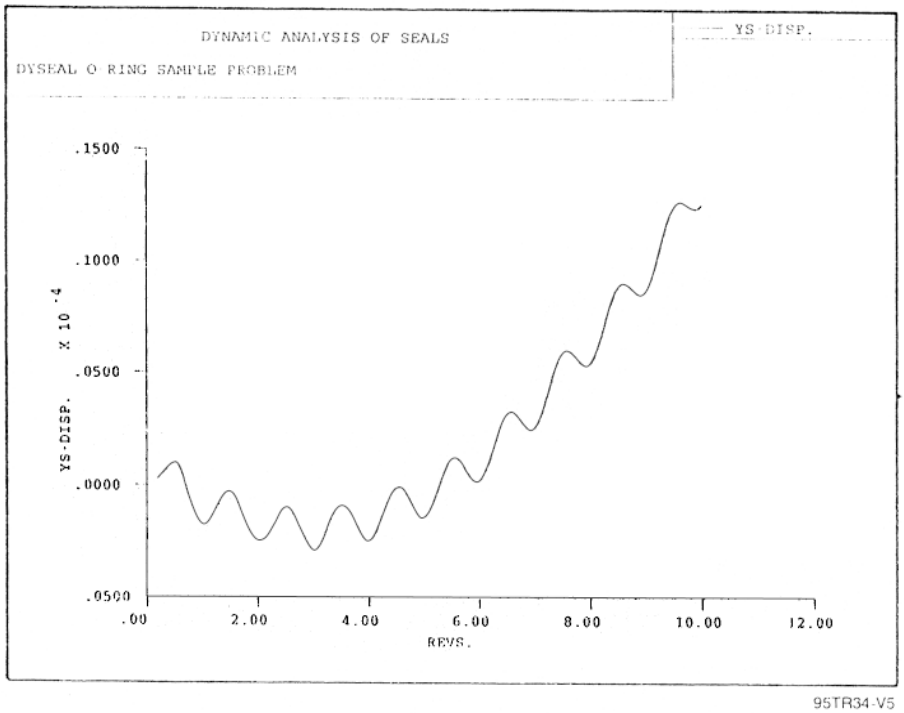

Figure 31. O-Ring Sample Problem y Displacement versus Shaft Revolutions

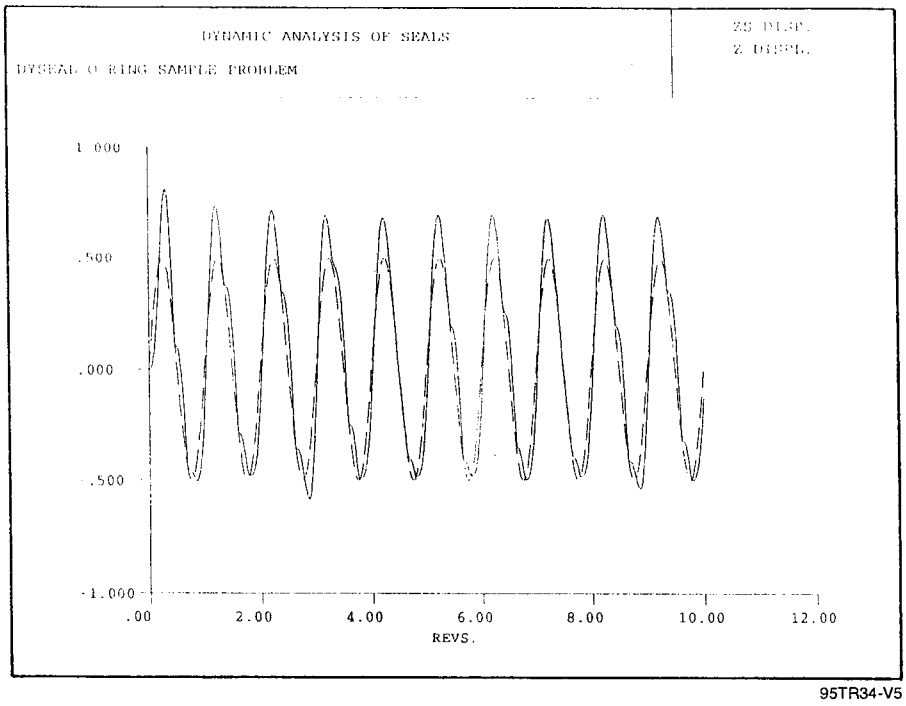

Figure 32. O-Ring Sample Problem Axial Displacement versus Shaft Revolutions

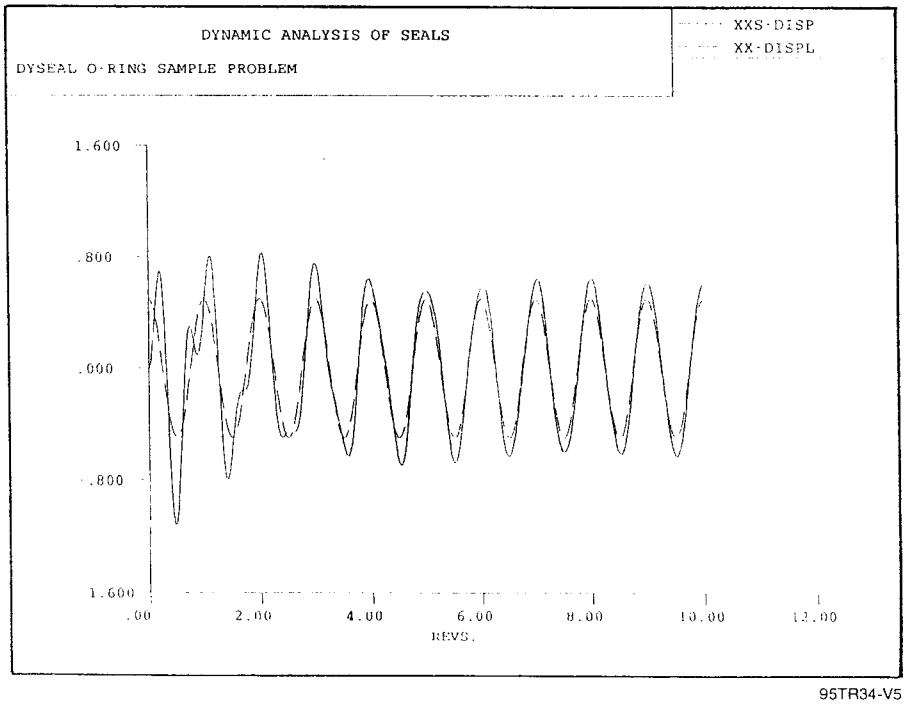

Figure 33. O-Ring Sample Problem Rotation About x Axis versus Shaft Revolutions

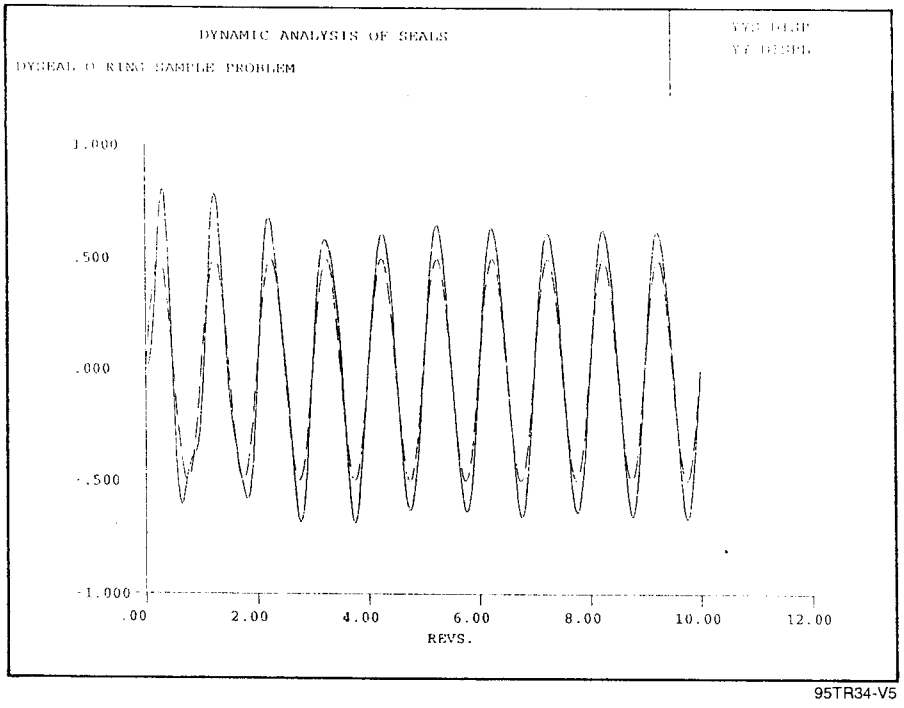

Figure 34. O-Ring Sample Problem Rotation About y Axis versus Shaft Revolutions

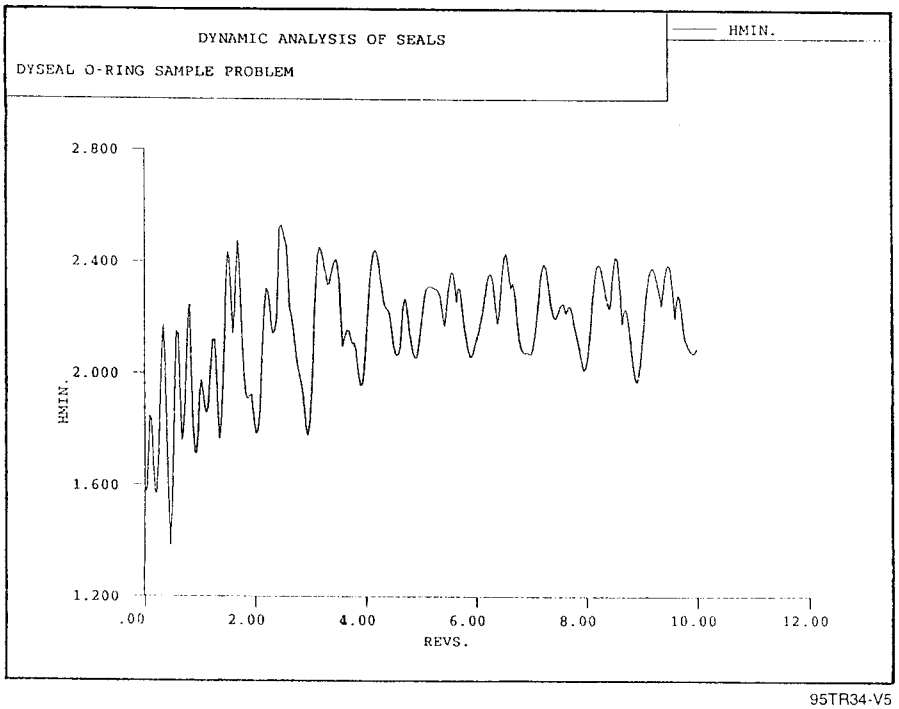

Figure 35. O-Ring Sample Problem Minimum Film Thickness versus Shaft Revolutions

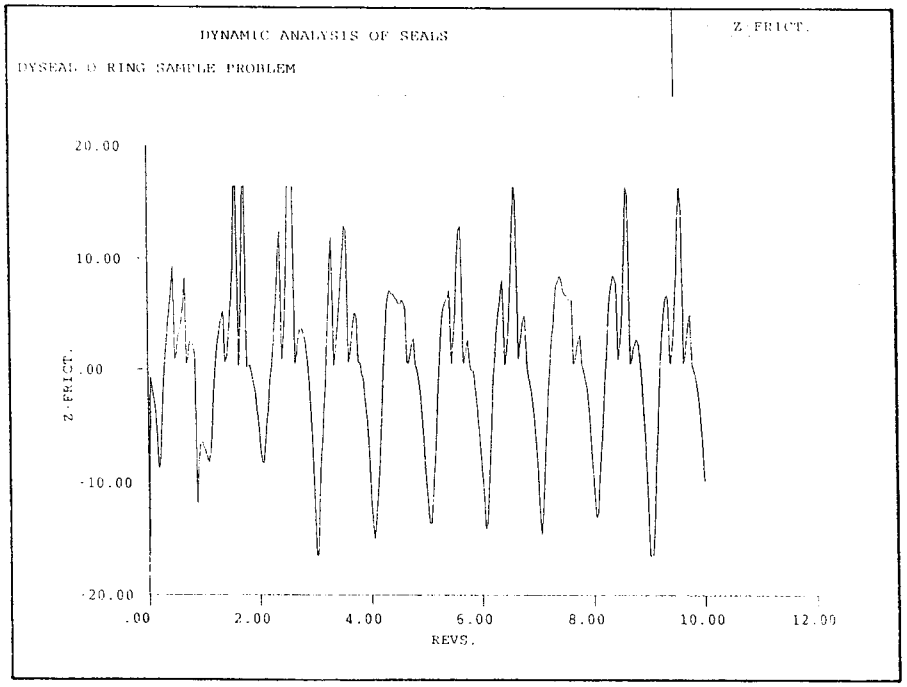

Figure 36. O-Ring Sample Problem Axial Friction versus Shaft Revolutions

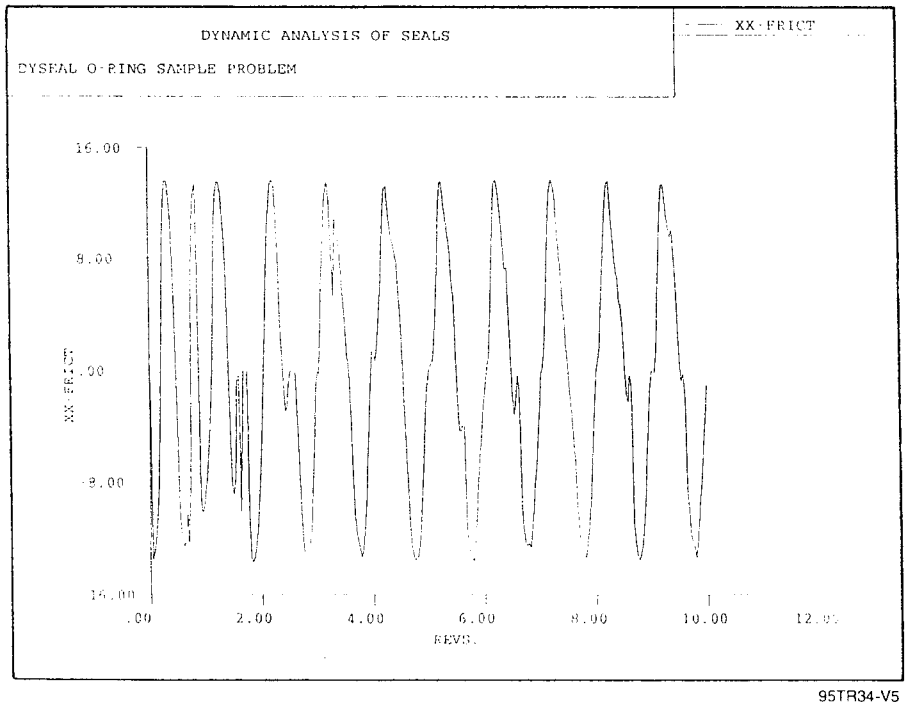

Figure 37. O-Ring Sample Problem Rotational Friction About x Axis versus Shaft Revolutions

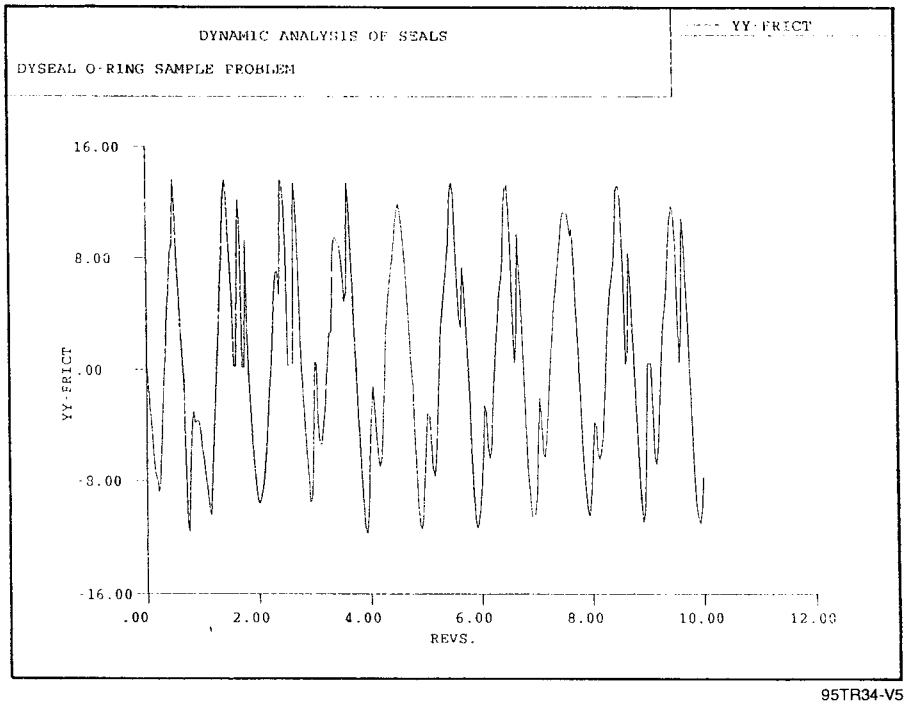

Figure 38. O-Ring Sample Problem Rotational Friction About y Axis versus Shaft Revolutions

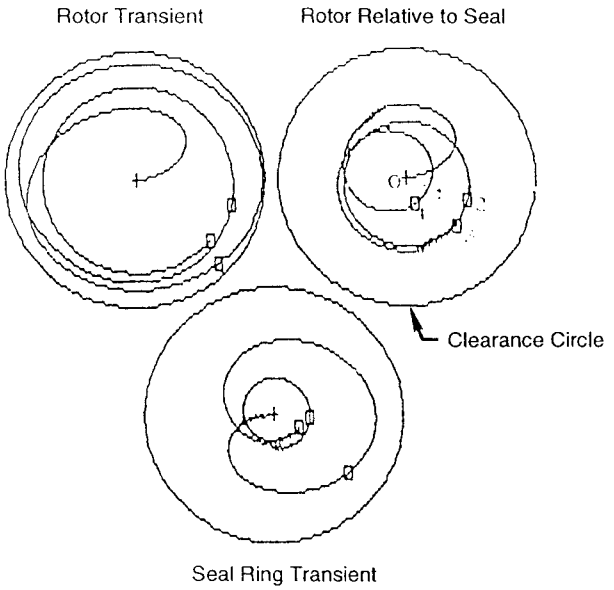

814.0		86.1	
WJ	= 200.00	N	= 1780.0
H/V	= 0.00	EMU	= 0.800
WSR	= 2.13	RJ	= 2.090
CR	= 0.0030	L	= 0.904
Viscosity	= 0.8125E-07	Mu-F	= 0.150
F-A	= 20.9000	P-L	= 60.00
P-H	= 72.00	TMAX	= 6.280
P-C	= -14.70	TH-N	= 36
H	= 0.03140		
NZ	= 6		

WJ	=	Modal mass of rotor shaft (lb_m)
N	=	Rotor shaft speed (rpm)
H/V	=	Horizontal or vertical indicator (1 ≡ horizontal; 0 ≡ vertical)
EMU	=	Rotor shaft modal mass eccentricity relative to seal clearance (DIM)
WSR	=	Seal ring mass (lb_m)
RJ	=	Seal journal radius (in.)
CR	=	Seal radial clearance (in.)
L	=	Seal axial length (in.)
Viscosity	=	Absolute viscosity of sealing fluid (lb-sec/in.^{2})
Mu-F	=	Face friction factor (DIM)
P-H	=	Seal high pressure (lb/in.^{2})
P-L	=	Seal low pressure (lb/in.^{2})
P-C	=	Seal liquid cavitation pressure (lb/in.^{2})
H	=	Time step for transient simulation (rad)
TMAX	=	Maximum time for each segment of response (rad)
NZ	=	Axial grid points for pressure profile
TH-N	=	Pressure profile grid points around circumference of seal

95TR34-V5

Figure 39. Pump Seal Transient with Three Cycles of Motion Showing Seal Tracking Rotor at 0.5 Eccentricity (N = 1780 rpm = 29.7 Hz)

03/30/1995 00:03 Filename: KIRK7.INP Page 1

```
KIRK7
CHECK AGAINST G. KIRKS RESULTS, FIG.7
*
*HELP
*GEOMETRY
RING
EMOD          30E06
ROS           2.112
RIS           2.090
RSC           2.090
RSP           2.3
NELM          2
ZSPO          0.904
THETO         0.0
DTHET         0.0
RIEL(20)      2.090 2.090
ROEL(20)      2.112 2.647
ELEML(20)     .125 .779
DENS(20)      0.328 0.328
ZL(20)         0.0 .125
*SPRING AND DAMPING
SPPRE        0.
NOSP         0.
SKXX         0.
SKXY         4157.
SKYX        -2356.
SKYY         0.
DXX          25.6
DXY          0.
DYX          0.
DYY          45.4
CO            0.003
HO            0.0
FFL           0.0
*OPERATING CONDITIONS
OMEGA        186.4
POO          72.
PID          60.
COFSC          0.075
VISC          0.8125E-07
DT            3.3708E-04
NTS           1000
NT               1
*INITIAL CONDITIONS
XO                .0024
YO                .0024
ZO                .000
AO                .00000
BO                .00000
OMEGAX       186.4
OMEGAY       186.4
OMEGAZ       0.
TINIT        0.0
END
```

95TR34-V5

Figure 40. Kirk's Figure 7 DYSEAL Input (mil)

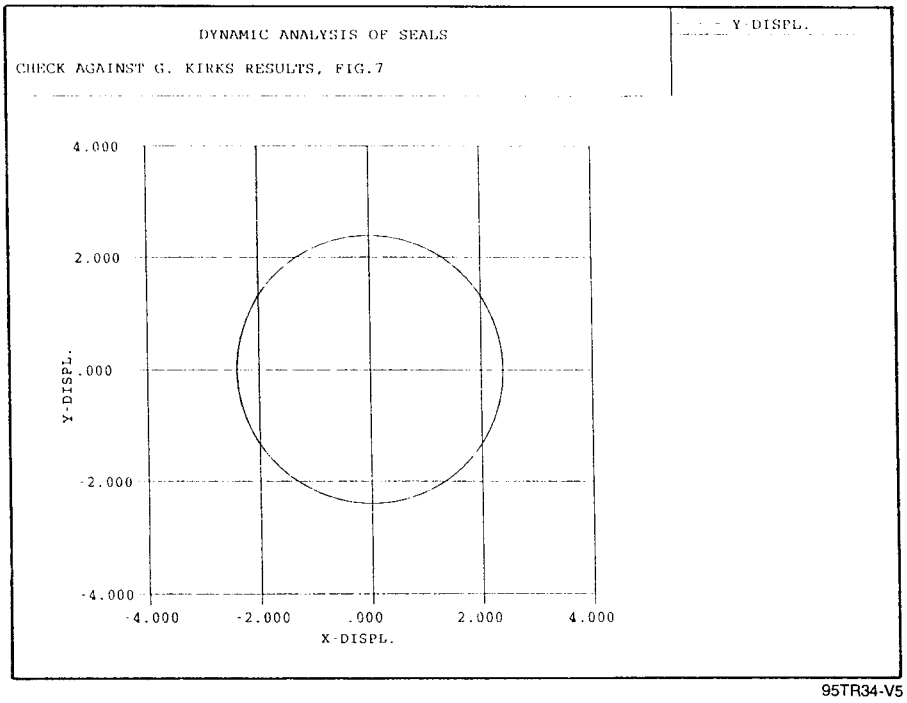

Figure 41. Kirk's Figure 7 Rotor Orbit (mil)

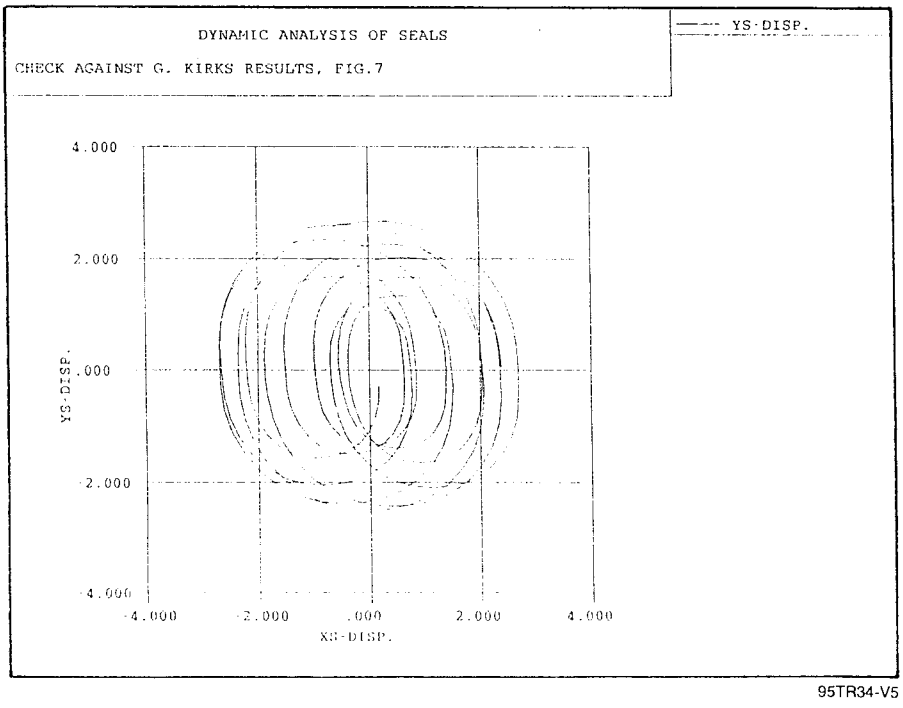

Figure 42. Kirk's Figure 7 DYSEAL Seal Ring Orbit (mil)

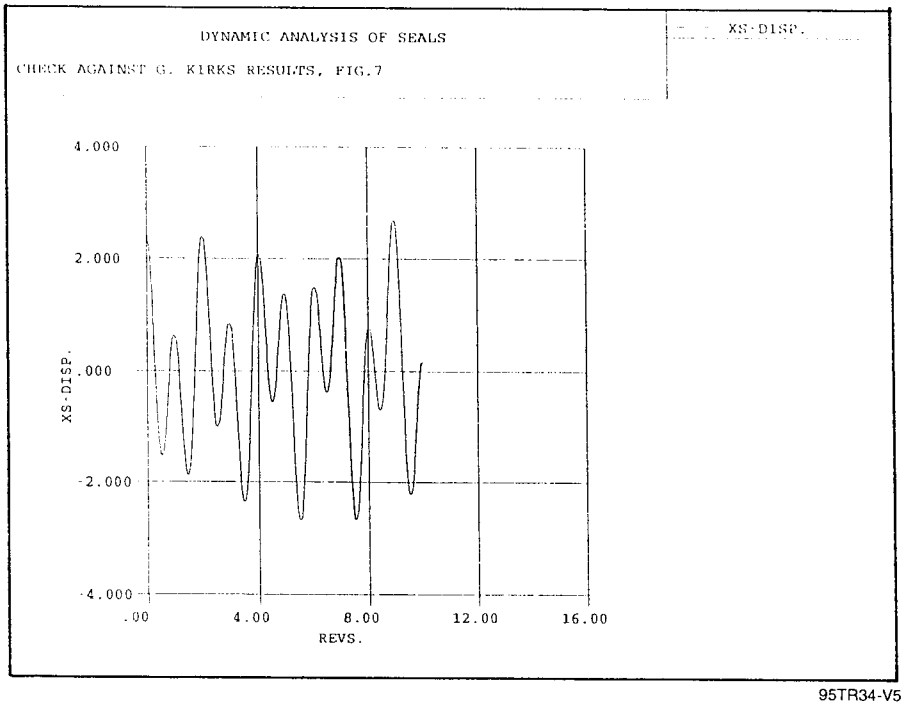

Figure 43. Kirk's Figure 7 DYSEAL x Displacement (mil)

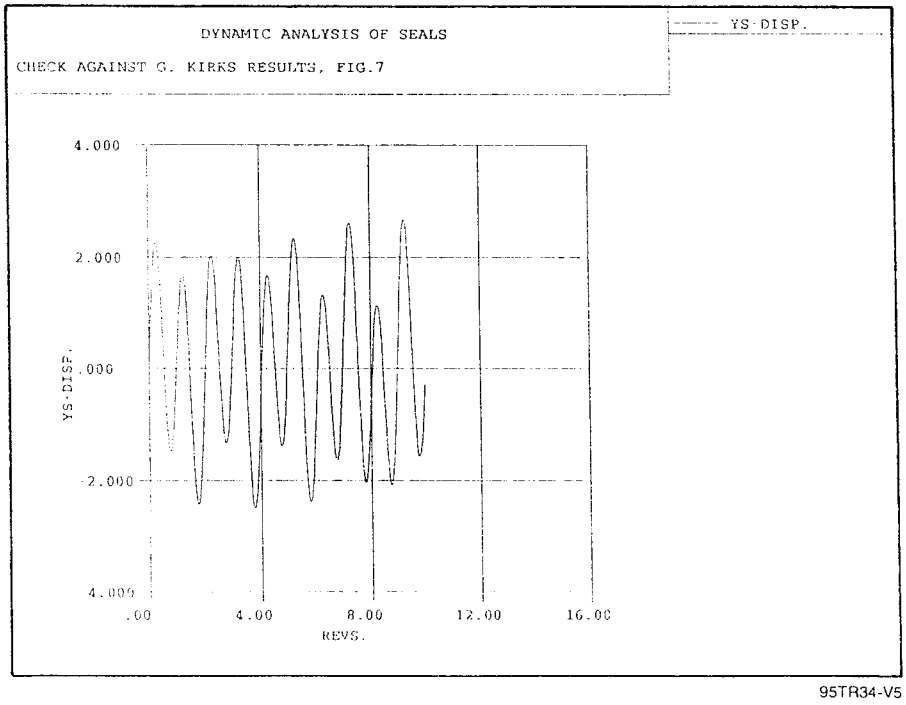

Figure 44. Kirk's Figure 7 DYSEAL y Displacement (mil)

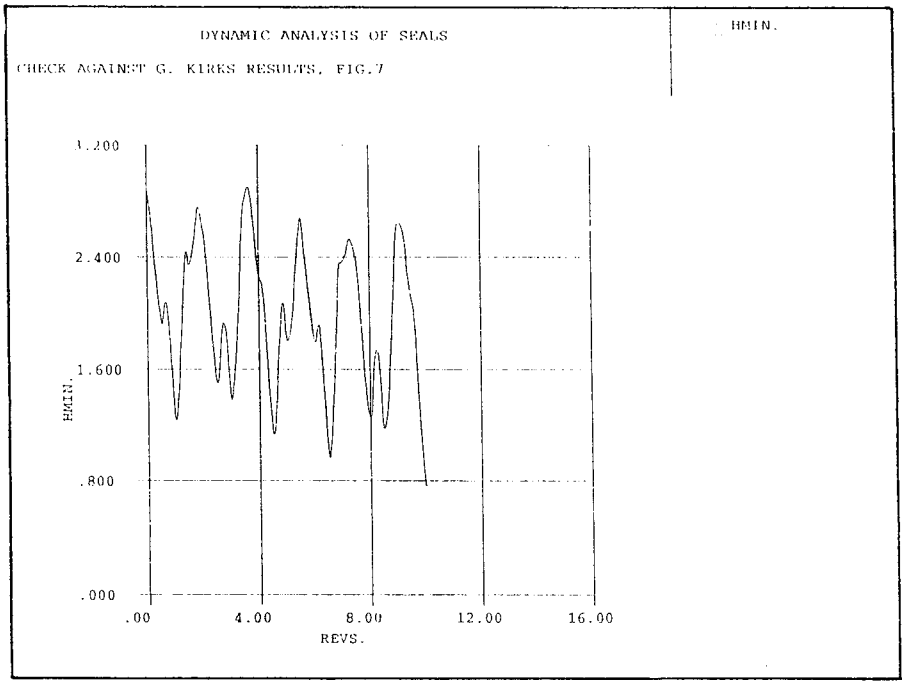

Figure 45. Kirk's Figure 7 DYSEAL Minimum Film Thickness (mil)

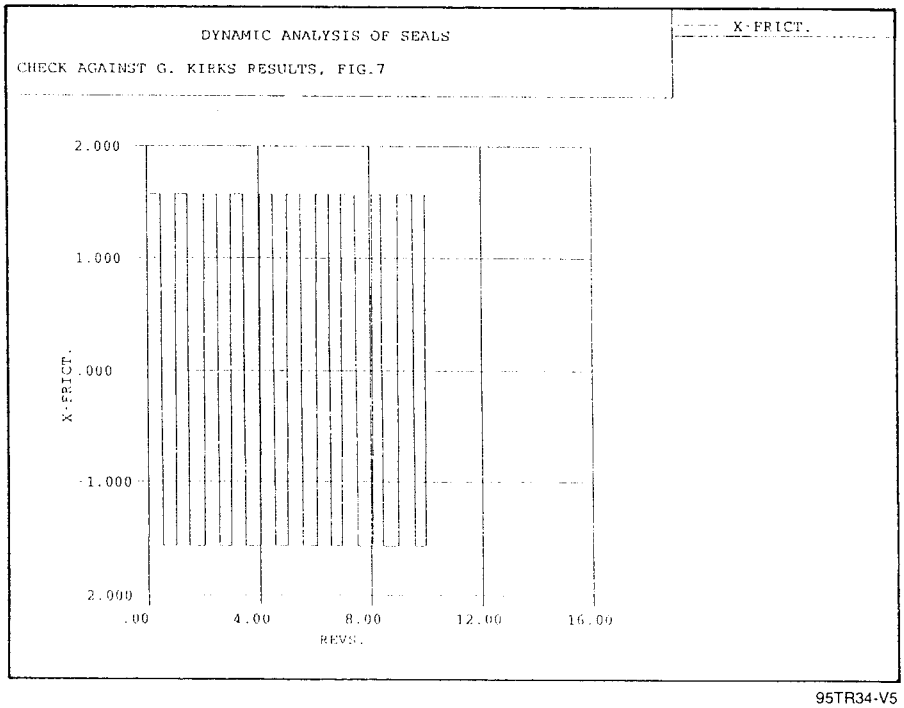

Figure 46. Kirk's Figure 7 DYSEAL x Friction (lb)

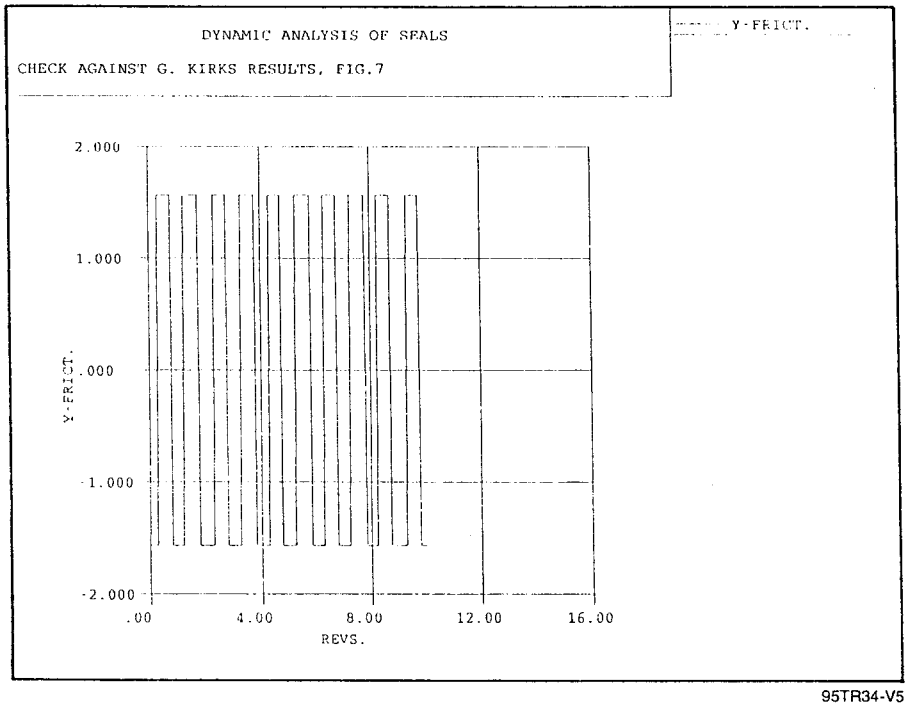

Figure 47. Kirk's Figure 7 DYSEAL y Friction (lb)

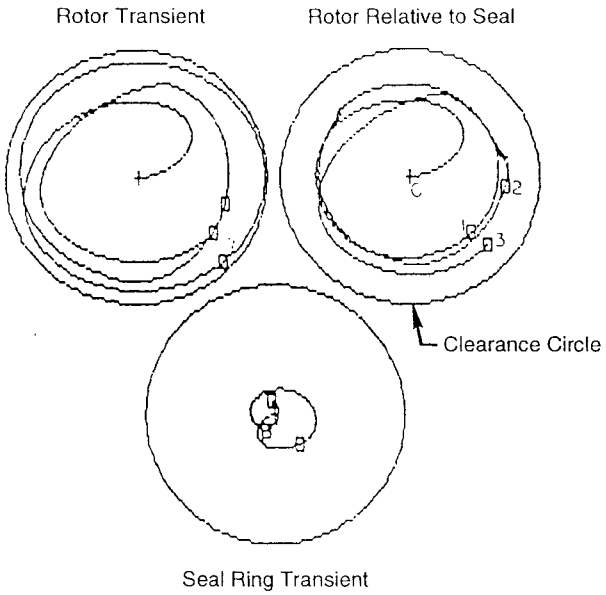

814.0		86.1	
WJ	= 200.00	N	= 1780.0
H/V	= 0.00	EMU	= 0.800
WSR	= 2.13	RJ	= 2.090
CR	= 0.0030	L	= 0.600
Viscosity	= 0.8125E-07	Mu-F	= 0.150
F-A	= 20.9000	P-L	= 60.00
P-H	= 72.00	TMAX	= 6.280
P-C	= -14.70	TH-N	= 36
H	= 0.03140		
NZ	= 6		

WJ	=	Modal mass of rotor shaft (lb_m)
N	=	Rotor shaft speed (rpm)
H/V	=	Horizontal or vertical indicator (1 ≡ horizontal; 0 ≡ vertical)
EMU	=	Rotor shaft modal mass eccentricity relative to seal clearance (DIM)
WSR	=	Seal ring mass (lb_m)
RJ	=	Seal journal radius (in.)
CR	=	Seal radial clearance (in.)
L	=	Seal axial length (in.)
Viscosity	=	Absolute viscosity of sealing fluid (lb-sec/in.^{2})
Mu-F	=	Face friction factor (DIM)
P-H	=	Seal high pressure (lb/in.^{2})
P-L	=	Seal low pressure (lb/in.^{2})
P-C	=	Seal liquid cavitation pressure (lb/in.^{2})
H	=	Time step for transient simulation (rad)
TMAX	=	Maximum time for each segment of response (rad)
NZ	=	Axial grid points for pressure profile
TH-N	=	Pressure profile grid points around circumference of seal

95TR34-V5

Figure 48. Pump Seal Transient for a Reduced-Length Seal Showing Seal Ring Tracking Rotor at an Eccentricity of $\varepsilon = 0.75$ *(N = 1780 rpm = 29.7 Hz)*

```
04/11/1995  15:16        Filename: KIRK8.INP                        Page   1

KIRK8
CHECK AGAINST G. KIRKS RESULTS, FIG.8
*
*HELP
*GEOMETRY
RING
EMOD          30.0E06
ROS           2.112
RIS           2.090
RSC           2.090
RSP           2.3
NELM          2
ZSPO          0.6
THETO         0.0
DTHET         0.0
RIEL(20)      2.090 2.090
ROEL(20)      2.112 2.647
ELEML(20)     .125 .475
DENS(20)      0.536 0.536
ZL(20)         0.0 .125
*SPRING AND DAMPING
SPPRE        0.
NOSP         0.
SKXX         0.0
SKXY         9068.
SKYY         0.
SKYX         -1747.
DXX          18.9
DYX          0.
DXY          0.
DYY          107.
CO             0.003
HO             0.0
FFL            0.0
*OPERATING CONDITIONS
OMEGA        186.4
POO          72.
PID          60.
COFSC          0.075
VISC         0.8125E-07
DT           3.3708E-04
* CONTINUATION 1
NTS          1000
NT           1
*INITIAL CONDITIONS
XO                .0024
YO                .0024
ZO                .000
AO                .00000
BO                .00000
OMEGAX       186.4
OMEGAY       186.4
OMEGAZ       0.
TINIT        0.0
END
                              95TR34-V5
```

Figure 49. Kirk's Figure 8 DYSEAL Input

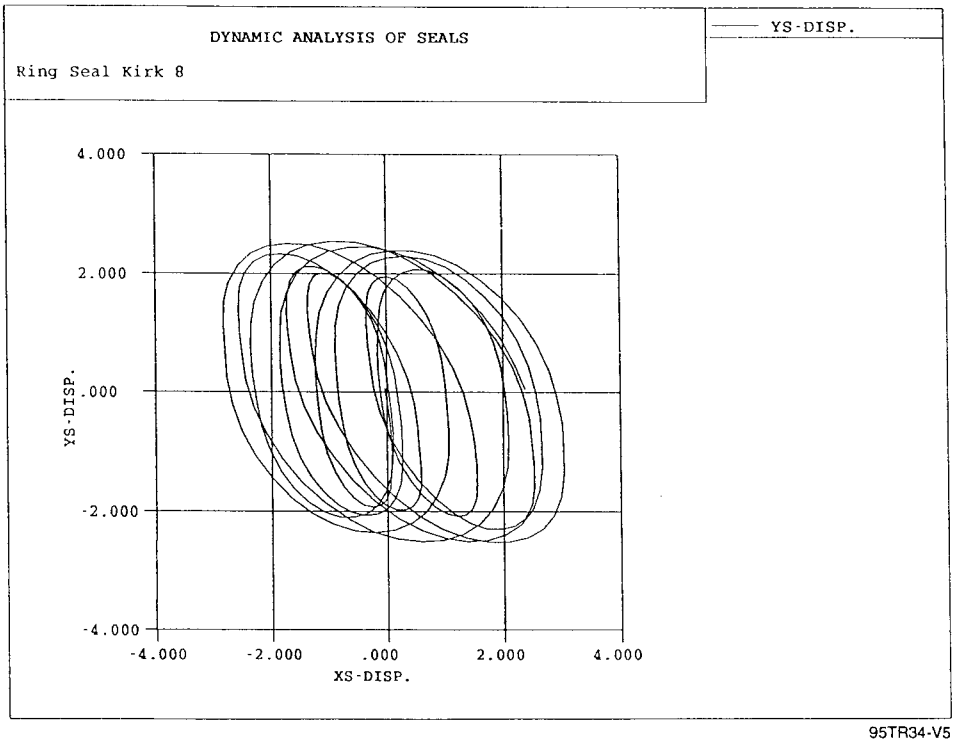

Figure 50. Kirk's Figure 8 DYSEAL Seal Ring Orbit (mil)

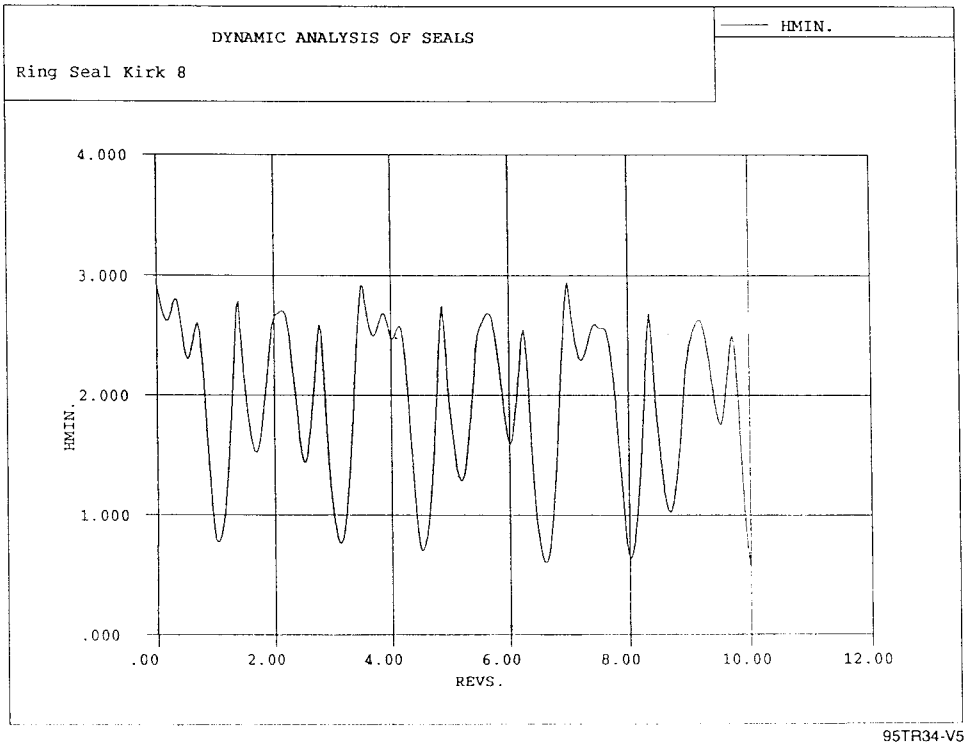

Figure 51. Kirk's Figure 8 DYSEAL Minimum Film Thickness (mil)

4.0 VERIFICATION FOR CODE DYSEAL

Several methods of verification were accomplished. Internal checks were made against closed-form solutions. Some mass, spring, and damper vibration problems were examined and compared against closed-form solutions. Also, comparisons were made against experimental data available in the literature. Ring seal verification was presented in the preceding section.

4.1 Internal Checks

An example of internal checks of the code was evaluation of spring forces and moments. The numerical approach used in the code can be compared against a closed-form solution. For the ith spring, the moment is

$$\overline{M}_s^i = \overline{r}_{sp}^i \times \overline{F}_s^i = \left(z_{sp} - z_{cg}\right)\hat{k} + \left(R_{sp}\cos\theta_i \hat{i} + R_{sp}\sin\theta_i \hat{j}\right) \times \left(-k_s z_i \hat{k}\right) \tag{4.1}$$

where:

$\overline{M}_s^i$ = moment from ith spring located at θ_i
$\overline{F}_s^i$ = force from ith spring
z_{sp} = z distance to ith spring
R_{sp} = spring radius
θ_i = angular coordinate to ith spring
z_i = displacement of ith spring in z direction
z_{cg} = z distance to CG

The seal ring motion in the z direction, z_i, is given by

$$z_i = z_s + R_{sp}\left(\beta_s \sin\theta_i - \alpha_s \cos\theta_i\right) \tag{4.2}$$

where the variables have been previously defined.

After substituting Equation (4.2) into Equation (4.1), expanding and summing over all springs, the following equation results:

$$\begin{aligned}\overline{M}_s = &\left(R_{sp}k_s z_s \sum\cos\theta_i + R_{sp}^2 k_s \beta_s \sum\sin\theta_i \cos\theta_i - R_{sp}^2 k_s \alpha_s \sum\cos^2\theta_i\right)\hat{j} \\ &-\left(R_{sp}^2 k_s z_s \sum\sin\theta_i + R_{sp}^2 k_s \beta_s \sum\sin^2\theta_i - R_{sp}^2 k_s \alpha_s \sum\sin\theta_i \cos\theta_i\right)\hat{i}\end{aligned} \tag{4.3}$$

where the $\hat{j}$ component equals the moment about the y axis and the $\hat{i}$ component equals the moment about the x axis.

Consider six springs with the first spring starting at an angle of 10°. The summation coefficients are indicated on Table 3.

Table 3. Summation Coefficients

K_{sp} = 2; N_{sp} = 6; k = 100 lb/in.

θ	sinθ	cosθ	sinθ cosθ	$\sin^2$	$\cos^2$
10	0.1736	0.9848		0.0301	0.9698
70	0.9397	0.342		0.883	0.117
130	0.7660	-0.6428		0.5866	0.4132
190	-0.1736	-0.9848		-0.301	0.9698
250	-0.9397	-0.342		0.883	0.117
310	-0.7660	0.64281		0.5868	0.4132
Σ	0	0	0	3.0	3.0

95TR34-V5

Referring to Equation (4.3),

$$K_{x\alpha} = R_{sp} k_s \sum \cos\theta = 0$$

$$K_{\beta\alpha} = R_{sp}^2 k_s \sum \sin\theta\cos\theta = 0$$

$$K_{\alpha\alpha} = R_{sp}^2 k_s \sum \cos^2\theta = 2^2(100)(3) = 1200 \text{ lb / in.}$$

Similarly,

$$K_{z\beta} = K_{\alpha\beta} = 0, K_{\beta\beta} = 1200$$

Also, the axial stiffness = 6 × 100 = 600 lb/in. The spring stiffness matrix as computed by the program is as follows:

paste up little table here

This checks precisely with the closed-form solutions. Similar results were obtained for varying the number of springs and the independent stiffness values.

4.2 Mass, Spring, Damper Vibrations

Several mass, spring, and damper vibration problems can be used to check out portions of the code. First, consider a forced vibration problem, as depicted in Figure 52. The base represents the shaft; the mass represents the seal ring. The base is the source of excitation, and the response of the seal ring or mass, M, is desired. The initial parameters tested were:

k = 10,000 lb/in.
ℓ = 10 lb-sec/in.
M = 10 lb = 10/386.4 = 0.02588 lb-sec²/in.
X = 0.002 in.
ω = 1000 rad/sec
C = 10 lb-sec/in.

As derived from Thomson [7], the maximum relative displacement, Z, (= y - x) is given by

$$Z = \frac{m\omega^2 X}{\sqrt{\left(k - m\omega^2\right)^2 + (C\omega)^2}} = \frac{(0.02588)(1000)^2(0.002)}{\sqrt{\left(10,000 - 0.0259(1000)^2\right)^2 + \left(10(1000)\right)^2}} \qquad (4.4)$$

$$= 0.002758 \text{ in.} = 2.758 \text{ mil}$$

Z represents the maximum difference between the amplitude of the mass, y, and the excitation, X. As shown on the computer output graph (Figure 53), the measured difference equals 2.74 mil. The phase angle as a function of frequency and damping is shown on Figure 54.

$$\frac{\omega}{\omega_n} = \frac{\omega}{\sqrt{\frac{k}{m}}} = \frac{1000}{\sqrt{\frac{10{,}000}{0.0258}}} = 1.6 \tag{4.5}$$

$$\rho = \frac{C}{C_c} = \frac{C}{2m\omega_n} = \frac{10}{2(0.02588)(622)} = 0.3106 \tag{4.5}$$

From Figure 54, the phase angle, ϕ, is approximately 135°. The computed value is estimated to be 136° as measured from the output curves of Figure 53. Considering graphical interpretations, the corroboration is excellent. Similar results were obtained using the ring seal option of the code exciting the shaft in the x direction, as shown on Figure 55.

4.3 Verification Against Data in the Literature

Di Russso [8] did extensive dynamic testing of spiral-groove face seals. The seals were subjected to constant load rotation, with installation runout of the seal seat (rotating member) and then to constant load rotation with installation runout plus an axial excitation of 50 μm (2 mil) at 100-Hz frequency. Figure 56 schematically shows the seal seat vibrational modes. The installation misalignment of the seal seat was approximately 35 μrad about both the x and y axes. Tests were run with and without secondary seals.

Figure 57 shows response of the seal at 14,000 rpm without a secondary seal in place. The film thickness frequency is approximately 6 times synchronous for the 14,000-rpm case. The case was simulated by determining the stiffness and damping characteristics of the spiral groove and establishing the physical characteristics of the seal ring. The input for the DYSEAL run is shown in Figure 58. The minimum film thickness in mils versus shaft revolutions, computed by the code is shown in Figure 59. The 6 per rev frequency is shown in Figure 60. The results are nearly identical to the steady mode without the axial excitation. The implication is that the seal ring tracks the exciting shaft perfectly. The input for the computer studies is identical to Figure 58, except that Z0 is give a value of 0.002. Computer results of film thickness are shown in Figure 61. The film thickness shows a definite trace of the excitation frequency. A blown-up view of the film thickness is shown in Figure 62, and the six times synchronous frequency is clearly discernible. The axial displacement of the seal seat (ZS) and seal ring (Z) are shown in Figure 63. They are in unison, confirming the tracking capability of the seal as experienced on test. The variations indicated by the film thickness curves do not show in the axial mode but are indicated by the rotational response about the x and y axes. Figure 64 shows the rotational response about the x axis superimposed on the pure sinusoidal excitation. The jagged sine curve provides the differences between excitation and response. In general, the computational results agree very favorably with the experimental data.

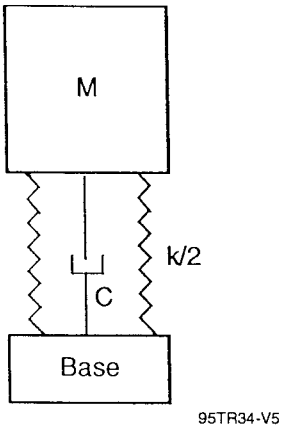

Figure 52. Mass, Spring, and Damper System

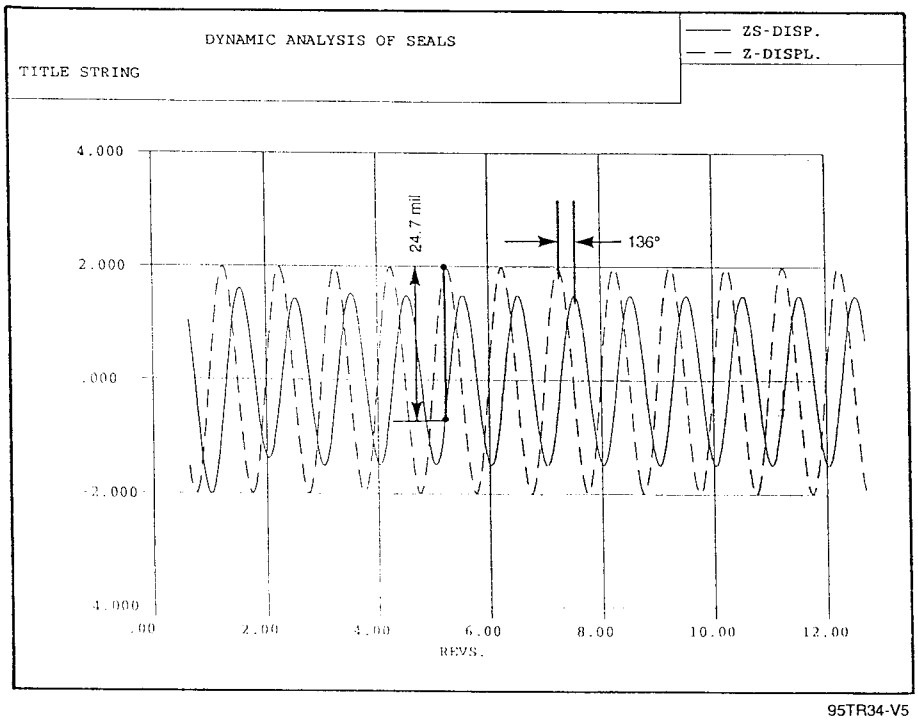

Figure 53. Single-Degree-of-Freedom Forced Vibration

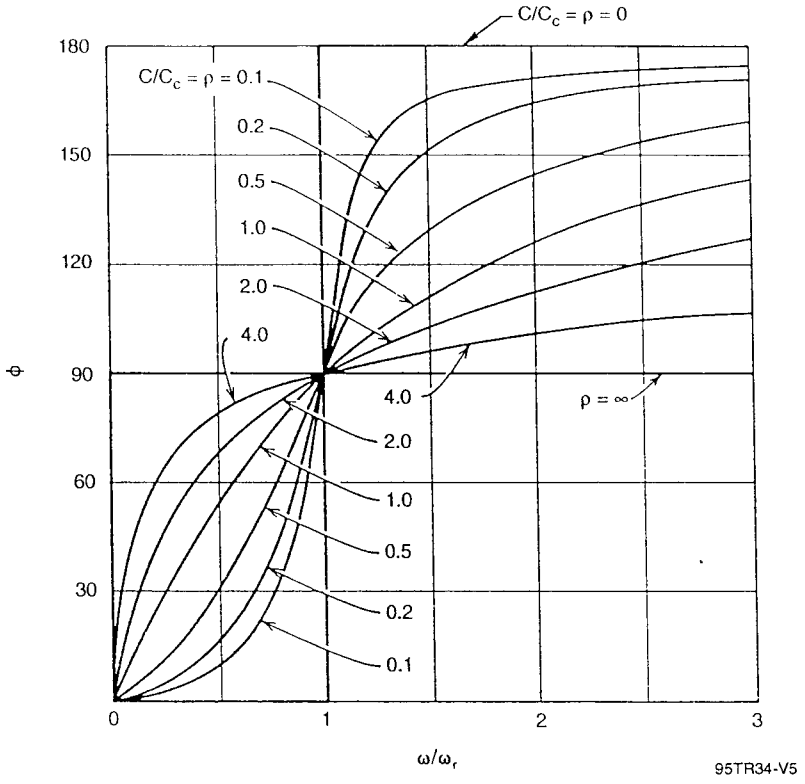

Figure 54. Phase Angle as a Function of Damping and Frequency

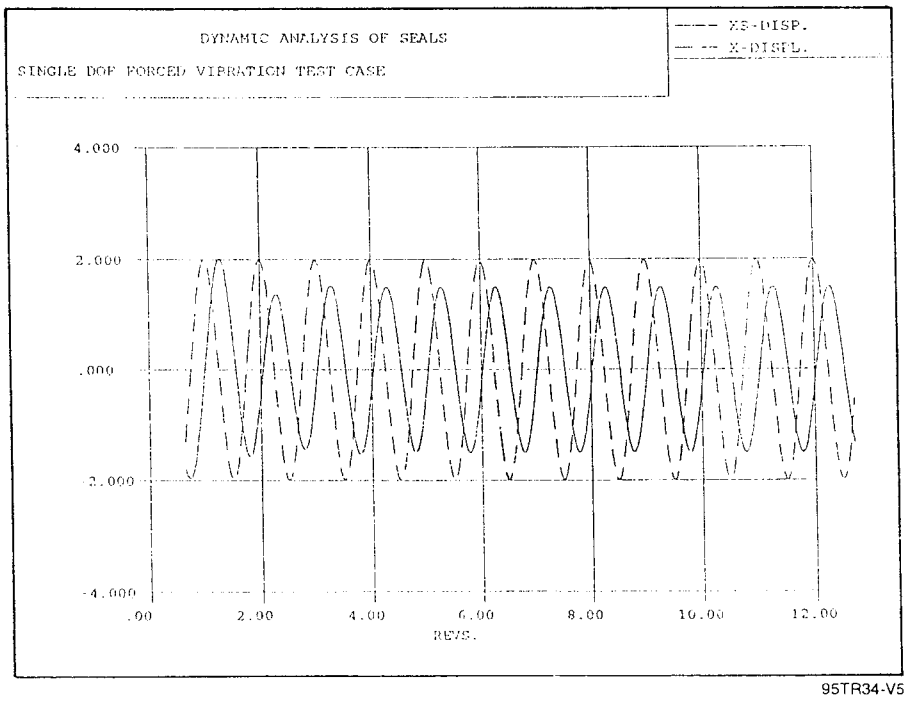

Figure 55. Ring Seal Option: Single-Degree-of-Freedom Forced Vibration Problem

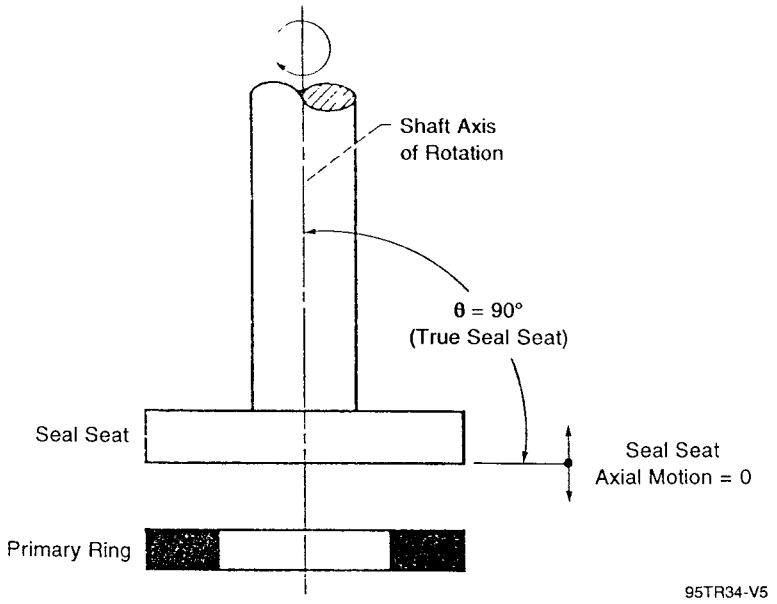

a) Steady Seal Seat Mode with True Seal Seat

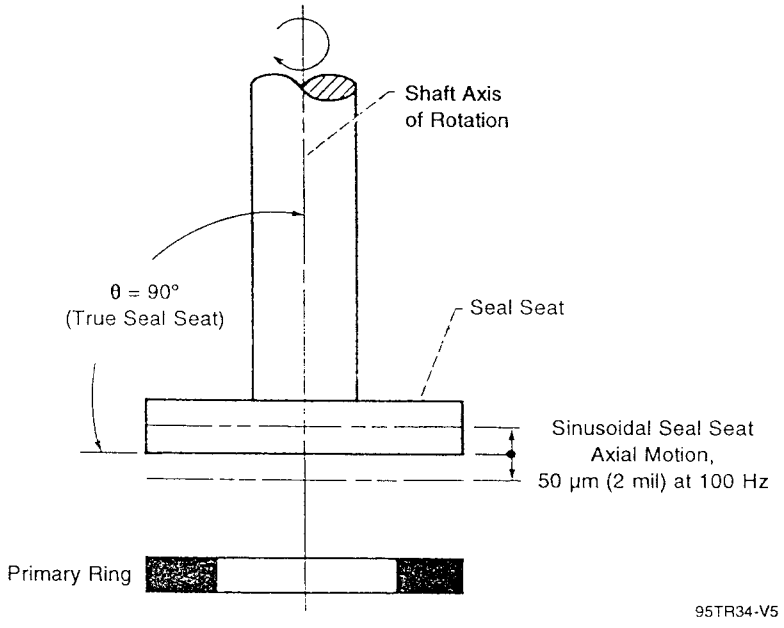

b) Sinusoidal Seal Seat Mode with True Seal Seat

Figure 56. Schematic Showing Seal Seat Vibrational Modes

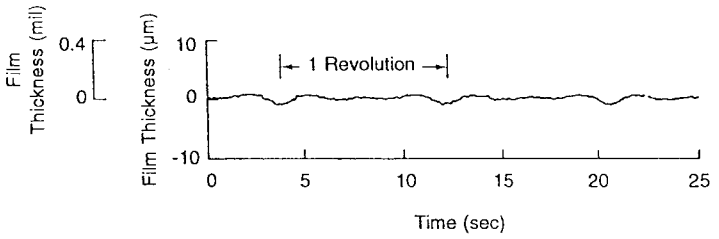

a) Shaft Speed = 7,000 rpm

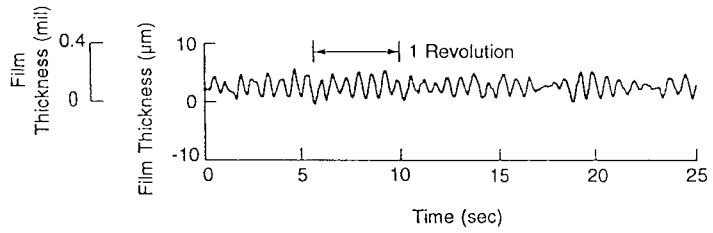

b) Shaft Speed = 14,000 rpm

95TR34-V5

Figure 57. Film Thickness as a Function of Time (Probe 1) for Inward-Pumping Spiral-Groove Seal (No Secondary Seal) and Steady Seal Seat Mode

03/30/1995 08:35 Filename: DIRUSS2A.INP Page 1

```
DIRUSS2A
14000 RPM ALIGNED, NO AXIAL EXCITATION, 35 MICRO-RADIANS MISALIGNMENT
*
HELP
*GEOMETRY
PISTON
ZSCO          0.6
ROS           1.850
RIS           1.608
RSCI          1.65
RSCO          1.71
RSP           1.80
NELM          5
ZSPO          0.35
THETO         0.0
DTHET         .5236
RIEL(20)       1.545  1.845  1.945 1.390 1.390
ROEL(20)       1.845  1.945  2.005 1.945 1.510
ELEML(20)      0.25  0.200  0.300 0.08 0.46
DENS(20)       0.0361 0.284  .450 0.45 0.45
ZL(20)         0.0 .05  0.08 0.29 0.38
APR           .633
WPR           .060
*SPRING AND DAMPING
SPPRE         0.0
NOSP          12
SKZZ          178520.
SKZA          0.0
SKZB          0.0
SKBZ          0.0
SKBB          256580.
SKBA          9288.
SKAZ         0.0
SKAB          -9288.
SKAA          256580.
DZZ          0.4
DZB             0.0
DZA             0.0
DBZ             0.0
DBB            0.8
DBA            0.0
DAZ             0.0
DAB            0.0
DAA            0.8
SPRST           5.583
HO            .00018
EFL           16.4
*OPERATING CONDITIONS
OMEGA         1466.0766
POO         7.4575
PID           0.0
COFSC          0.0
VISC          2.63E-09
DT           85.71875E-06
NTS           1000
NT            1
*INITIAL CONDITIONS
XO               .000
YO               .000
ZO               .000
AO              0.000035
BO              0.000035
OMEGAX       0.
OMEGAY       0.
OMEGAZ       628.32
TINIT          0.0
```

03/30/1995 08:35 Filename: DIRUSS2A.INP Page 2

```
OMEGAB        1466.0766
OMEGAA        1466.0766
END
```

95TR34-V5

Figure 58. Input for Spiral-Groove Seal; 14,000 rpm, No Axial Excitation

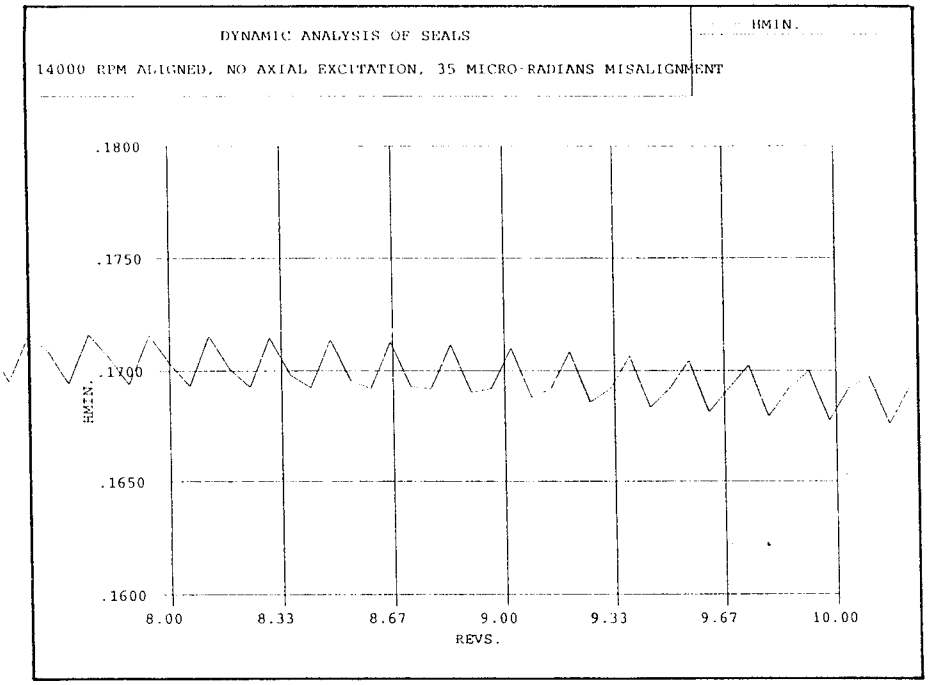

Figure 59. Results of DYSEAL Analysis; Film Thickness versus Revolutions (Steady Seal Seat Mode)

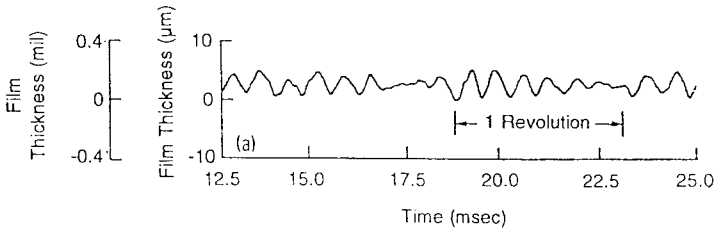

a) Steady Seal Seat Mode

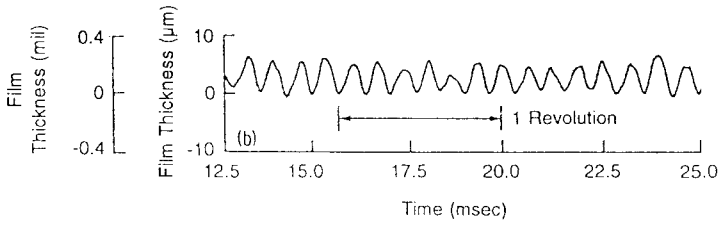

b) Sinusoidal Seal Seat Mode; Amplitude = 50 μm (2 mil); Frequency = 100 Hz

95TR34-V5

Figure 60. Film Thickness; Sinusoidal Axial Vibration

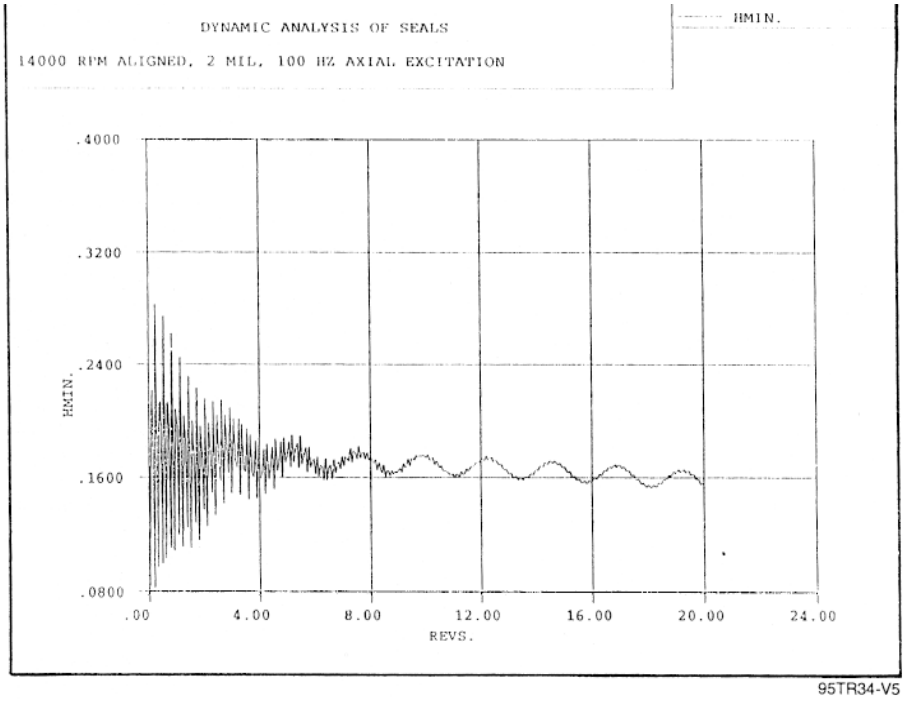

Figure 61. DYSEAL Film Thickness; Sinusoidal Axial Vibration

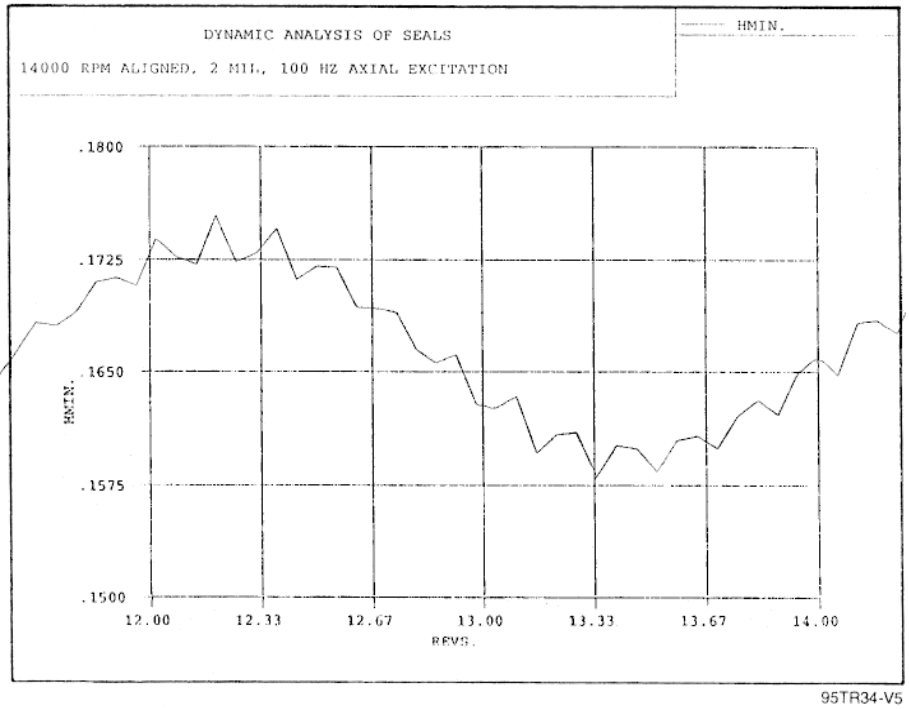

Figure 62. DYSEAL Magnified View of Film Thickness; Sinusoidal Axial Vibration

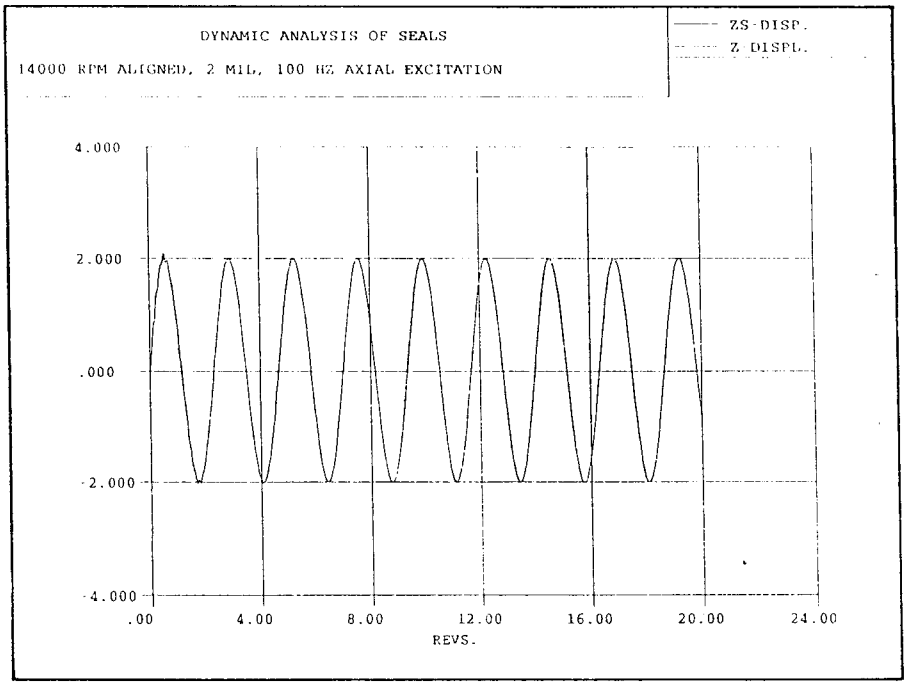

Figure 63. Axial Motion of Shaft and Seal

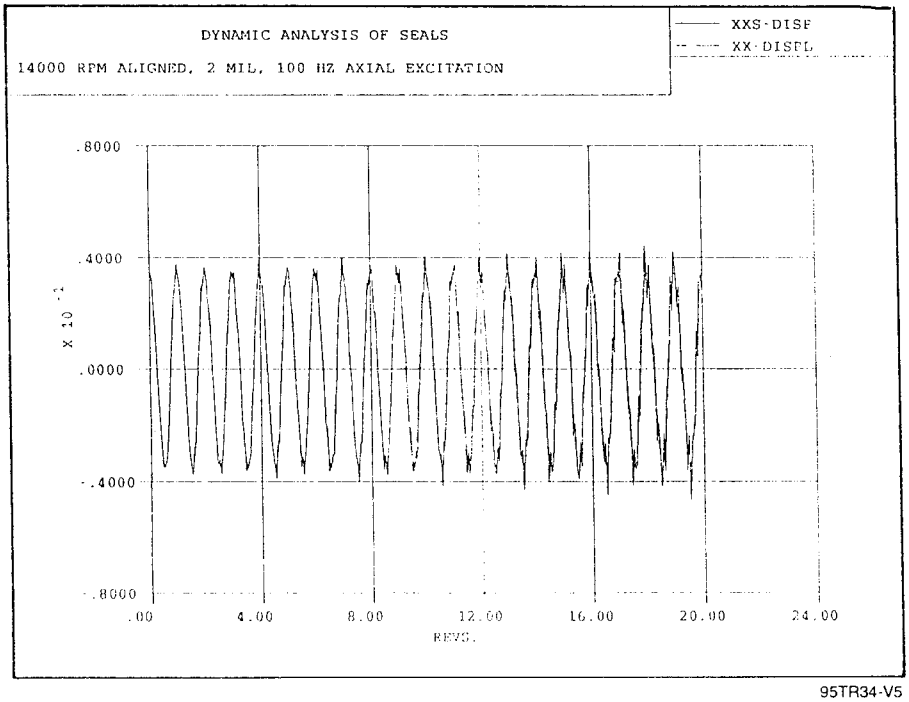

Figure 64. Rotational Response About x Axis for Axial Sinusoidal Excitation

5.0 DESIGN MODEL DESCRIPTION OF CODE KTK

The labyrinth seal design model is an expansion of the knife-to-knife (KTK) analyses reported in the literature. In such approaches, one-dimensional flow parameters in the knife throats are computed and linked together by a total pressure loss calculation. Flow coefficients are used for individual knives or groups of knives to account for the vena contracta in knife throats. Velocity head carry-over from upstream knives is accounted for by reducing the head loss between knives based on the flow expansion angle.

The design model is similar to previous KTK approaches except that the loss for each knife is broken down further into three losses as shown in Figure 65:

- Contraction: stations 1 to 2 and 4 to 5
- Venturi and friction: stations 2 to 3 and 5 to 6
- Partial or full expansion: stations 3 to 4 and 6 to 7.

The three loss coefficients aid in understanding the effects that each seal parameter has on the pressure drop across a knife. They reflect the types of pressure drops that the flow experiences more specifically than a knife flow coefficient used in previous KTK models. Specifically, the design model consists of :

- One-dimensional flow calculation at three locations for each knife
- Calculation of the individual loss coefficient values from the flow and geometric conditions
- Correction of loss coefficient values due to the presence of adjacent knives
- Linking of the total pressure between stations based on the total pressure drop from the loss coefficient and local velocity head.

Figure 66 lists the basic flow equations used in the design model.

Early in the development of the design model, knife loss coefficients were specified in the input data. The loss coefficients were then corrected by applying the model to the data base. The corrected coefficients were correlated against the independent seal parameters using a linear regression analysis. This iterative process was continued until equations were obtained which, not only, fit the data but were also physically relevant. The correlating equations were put into the model code and then the model accuracy was assessed by comparing the calculated flow results with the flow results in the entire data base.

Detailed information about the design model is summarized in the following paragraphs. This includes a discussion of the parameters considered and the model development for single knives, straight seals and stepped seals.

5.1 Parameters Considered

Based on the literature survey and previous experience at Allison [9], the parameters selected for consideration in the design model were those listed in Table 4. Schematics are given in Figures 67 and 68 which define these parameters. The effect of rotational speed was not included because of the lack of accurate and complete experimental data for labyrinth seals at knife tip speeds typical of those found in gas turbine engines.

The parameters listed in Table 4 were incorporated into the model to define the seal geometry. The geometric parameters were combined to obtain the data correlations in a manner that would make the correlations physically relevant. The ranges of these geometric parameter combinations in the data base are given in Table 5. The design model is valid primarily within these ranges.

5.2 Single Knife

Analyzing the flow data for a single knife affords the advantage of isolating the individual knife losses from the influence of adjacent knives. For the design model approach the three loss coefficients for the knife were separated using overall flow characteristic data. This was done by first noting that the expansion loss (K_e) would be unity because of the complete expansion downstream of a single knife. The other two loss coefficients, contraction (K_c) and venturi with wall friction (K_{vf}), were separated by considering data from several authors who varied the leading-edge sharpness and the thickness of the knife tip independently. It was assumed that the leading-edge radius affected only K_c and that the knife tip thickness affected only K_{vf}. The resulting correlations for K_c and K_{vf} are given in Figures 69 and 70. In these correlations, the local flow factor, ϕ, is an independent parameter. Several values for knife tip radius (KR) are listed in Figure 69 from the five data sources.

Single knife flow data for slanted knives were also analyzed to determine the effect of knife angle. Figure 69 gives the results. For $K\theta < 90°$, it was found that a parametric function of $K\theta$ added to K_c for a 90° knife gave the best fit of the data. For $K\theta > 90°$, i.e., $K\beta = 0$, data from Idel'chik [14] indicated that a multiplier applied to K_c for a 90° knife would be the most appropriate.

The relationships for the three loss coefficients as summarized in Figure 69 represent one approach that could be taken to correlate overall flow characteristics of single knife data. In combination, they accurately define the overall flow characteristics for the data sources and parameter ranges considered. The individual correlations involve the interactions of seal geometry with the flow parameters in a physically realistic way so that the overall results are valid for interpolated and some limited extrapolated data.

5.3 Straight Seals

Multiknife seals are analyzed in the design model by linking the triplet losses for each knife in series so that a seal has a total of 3 times KN losses. The overall pressure loss is a summation of the individual total pressure losses. The losses are calculated sequentially starting with the known inlet pressure because the loss coefficients and Mach number are functions of the local total

pressure through the parameter ϕ. For a straight seal, there is a carry-over of the velocity head from one knife to the next. This carry-over affects the K_{vf} and K_c of the upstream knife and the K_c and K_{vf} of the downstream knife. Thus, all the loss coefficients of a multiknife straight seal are influenced except the K_c of the first knife and the K_e of the last knife. The approach followed in multiknife seals is to determine the three loss coefficients for a given knife location from single knife correlations (Figure 69) and then correct them for the influence of adjacent knives. The correction is based on the characteristics of the expansion angle of the jet discharging from the clearance gap over a knife. This approach has been discussed by Abramovich [16] and utilized by Komotori and Miyake [11] in their KTK model. Figure 71 shows a schematic of a straight seal with the expansion angle, α, defined. The flow expands until it impinges on the front edge of the next knife. The maximum downstream flow height is CL + δ so that the expansion area ratio is (CL + δ)/CL instead of (CL + KH)/CL if the next knife were not present. This jet expansion ratio not only represents the amount the flow expands from the upstream knife but also the contraction into the downstream knife gap. The equations for δ in terms of α and the other geometric parameters are given in Figure 71.

To incorporate the effect of α on the three loss coefficients, relationships given in Figure 72 were used which are recommended in the literature [17] for various types of losses. The ratios A_o/A_1 and A_o/A_2 are simply the ratio CL/(CL + δ) relative to the upstream and downstream sides of a given knife, respectively.

The expansion angle, in general, will vary from knife to knife because the pressure ratio varies. This was observed in the flow visualization test results. This expansion angle variation, however, was not modelled because of the lack of good, complete seal data with interknife pressure data. Future design model development could be done to include variation through the seal based on results from analysis model calculations and/or test data.

The equations in Figures 71 and 72 were incorporated into the design model with α as an input value. Results were then obtained for the straight seal geometries in the data base using a range of α values. Comparing model results with the test performance data yielded the correct α values. Table 6 summarizes the range of values obtained from the various data sources. The α range obtained from Komotori's data [11] compares well with the value of 6° reported in a discussion of their paper. A linear regression analysis was performed on the α results. The equation obtained in given in Figure 73.

The effect of land roughness was included in the model by adding a frictional head loss term to the venturi with a wall friction loss coefficient (K_f) in the model for a smooth land (see Figure 73). Also, the flow area in each knife throat was increased to account for the increase in clearance due to the land roughness. The frictional head loss coefficient was determined from published rough-pipe turbulent flow friction factor correlations and a length equal to the knife pitch for knives 2, 3, and equal to knife-tip thickness for the first knives.

5.4 Stepped Seals

Stepped seals are designed to minimize carry-over from one knife to the next. Accordingly, one model approach could be to simply derive a new correlation for the expansion angle in terms of cavity dimensions. This method, however, is not acceptable because stepped seals flow both more and less than equivalent straight seals without carry-over depending primarily on the clearance. An expansion angle approach can only account for a flow equal to or greater than that without carry-over.

Physically, the flow between knives in a stepped seal does carry over some of the velocity head to the next knife. But while the intervening flow path dissipates some of the velocity head it also affects how the flow enters the next knife and thereby influences the loss coefficients of that knife. The complex flow patterns involved would make correction correlations to the loss coefficients difficult to determine accurately. Consequently, a simpler approach was taken to introduce an area correction factor (XMUL) for a knife throat downstream of a step. This factor is a multiplier on the flow area and can be less than or greater than unity. It accounts for carry-over, additional pressure loss in flowing between the knife face and step which is important for small distances to contact (DTC), and flow distortion into the next knife throat.

A correlation for XMUL was obtained through a procedure similar to that followed for α for straight seals. Model results were calculated for stepped seal configurations in the data base for a range of input XMUL values. Comparing these results with test data yielded the correct XMUL value. The area multiplier was found to vary from 0.55 to 1.32. A correlating equation for XMUL in terms of the various geometric parameters was derived using a linear regression analysis. This was done first for STLD flow direction, backward facing stator steps, because there were 62 configurations for STLD flow direction compared to 15 for LTSD flow. A correlation for the LTSD flow direction was obtained by comparing the STLD equation to the LTSD data and deriving a correction expression. This approach gives the best chance to extrapolate the narrower parameter ranges for the LTSD data. Figure 74 gives the two correlating equations for XMUL and respective parameter ranges.

Roughened surface land effects for stepped seals were handled in the model using a procedure similar to that used for straight seals, i.e., adding a friction head loss term to K_{vf} for a smooth wall plus increasing the throat area due to roughness. However, the length of the roughened passage was taken to be the knife-tip thickness to give the best agreement between the model and test data.

5.5 Design Model Optimization

The design model is an abbreviated analysis tool. Design is typically accomplished using this model by (1) determining the overall design constraints, (2) selecting the allowable range of each parameter to meet design and model constraints, (3) using the design model to calculate the leakage flow rate for a matrix of possible seal configurations, and (4) optimizing the seal design from the performance matrix, i.e., finding the seal geometry with the lowest leakage. This process has been automated by coupling the design model with a numerical optimization algorithm. As a

result, a minimum amount of input information is needed to optimize a seal configuration using the design model. In the following subsections, a brief description will be given for the parameters considered in the optimization algorithm.

5.5.1 Optimization Parameters

The parameters considered in the optimization code are listed in Table 7. The parameters are of three types: (1) input parameters which define the seal configuration but are not optimized, (2) optimized parameters, and (3) constrained correlation parameters. The input parameters are not optimized because of their nature (T, P_1, P_R) or the design defines their value (CL, KR, Kθ, L_{max}, H_{max}, DTC, DIA, KP_{min}). The parameters L_{max} and H_{max} are optional and constrain the calculations only if input. The optimized parameters listed in Table 7 are of two types: continuous and discrete. These types are handled differently by the optimization algorithm. The third type of parameter constrains the selection of the best design so that the various correlations in the design model are not extrapolated.

5.5.2 Optimization Algorithm

Determining the best seal design is an iterative selection procedure which is the subject of a branch of mathematics known as optimization theory. The characteristics of the problem solved determine the type of theory; the most general is nonlinear constrained optimization. In this case, a nonlinear objective function is optimized with respect to the design requirements, also called independent variables or parameters, that are subject to equality or inequality constraints which are also nonlinear functions of the independent variables. The method selected for the design model optimization code involves the use of a penalty function to convert the constrained optimization problem into an unconstrained one which is solved using the Fletcher-Power-Davidon variable metric method. This algorithm includes a parabolic cubic spline fit search routine to locate the optimum. This approach is reliable even for erratic functions often encountered in design problems.

The optimization algorithm described applies only to continuous variables, i.e., the first six optimized parameters listed in Table 7. The discrete variables were optimized by trial and comparison in which the entire matrix of these variables is considered. The code performs the continuous variable optimization for each set of discrete variable values and the overall optimum design is selected from the individual optimum designs.

Constraints have been included in the algorithms to ensure that the optimized seal configuration satisfies the design requirements. The constraints imposed are given in Table 8. Constraints on the discrete variables (KN, seal type, and flow direction) simply limit the matrix of values considered in the trial and comparison procedure. Constraints on the other variables are imposed by adding inequality penalty functions to the functions being optimized. A penalty function equals zero if the design meets a given constraint. It is greater than zero if the constraint is violated and the penalty varies parabolically with the magnitude of the violation. Each continuous variable constraint has one penalty function associated with it.

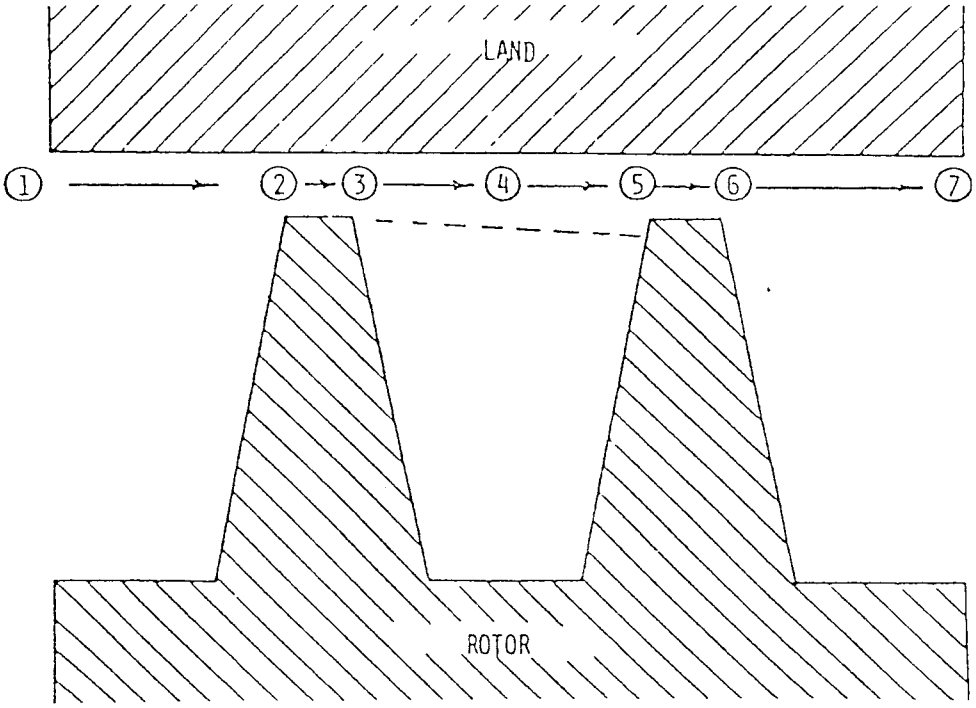

Figure 65. Seal Loss Zone Schematic

Compressible flow equations applied at the knife throat are:

the isentropic pressure relationship

$$\frac{P_t}{P_s} = \left(1 + \frac{\gamma - 1}{2} M^2\right)^{\frac{\gamma}{\gamma - 1}}$$

combined with the compressible flow equation of SAINT VENANT-WANTZEL,

$$\phi = \sqrt{\frac{2g_c\gamma}{R(\gamma - 1)}} \left(\frac{P_s}{P_t}\right)^{\frac{1}{\gamma}} \sqrt{1 - \left(\frac{P_s}{P_t}\right)^{\frac{\gamma-1}{\gamma}}}$$

in the form

$$\phi = \sqrt{\frac{g_c\gamma}{R}} \quad \frac{M}{\left(1 + \frac{\gamma - 1}{2} M^2\right)^{\frac{\gamma + 1}{2(\gamma-1)}}}$$

The drop in total pressure between any two stations in the flow is:

$\Delta P_t = K_c \frac{\gamma}{2} P_s M^2$ contraction loss

$\Delta P_t = K_{vf} \frac{\gamma}{2} P_s M^2$ venturi and friction loss

$\Delta P_t = K_e (P_t - P_s)$ expansion loss

95TR34-V5

Figure 66. Basic Flow Equations Used in the Design Model

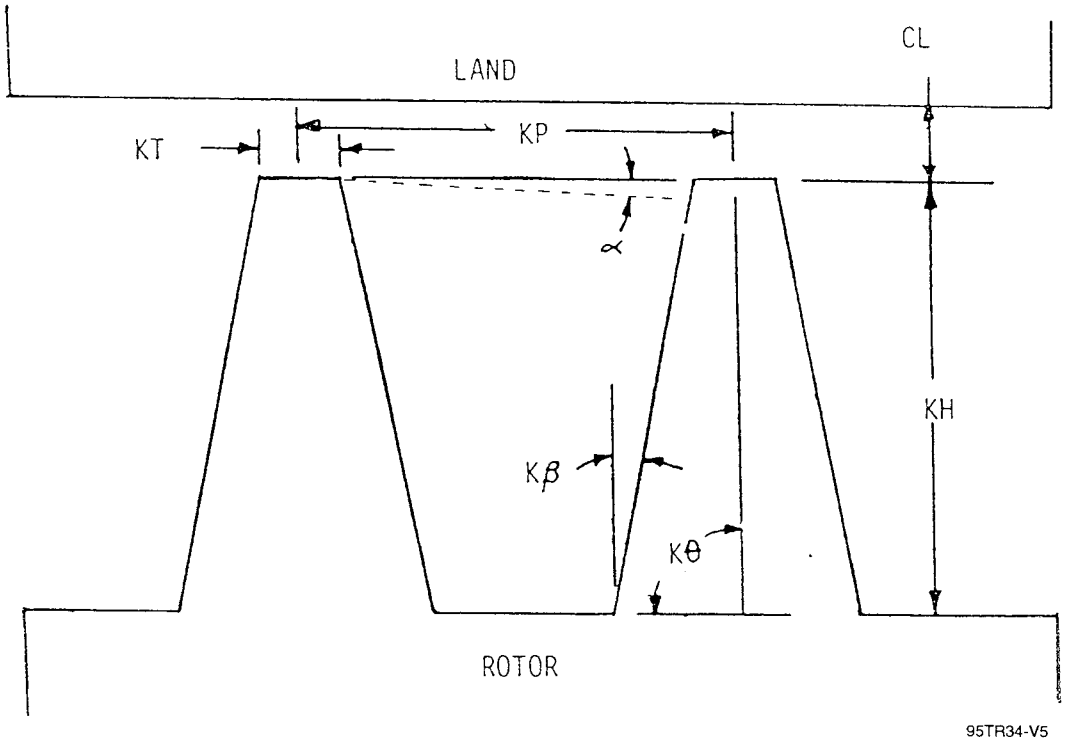

Figure 67. Seal Nomenclature for Straight Seals

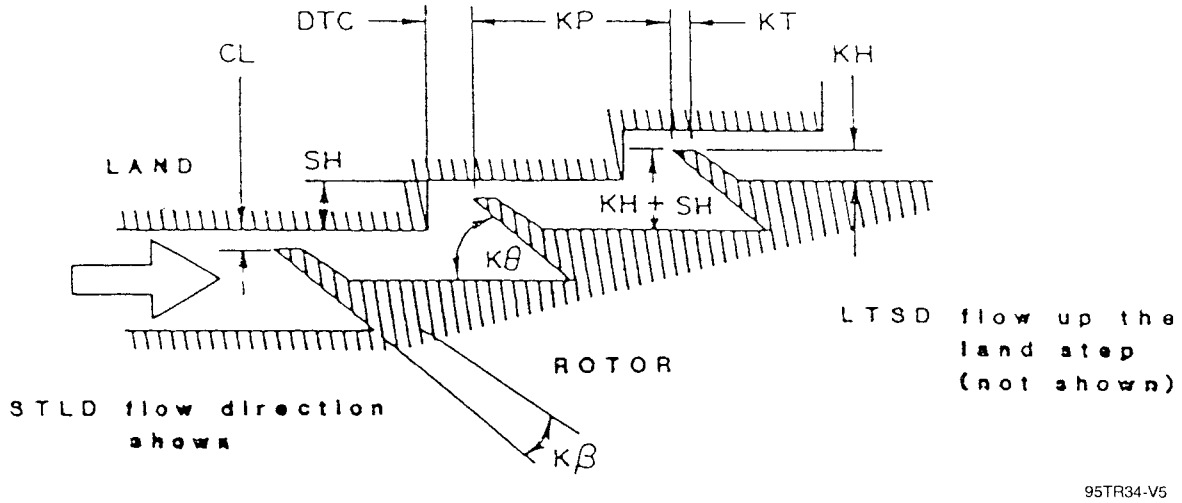

Figure 68. Seal Nomenclature for Stepped Seals

Table 4. Parameters in the Design Model

Geometric parameters for straight and stepped seals

- Knife height (KH)
- Knife pitch (KP)
- Number of knives (KN)
- Knife angle (Kθ)
- Knife tip thickness (KT)
- Knife taper angle (Kβ)
- Knife tip leading edge radius (KR)
- Clearance (CL)
- Surface roughness (ϵ)

Additional parameters considered for stepped seals

- Step height (SH)
- Distance to contact (DTC)
- Flow direction (LTSD or STLD)

Flow parameters

- Overall pressure ratio (P_R)
- Inlet stagnation pressure (P_U)
- Fluid temperature distribution (T)
- Flow rate (w)

95TR34-V5

Table 5. Parameter Ranges of Data in Labyrinth Seal Data Base

		Seal type		Stepped seal	
Parameter		Single knife	Straight seal	STLD dir.	LTSD dir.
KN	min	1	2	2	2
	max	1	12	6	6
KT/CL	min		0.21	0.21	0.50
	max	3.3	4.4	2.64	1.50
Kθ	min	30	60	50	50
	max	90	90	90	90
KH/CL	min	-	2.7	5.1	5.1
	max	-	31.3	29.4	28.0
KP/CL	min	-	4.0	6.4	9.2
	max	-	56.3	53	40
ε/(2CL)	min	0	0	0	0
	max	0	0.030	0	0.030
SH/CL	min	-	-	2.0	4.0
	max	-	-	29.4	12.5
DTC/CL	min	-	-	0.85	4.1
	max	-	-	40	19.4
(KP-KT)/CL	min	-	3.5	6.2	8.9
	max	-	55.0	51.8	38.5

95TR34-V5

K_e = 1.0

K_{vf} = $f(\phi, KT/CL)$

Figure 70: $0.77 \leq KT/CL \leq 3.3$, but good for $0.0 \leq KT/CL \leq 3.3$ [Derived from Kearton and Keh data for K_c = 0.70 (KR very small)]

$$K_{c\ @\ 90^\circ} = 0.7\left\{1. - EXP\left[C_1 - C_2\,\phi^2\left(\frac{CL}{KR}\right)^{0.25} + C_3\left(\frac{KR}{CL}\right)\right]\right\}$$

where

KR - in.	from	Data Source
0.0		KEARTON & KEH [10]
0.00167		Allison
0.005		KOMOTORI & MIYAKE [11]
0.005		HARRISON [12]
0.010		CAUNCE & EVERITT [13]

$K_c = K_{c\ @\ 90^\circ}$ for $K\theta = 90^\circ$

$K_c = K_{c\ @\ 90^\circ} \times [1. - C_4\,(K\theta - 90^\circ)]$ for $K\theta > 90^\circ$ [from IDEL'CHIK [14]]

$K_c = K_{c\ @\ 90^\circ} + C_5\,[1. - SIN\,(K\theta)]$ for $30^\circ \leq K\theta \leq 90^\circ$ [from Allison plus MEYER AND LOWRIE data [15]]

NOTE: $K\theta$ is actual front surface angle relative to the flow direction so that $K\theta = 90^\circ + K\beta/2$ when the specified knife angle is vertical or beyond, $K\theta \geq 90^\circ$.

C_n = constant

95TR34-V5

Figure 69. Loss Coefficient Correlations for Single-Knife Seal

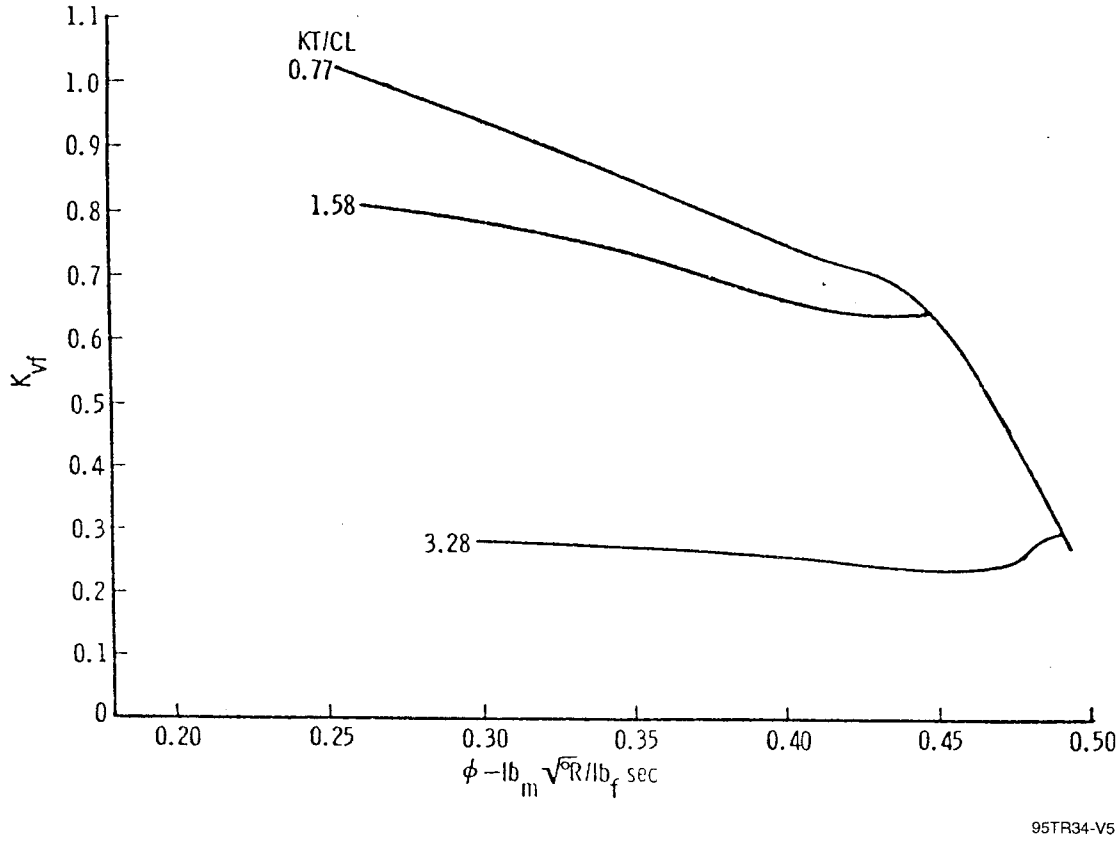

Figure 70. Venturi-Friction Coefficient from Kearton and Keh Data

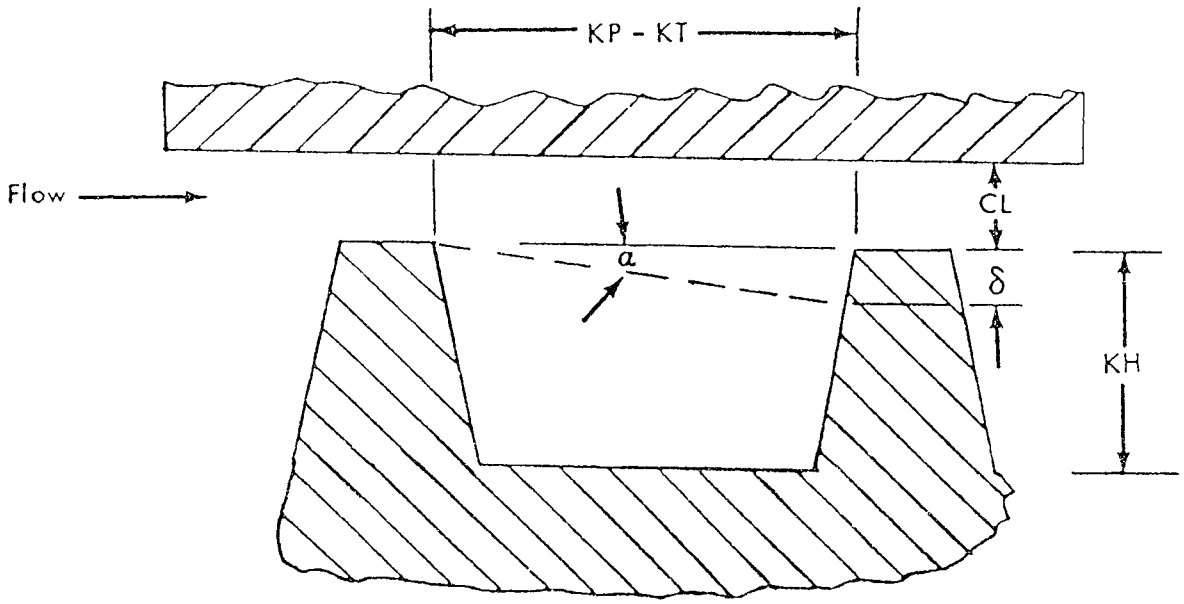

Figure 71. Schematic of the Flow Expansion Angle for a Straight Seal

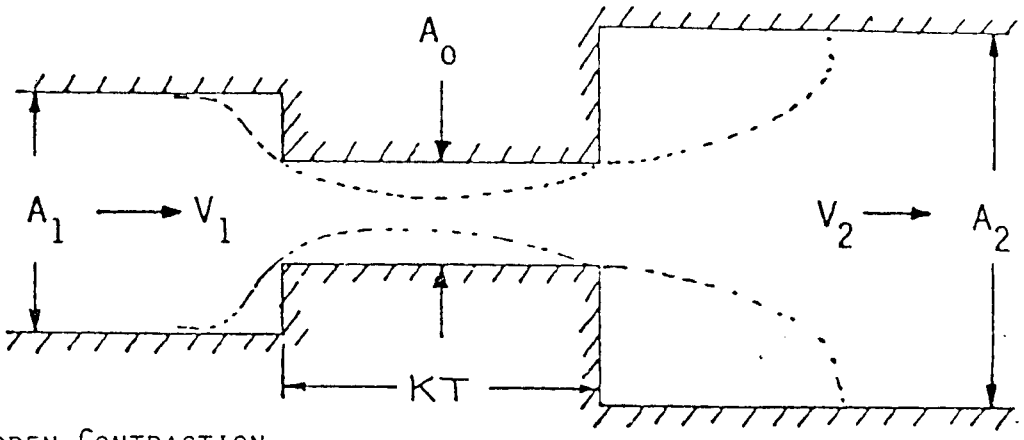

SUDDEN CONTRACTION

$$K_c = K_c' \left[1 - \frac{A_0}{A_1}\right]$$

VENTURI/FRICTION

$$K_{vf} = K_{vf}' \left[1 - \frac{A_0}{A_1}\right]^{1/2} \left[1 - \frac{A_0}{A_2}\right]$$

SUDDEN EXPANSION

$$K_e = K_e' \left[1 - \frac{A_0}{A_2}\right]^2$$

95TR34-V5

Figure 72. Effect of Upstream and Downstream Area on Loss Coefficient

Table 6. Expansion Angle (α) Determined by Correlation

o	Caunce and Everett, 6 knife	= 6 - 8 deg
o	Komotori 2, 4, 8, and 10 knife	= 4 - 6 deg
o	AGT 4 knife	= 2 - 4 deg
o	AGT 8 knife	= 4 - 5 deg
o	AGT 4, 5 knife slanted	= 2 - 4 deg

JET EXPANSION ANGLE

$$\alpha = C_6 \sqrt{\frac{KP-KT}{KH}}$$

for

$$0.54 \leq \frac{(KP-KT)}{KH} \leq 4.0$$

Average deviation = 25%

C_6 = constant. The value of this constant is given in the program listing for the Design Model, Appendix "D".

WALL ROUGHNESS

$$K_{vf} = K_{vf\ smooth}\ (\text{Correction for upstream and downstream knives}) + K_{f\ rough}$$

where

$$K_{f\ rough} = f\ (\epsilon/H,\ Re,\ KP)$$

$$A_t = A_{t\ smooth}\left(\frac{CL + \epsilon}{CL}\right)$$

95TR34-V5

Figure 73. Straight Seal Correlations in the Design Model

STEPPED SEAL AREA MULTIPLIER, XMUL

STLD Flow Direction

$$XMUL = C_7 (DTC/CL) (KT/CL)^{C_8} (DTC/(KP-KT))^{C_9} (KH/CL)^{C_{10}} \cdots$$
$$\cdots ((KP-KT)/KH)^{C_{11}} (SH/CL)^{C_{12}} \Big/ \sqrt{(DTC/CL)^2 + C_{13}}$$

$0.85 \leq DTC/CL \leq 40$, $0.21 \leq KT/CL \leq 2.6$, $0.09 \leq DTC/(KP-KT) \leq 1.0$,

$5.1 \leq KH/CL \leq 19.4$, $1.16 \leq (KP-KT)/KH \leq 1.76$, $2.0 \leq SH/CL \leq 29.4$

LTSD Flow Direction

$$XMUL = XMUL_{STLD} \quad C_{14} \quad (KH/CL)^{C_{15}}$$

$4.0 \leq DTC/CL \leq 19.4$, $0.50 \leq KT/CL \leq 1.5$, $0.35 \leq DTC/(KP-KT) \leq 0.50$

$5.1 \leq KH/CL \leq 28$, $1.02 \leq (KP-KT)/KH \leq 1.9$, $4.0 \leq SH/CL \leq 12.5$

Note: The limits on the seal parameters result from the range of the seal geometries used in developing the correlation equations.

WALL ROUGHNESS

$$K_{vf} = K'_{vf} + K_{f\ rough}$$

$$K_{f\ rough} = f(\epsilon/H, Re, KT)$$

$$A_t = A_{t\ smooth} \left(\frac{CL + \epsilon}{CL} \right)$$

95TR34-V5

Figure 74. Stepped Seal Correlations in the Design Model

Table 7. Design Model Optimization Parameters

Input Parameters

Straight and Stepped Seals

Clearance (CL)
Temperature (T)
Inlet total pressure (P_U)
Pressure ratio (P_R)
Knife radius (KR)
Knife taper angle (KB)
Maximum axial length (L_{max})*

Stepped Seals Only

Maximum seal height (H_{max})*
Distance to contact (DTC)
Maximum or minimum diameter (D_{max}, D_{min})
Minimum knife pitch (KP_{min})
(= 2X maximum allowable axial travel)

Optimized Parameters

Continuous Variables

Knife height (KH)
Knife pitch (KP)
Knife tip thickness (KT)
Knife angle (Kθ)
Roughness (ϵ)
Step height (SH)**

Discrete Variables

Seal type (straight, stepped)
Number of knives (KN)
Flow direction (LTSD, STLD)**

* Optional
** Stepped seals only

Constraining Correlation Parameters

Straight Seals

KT/CL
Kθ
(KP-KT)/KH
(ϵ - 30)/CL

Stepped Seals

KT/CL
Kθ
(KP-KT)/KH
DTC/CL
SH/CL
KH/CL
(ϵ - 30)/CL

95TR34-V5

Table 8. Constraints Imposed in Design Model Optimization Code

Overall length (L_{max})*
Overall height (H_{max})*

Minimum and maximum limits for all optimized parameters, i.e.,

KH, KP, KT, Kθ, ϵ, SH, KN**, seal type**, flow direction**

Minimum and maximum limits for correlation parameters to avoid extrapolation beyond data ranges in the data base, i.e.,

KT/CL, Kθ, (KP-KT)/KH, DTC/CL, SH/CL, (ϵ - 30)/CL

* Optional constraints
** Discrete variable constraints not imposed by inequality penalty functions

95TR34-V5

6.0 COMPUTER PROGRAM FEATURES OF CODE KTK

The design model computer program described in this report has several features to enhance its use. The program can be run in an analysis mode by defining the labyrinth seal geometry to be considered and executing the program. Also, the program can be run in an optimization mode by defining certain parameters and letting the program determine the optimum values for the remaining ones. The first mode will be referred to as the design model code and the second one as the design model optimization code. Various features of these two parts will be described separately in the following paragraphs.

6.1 Design Model Code Features

Features available in the design model code include:

- The input is abbreviated where possible.
- An override is available for many of the loss coefficient parameters.
- A function loss is available instead of, or in addition to, the three loss coefficients.
- Straight seals, stepped seals, or a mixed combination of the two can be analyzed. (Steps can be for either increasing or decreasing diameter.)
- Geometric parameter values can be varied from knife to knife.
- Two-dimensional or three-dimensional seals can be analyzed. (Calculations for two-dimensional seals are important to compare model results with nonrotating labyrinth seal rigs that utilize a rectangular test section).
- Various calculation options can be selected. The program can calculate:
  - Seal pressure distribution for a given flow rate
  - Seal pressure distribution and flow rate for a given overall pressure ratio
  - A flow characteristics curve (ϕ versus P_R)
- A flow characteristic curve can be punched out for input to plotting routines or to flow network solution codes.
- A summary is printed out of the various parameters with their applicable ranges. (If a parameter is outside its range, a warning message is printed, and the calculations are continued with either the input parameter value or one at the end of the range depending on whether or not extrapolation is considered acceptable for that particular parameter.)

6.2 Optimization Code Features

The optimization code is the design model code coupled with a driver routine. The latter calculates the independent parameter values to be used in the design model to search for an optimum configuration. Features of the code are:

- Constant geometry straight and stepped seals can be considered. However, variable parameters from knife-to-knife or mixed straight and stepped seal geometries cannot be considered.

- Each independent parameter has a default range which may be overridden. Even the correlation parameter ranges may be overridden if desired.
- An independent parameter may be held constant (by inputting both its minimum and maximum values equal to the one desired).
- An optimum configuration may be determined for both seal types and both directions for the stepped seals. Any subset of these may be considered.
- Before optimization is attempted, the parameter values and ranges are checked to be sure a solution is possible, e.g., a solution is impossible if L_{max} is less than the minimum KP divided by the maximum KN. If a solution does not exist, information is printed describing the problem and the execution of the data set is halted.
- Intermediate output information is given for each combination of discrete variables employed. This output information includes algorithm parameter values, derivatives of the optimized function with respect to each continuous variable, and comparisons of the continuous variable values with the allowable ranges.
- Final output information includes sensitivity results for each discrete variable step and summary data of the optimum seal configuration designated.

The output information not only defines the optimum seal configuration but indicates the effect, if any, of imposing each constraint. Also, the improvement in decreased leakage of the optimum configuration compared to the other possible configuration is given. This information can be used to assess the penalty caused by each limiting constraint and the penalty for choosing an alternate design.

6.3 Description of Output

The design model code printed output provides a detailed description of the seal geometric parameters and the predicted aerodynamic performance. A listing of a sample output data set is given in Appendix A. The output associated with a seal that is being optimized differs significantly from a nonoptimized seal. Therefore, the two outputs will be discussed separately.

6.3.1 Nonoptimized Output

A description of the output corresponding to sample data sets 1 through 3 in Appendix A is presented in the following paragraphs. An overview is presented first, followed by a more detailed description of the output.

The first section of the output echoes some of the parameters input. The second section, "KNIFE GEOMETRY DATA," lists the geometric parameters associated with each knife of the seal. The third section, labelled "INPUT DATA RANGE CHECK," records the results from a check of the input data against the data ranges used in the design model correlations. Warnings are issued when input data forces an extrapolation outside the empirical data range. If a seal parameter is outside the empirical range, this output section is printed before the first section described above. The next section of the output lists the aerodynamic parameters for each of the three flow "stations" associated with each knife. The values shown correspond to the choked flow condition unless a seal flow or pressure ratio is specified in the input. The fifth and final output section is

labeled "FLOW CURVE" and prints the values which make up the flow curve for the seal (if applicable). The flow curve (a function of pressure ratio and WRT/PTA) is printed out in standard and elliptical coordinates.

The "KNIFE GEOMETRY DATA" is printed for the three stations of each knife. The first 16 column headings correlate closely with the input variable names. The remaining column headings, beginning with "DEL C," identify the values for other parameters determined by the code as listed below:

- DEL C: Radial expansion of flow jet between knives used to calculate contraction area ratio.
- DEL E: Radial expansion of flow jet between knives used to calculate expansion area ratio.
- AREA MULT: Area multiplier on flow area for stepped seals.
- ALPHA: Jet expansion angle used for carry-over calculation.

The "INPUT DATA RANGE CHECK" is printed after the "KNIFE GEOMETRY DATA" except when a knife parameter is outside the empirical data range. In such cases this section is printed at the beginning of the output to draw attention to the warning messages printed. The output consists of the knife parameter being considered, the minimum value of the empirical data, the value input (or calculated) for the knife, and the maximum value of the empirical data. Asterisks are printed near the minimum or maximum value of the knife parameter when the minimum or maximum value (respectively) of the data base has been exceeded. A warning message is printed to this effect.

The fourth section of output lists the aerodynamic performance data predicted by the design model for each knife station. The column headings are defined below beginning with the third column.

- AREA: The flow area over the knife tip calculated by the equation: $A = \pi * DIA * CL * AREA\ MULT\ (in.^2)$.
- TEMP: The temperature of the air entering the seal as input (°R)
- WRT/PTA: Flow function $W * \sqrt{Tin} / Ptin * Aref (lbm\sqrt{R} / sec / lbf)$
- WRT/PSA: Flow function $W * \sqrt{Tin} / Psin * Aref (lbm\sqrt{R} / sec / lbf)$
- 4FL/D: Friction factor calculated for the seal land
- KFACT: Corrected dynamic head loss factor (K-factor)
- LOSS TYPE: Pressure loss mechanism (sudden contraction, "long hole," sudden expansion)
- PT: Total pressure (lbf/in.**2)
- PS: Static pressure (lbf/in.**2)
- MN: mach number.
- KFACT METHOD: Method of calculating total pressure loss (total pressure minus static pressure of 1/2 * density * velocity**2)
- PARM: Correction parameter
- AMUL: Multiplier on the "XKUNC" to calculate corrected dynamic head loss factor

- ADDER: Quantity added to the quantity "XKUNC" times "AMUL" to calculate corrected dynamic head loss factor
- XKUNC: Uncorrected dynamic head loss factor
- MOD AREA: Modified flow area calculated by multiplying "AREA MULT" (from KNIFE GEOMETRY DATA printed output) by "AREA."

The final section of printed output is labelled "FLOW CURVE" and prints the coordinates of a curve relating $W\sqrt{Tin} / PtAref$ to seal pressure ratio. Also shown are coordinates for curves relating a function of pressure ratio to functions of $W\sqrt{Tin} / PtAref$ in elliptical coordinates. Coordinates for a flow curve relating $W\sqrt{Tin} / PtAref$ and pressure ratio are also "punched" out on Fortran I/O unit 7. The row headings are defined below:

- PR: Seal pressure ratio
- PHI: Flow function ($W\sqrt{Tin} / PtAref$)
- 1.-1./PR**2: One minus the reciprocal of seal pressure ratio squared
- PHI**2: Flow function ($W\sqrt{Tin} / PtAref$) squared
- R/G * PHI**2: Gas constant for air divided by the gravitational constant times flow function $W\sqrt{Tin} / PtAref$) squared.

6.3.2 Optimized Output

A description of the output corresponding to sample data set 4 in Appendix A is presented in the following paragraph.

The first section of output prints the input values for the variables on input record type 7. The second section of the printout lists some of the information input on record types 1 through 4. The third section, "KNIFE GEOMETRY DATA," lists the geometric parameters associated with each knife of the seal for the maximum number of knives allowed by input. The fourth section lists some information relating to the first optimization iteration. The fifth output section ("KNIFE GEOMETRY DATA") lists knife geometric data for the initial optimization configuration. The resulting calculated flow rate is then printed followed by a table of aerodynamic parameters for each knife station for the configuration being considered. The seventh section lists the optimum value for each seal parameter with the range associated with each (set by input or default). Parameters that are "binding constraints" are flagged. Output sections 4 through 7 are repeated each time the number of seal knives is indexed. The last section of output lists the seal input parameters that are not optimized and summarizes the optimized knife configurations. The optimum seal configuration (i.e., minimum leakage flow) is flagged.

7.O REFERENCES

1. Munson, J. and B. Steinetz. "Specific Fuel Consumption and Increased Thrust Performance Benefits Possible with Advanced Seal Technology." Preprint AIAA-94-2700, presented at 1994 Joint Propulsion Conference, Indianapolis, IN, June 27, 1994.

2. Shapiro, W. "Users Manual for Computer Code DYSEAL (Dynamic Response of Seals)." MTI Technical Manual 95TM1.

3. "Users Manual for Labyrinth Seal Design Model (KTK)." MTI Technical Manual 94TM6.

4. Timoshenko, S., D.H. Young, and W. Weaver, Jr. *Vibration Problems in Engineering*. Fourth Edition, Copyright 1974 by John Wiley & Sons, Inc., Paragraph 2.6.

5. Shapiro, W. and R. Hamm. "Seal Tribology for Liquid Oxygen (LOX) Turbopumps." NASA CR-174866, February 1985.

6. Kirk, G."Transient Response of Floating-Ring Liquid Seals." Transactions of ASME, *Journal of Tribology*, Vol. 110, pp. 572-578, July 1988.

7. Thomson, W.T. *Mechanical Vibrations*. Prentice Hall, Copyright 1948.

8. DiRusso, E. "Dynamic Response of Film Thickness in Spiral-Groove Face Seals." NASA Technical Paper 2544, December 1985.

9. Tipton, D.L., T. E. Scott, and R. E. Vogel. "Labyrinth Seal Analysis: Volume III – Analytical and Experimental Development of a Design Model for Labyrinth Seals, AFWAL-TR-85-2103, Allison Gas Turbine Division, General Motors Corporation, Indianapolis, IN, January 1986.

10. Kearton, W.J. and T. H. Keh. "Leakage of Air through Labyrinth Glands of Staggered Type." *Proceedings of the Institution of Mechanical Engineers*, Series A, Vol. 166, No. 2, pp. 180-188 and 189-195, 1952.

11. Komotori, K. and K. Miyake. "Leakage Characteristics of Labyrinth Seals with High Rotating Speed." *Proceedings of the 1977 Tokyo Joint Gas Turbine Congress*, pp. 371-380, May 22-27, 1977.

12. Harrison, J. "An Investigation of Parameters Influencing Leakage through Labyrinth Seals with Solid and Honeycomb Lands." Masters Thesis, Brigham Young University, Provo, Utah, August 1980.

13. Caunce, D. and P. J. Everitt. "The Leakage of Air through Stepped Labyrinth Seals." University of Bristol, United Kingdom, June 1966.

14. Idel'chik, I.E. "Handbook of Hydraulic Resistance (Coefficients of Local Resistance and of Friction). AEC-TR-6630 (*Gosudarsivennoe Energetichedskoe Izdatel'stvo, Moskva-Leningrad*), pp. 354-357 and 372-373, 1960.

15. Meyer, C. A. and J. A. Lowrie. "The Leakage through Straight and Slant Labyrinths and Honeycomb Seals." Paper No. 74-WA/PTC-2, Transactions of ASME, *Journal of Engineering for Power,* Series A, Vol. 97, pp. 495-501, October 1975.

16. Abramovich, G. N. *The Theory of Turbulent Jets.* (Chapter 13, Jets in Finite Space), MIT Press, pp. 625-628, 1963.

17. Dodge, L. "Fluid Throttling Devices." Flow Resistance in Piping and Components, Product Engineering, Reprint R109, McGraw-Hill, New York, New York, pp. 14-20, March 1964.

APPENDIX A
CODE OUTPUT

K N I F E -- T O -- K N I F E S E A L D E S I G N M O D E L

Straight Labyrinth Seal
Data set #1

SPECIFIC HEAT RATIO (GAMMA)	=	1.3600	
MOLECULAR WEIGHT	=	28.9700	
NUMBER OF KNIVES	=	5	
SEAL TYPE	=	STRAIGHT	
FLOW DIRECTION	=		
SEAL LENGTH (2-D SEAL)	=	0.0000	(INCHES)
AVG. KNIFE DIAMETER (3-D SEAL)	=	2.6000	(INCHES)
INLET TOTAL PRESSURE	=	35.0000	(PSIA)

K N I F E G E O M E T R Y D A T A

KNIFE NO.	CL (IN)	KR (IN)	KT (IN)	KP (IN)	KH (IN)	SH (IN)	DTC (IN)	THETA (DEG)	BETA (DEG)	DIA (IN)	ROUGH (RMS)	TEMP (DEGR)	KCCO	KECO	4FL/D	DEL C (IN)	DEL E (IN)	AREA MULT	ALPHA (DEG)
1	0.0050	0.00170	0.0100	0.0400	0.0300	0.0000	0.0000	90.0	20.0	2.6000	0.00	900.0	-1	1	0.00	0.0000	0.0020	1.000	
2	0.0050	0.00170	0.0100	0.0400	0.0300	0.0000	0.0000	90.0	20.0	2.6000	0.00	900.0	1	1	0.00	0.0020	0.0020	1.000	3.790
3	0.0050	0.00170	0.0100	0.0400	0.0300	0.0000	0.0000	90.0	20.0	2.6000	0.00	900.0	1	1	0.00	0.0020	0.0020	1.000	3.790
4	0.0050	0.00170	0.0100	0.0400	0.0300	0.0000	0.0000	90.0	20.0	2.6000	0.00	900.0	1	1	0.00	0.0020	0.0020	1.000	3.790
5	0.0050	0.00170	0.0100	0.0400	0.0300	0.0000	0.0000	90.0	20.0	2.6000	0.00	900.0	1	-1	0.00	0.0020	0.0000	1.000	3.790

I N P U T D A T A R A N G E C H E C K

ALL KNIVES

VARIABLE	MIN	VALUE	MAX
THETA	30.	90.0	90.
KT/CL	0.0	2.000	3.3
(KP-KT)/KH	0.54	1.000	4.

F L O W R E S U L T S A T C H O K E P O I N T (W = 0.01814 LB/SEC ITERATIONS = 25)

STN NO.	KNIFE NO.	AREA (IN**2)	TEMP (DEG R)	WRT/PTA	WRT/PSA	4FL/D	KFACT	LOSS TYPE	PT (PSIA)	PS (PSIA)	MN	KFACT METHOD	PARM	AMUL	ADDER	XKUNC	MOD AREA (IN**2)
1		0.041	900.00	0.3799	0.4426				35.000	30.040	0.479						0.041
2	1	0.041	900.00	0.3979	0.4731	0.000	0.337	CONTR	33.419	28.104	0.511	Q	0.340	0.860	0.000	0.392	0.041
3	1	0.041	900.00	0.4081	0.4916	0.000	0.169	LHOLE	32.577	27.047	0.530	Q	2.000	0.282	0.000	0.599	0.041
4	1	0.041	900.00	0.4137	0.5020	0.000	0.080	EXPND	32.137	26.484	0.540	PT-PS	0.000	0.080	0.000	1.000	0.041
5	2	0.041	900.00	0.4211	0.5162	0.000	0.106	CONTR	31.578	25.759	0.555	Q	0.340	0.243	0.000	0.438	0.041
6	2	0.041	900.00	0.4274	0.5288	0.000	0.087	LHOLE	31.111	25.142	0.568	Q	2.000	0.150	0.000	0.579	0.041
7	2	0.041	900.00	0.4340	0.5426	0.000	0.080	EXPND	30.636	24.504	0.582	PT-PS	0.000	0.080	0.000	1.000	0.041
8	3	0.041	900.00	0.4432	0.5627	0.000	0.113	CONTR	30.001	23.631	0.602	Q	0.340	0.243	0.000	0.464	0.041
9	3	0.041	900.00	0.4506	0.5799	0.000	0.085	LHOLE	29.505	22.929	0.619	Q	2.000	0.150	0.000	0.569	0.041
10	3	0.041	900.00	0.4588	0.5998	0.000	0.080	EXPND	28.982	22.166	0.639	PT-PS	0.000	0.080	0.000	1.000	0.041
11	4	0.041	900.00	0.4708	0.6319	0.000	0.120	CONTR	28.244	21.041	0.671	Q	0.340	0.243	0.000	0.494	0.041
12	4	0.041	900.00	0.4782	0.6538	0.000	0.068	LHOLE	27.807	20.337	0.693	Q	2.000	0.150	0.000	0.453	0.041
13	4	0.041	900.00	0.4886	0.6883	0.000	0.080	EXPND	27.213	19.319	0.726	PT-PS	0.000	0.080	0.000	1.000	0.041
14	5	0.041	900.00	0.5050	0.7559	0.000	0.128	CONTR	26.329	17.589	0.791	Q	0.340	0.243	0.000	0.526	0.041
15	5	0.041	900.00	0.5265	0.9831	0.000	0.143	LHOLE	25.255	13.525	0.999	Q	2.000	0.531	0.000	0.270	0.041
16	5	0.041	900.00	0.9831		0.000	1.000	EXPND	13.525			PT-PS	0.000	1.000	0.000	1.000	0.041

F L O W C U R V E WHERE PR = PT UP / PT DOWN AND PHI = W * SQRT(TIN) / (PT UP * AREF) (WHERE AREF= 0.041)

I	1	2	3	4	5	6	7	8	9	10	11	12	13	14
1.-1./PR**2	0.00000	0.00668	0.03179	0.07401	0.13162	0.20284	0.28461	0.37238	0.46286	0.55390	0.64517	0.73033	0.78207	0.85068
PHI**2	0.00000	0.00175	0.00831	0.01870	0.03188	0.04689	0.06287	0.07903	0.09469	0.10923	0.12215	0.13300	0.14145	0.14432
R/G * PHI**2	0.00000	0.00290	0.01378	0.03101	0.05285	0.07774	0.10422	0.13102	0.15698	0.18110	0.20251	0.22051	0.23450	0.23927

K N I F E -- T O -- K N I F E S E A L D E S I G N M O D E L

Mixed Labyrinth Seal
Data set #2

I N P U T D A T A R A N G E C H E C K

KNIFE 1

VARIABLE	MIN	VALUE	MAX	
THETA	30.	90.0	90.	
KT/CL	0.0	1.111	3.3	
(E-30)/D	0.0	1111.1	27000.	

KNIFE 2

VARIABLE	MIN	VALUE	MAX	
THETA	30.	90.0	90.	
KT/CL	0.0	1.111	3.3	
(KP-KT)/KH	0.54	0.789	4.	
(E-30)/D	0.0	1111.1	27000.	

KNIFE 3

VARIABLE	MIN	VALUE	MAX	
THETA	30.	90.0	90.	
KT/CL	0.21	1.111	2.6	
KH/CL	5.1	21.111	29.4	
DTC/(KP-KT)	0.09	1.133	1.0	****
DTC/CL	0.85	18.889	40.0	
(KP-KT)/KH ****	1.16	0.789	1.76	
SH/CL	2.02	8.889	29.4	
(E-30)/D	0.0	1111.1	27000.	

KNIFE 4

VARIABLE	MIN	VALUE	MAX	
THETA	30.	90.0	90.	
KT/CL	0.21	1.111	2.6	
KH/CL	5.1	21.111	29.4	
DTC/(KP-KT)	0.09	1.067	1.0	****
DTC/CL	0.85	17.778	40.0	
(KP-KT)/KH ****	1.16	0.789	1.76	
SH/CL	2.02	8.889	29.4	
(E-30)/D	0.0	1111.1	27000.	

W A R N I N G SEAL CALCULATION MAY BE IN ERROR
**** INDICATES VARIABLES OUTSIDE RANGE OF DATA BASE
USED FOR EMPIRICAL CORRELATION

K N I F E -- T O -- K N I F E S E A L D E S I G N M O D E L

Mixed Labyrinth Seal
Data set #2

SPECIFIC HEAT RATIO (GAMMA)	=	1.3600	
MOLECULAR WEIGHT	=	28.9700	
NUMBER OF KNIVES	=	4	
SEAL TYPE	=	MIXED	
FLOW DIRECTION	=		
SEAL LENGTH (2-D SEAL)	=	0.0000	(INCHES)
AVG. KNIFE DIAMETER (3-D SEAL)	=	2.9850	(INCHES)
INLET TOTAL PRESSURE	=	35.0000	(PSIA)

K N I F E G E O M E T R Y D A T A

KNIFE NO.	CL (IN)	KR (IN)	KT (IN)	KP (IN)	KH (IN)	SH (IN)	DTC (IN)	THETA (DEG)	BETA (DEG)	DIA (IN)	ROUGH (RMS)	TEMP (DEGR)	KCCO	KECO	4FL/D	DEL C (IN)	DEL E (IN)	AREA MULT	ALPHA (DEG)
1	0.0090	0.00170	0.0100	0.1600	0.1900	0.0000	0.1600	90.0	20.0	3.1000	50.00	900.0	-1	0	0.00	0.0000	0.0087	1.000	
2	0.0090	0.00170	0.0100	0.1600	0.1900	0.0000	0.1600	90.0	20.0	3.1000	50.00	900.0	1	-1	0.00	0.0087	0.0000	1.000	3.368
3	0.0090	0.00170	0.0100	0.1600	0.1900	0.0800	0.1700	90.0	20.0	2.9400	50.00	900.0	-1	-1	0.00	0.0000	0.0000	1.088	3.368
4	0.0090	0.00170	0.0100	0.1600	0.1900	0.0800	0.1600	90.0	20.0	2.8000	50.00	900.0	-1	-1	0.00	0.0000	0.0000	1.081	3.368

F L O W R E S U L T S A T C H O K E P O I N T (W = 0.02728 LB/SEC ITERATIONS = 25)

STN NO.	KNIFE NO.	AREA (IN**2)	TEMP (DEG R)	WRT/PTA	WRT/PSA	4FL/D	KFACT	LOSS TYPE	PT (PSIA)	PS (PSIA)	MN	KFACT METHOD	PARM	AMUL	ADDER	XKUNC	MOD AREA (IN**2)
1		0.088	900.00	0.2646	0.2821				35.000	32.820	0.309						0.088
2	1	0.088	900.00	0.2691	0.2876	0.000	0.275	CONTR	34.415	32.191	0.315	Q	0.189	0.860	0.000	0.320	0.088
3	1	0.088	900.00	0.2781	0.2988	0.000	0.516	LHOLE	33.295	30.983	0.327	Q	1.111	0.493	0.060	0.927	0.088
4	1	0.088	900.00	0.2829	0.3048	0.000	0.243	EXPND	32.734	30.376	0.333	PT-PS	0.000	0.243	0.000	1.000	0.088
5	2	0.088	900.00	0.2858	0.3085	0.000	0.146	CONTR	32.398	30.011	0.337	Q	0.189	0.424	0.000	0.345	0.088
6	2	0.088	900.00	0.2995	0.3262	0.000	0.639	LHOLE	30.916	28.389	0.356	Q	1.111	0.702	0.004	0.905	0.088
7	2	0.088	900.00	0.3262	0.3592	0.000	1.000	EXPND	28.389	25.776	0.379	PT-PS	0.000	1.000	0.000	1.000	0.088
8	3	0.083	900.00	0.3256	0.3613	0.000	0.336	CONTR	27.541	24.825	0.393	Q	0.189	0.860	0.000	0.391	0.091
9	3	0.083	900.00	0.3543	0.4025	0.000	0.851	LHOLE	25.317	22.283	0.437	Q	1.111	1.000	0.004	0.847	0.091
10	3	0.083	900.00	0.4025	0.4965	0.000	1.000	EXPND	22.283	18.062	0.564	PT-PS	0.000	1.000	0.000	1.000	0.091
11	4	0.079	900.00	0.4619	0.6078	0.000	0.451	CONTR	20.523	15.597	0.647	Q	0.189	0.860	0.000	0.525	0.086
12	4	0.079	900.00	0.5265	0.9838	0.000	0.567	LHOLE	18.005	9.635	1.000	Q	1.111	1.000	0.004	0.563	0.086
13	4	0.079	900.00	0.9838		0.000	1.000	EXPND	9.635			PT-PS	0.000	1.000	0.000	1.000	0.086

F L O W C U R V E WHERE PR = PT UP / PT DOWN AND PHI = W * SQRT(TIN) / (PT UP * AREF) (WHERE AREF= 0.085)

I	1	2	3	4	5	6	7	8	9	10	11	12	13	14
1.-1./PR**2	0.00000	0.00971	0.04622	0.10448	0.17955	0.26697	0.36263	0.46260	0.56129	0.65488	0.73990	0.81563	0.88987	0.92421
PHI**2	0.00000	0.00092	0.00440	0.00989	0.01686	0.02479	0.03324	0.04179	0.05007	0.05776	0.06459	0.07033	0.07479	0.07631
R/G * PHI**2	0.00000	0.00153	0.00729	0.01640	0.02795	0.04110	0.05511	0.06928	0.08300	0.09576	0.10708	0.11659	0.12399	0.12651

K N I F E -- T O -- K N I F E S E A L D E S I G N M O D E L

Stepped Labyrinth Seal
Data set #3

I N P U T D A T A R A N G E C H E C K

KNIFE 1

VARIABLE	MIN	VALUE	MAX	
THETA	30.	90.0	90.	
KT/CL	0.50	1.111	1.5	
KH/CL	5.1	8.889	28.0	
DTC/(KP-KT)	0.35	2.267	0.5	****
DTC/CL	4.10	37.778	19.4	****
(KP-KT)/KH	1.02	1.875	1.90	
SH/CL	4.00	5.556	12.5	
(E-30)/D	0.0	1111.1	27000.	

KNIFE 2

VARIABLE	MIN	VALUE	MAX	
THETA	30.	90.0	90.	
KT/CL	0.50	1.111	1.5	
KH/CL	5.1	8.889	28.0	
DTC/(KP-KT)	0.35	1.067	0.5	****
DTC/CL	4.10	17.778	19.4	
(KP-KT)/KH	1.02	1.875	1.90	
SH/CL	4.00	5.556	12.5	
(E-30)/D	0.0	1111.1	27000.	

KNIFE 3

VARIABLE	MIN	VALUE	MAX	
THETA	30.	90.0	90.	
KT/CL	0.50	1.111	1.5	
KH/CL	5.1	8.889	28.0	
DTC/(KP-KT)	0.35	1.067	0.5	****
DTC/CL	4.10	17.778	19.4	
(KP-KT)/KH	1.02	1.875	1.90	
SH/CL	4.00	5.556	12.5	
(E-30)/D	0.0	1111.1	27000.	

KNIFE 4

VARIABLE	MIN	VALUE	MAX	
THETA	30.	90.0	90.	
KT/CL	0.50	1.111	1.5	
KH/CL	5.1	8.889	28.0	
DTC/(KP-KT)	0.35	1.067	0.5	****
DTC/CL	4.10	17.778	19.4	
(KP-KT)/KH	1.02	1.875	1.90	
SH/CL	4.00	5.556	12.5	
(E-30)/D	0.0	1111.1	27000.	

W A R N I N G SEAL CALCULATION MAY BE IN ERROR
**** INDICATES VARIABLES OUTSIDE RANGE OF DATA BASE
USED FOR EMPIRICAL CORRELATION

K N I F E -- T O -- K N I F E S E A L D E S I G N M O D E L

Stepped Labyrinth Seal
Data set #3

SPECIFIC HEAT RATIO (GAMMA)	=	1.3600	
MOLECULAR WEIGHT	=	28.9700	
NUMBER OF KNIVES	=	4	
SEAL TYPE	=	STEPPED	
FLOW DIRECTION	=	LTSD	
SEAL LENGTH (2-D SEAL)	=	0.0000	(INCHES)
AVG. KNIFE DIAMETER (3-D SEAL)	=	3.1700	(INCHES)
INLET TOTAL PRESSURE	=	35.0000	(PSIA)

K N I F E G E O M E T R Y D A T A

KNIFE NO.	CL (IN)	KR (IN)	KT (IN)	KP (IN)	KH (IN)	SH (IN)	DTC (IN)	THETA (DEG)	BETA (DEG)	DIA (IN)	ROUGH (RMS)	TEMP (DEGR)	KCCO	KECO	4FL/D	DEL C (IN)	DEL E (IN)	AREA MULT	ALPHA (DEG)
1	0.0090	0.00170	0.0100	0.1600	0.0800	0.0500	0.3400	90.0	20.0	3.3200	50.00	900.0	-1	-1	0.00	0.0000	0.0000	1.320	
2	0.0090	0.00170	0.0100	0.1600	0.0800	0.0500	0.1600	90.0	20.0	3.2200	50.00	900.0	-1	-1	0.00	0.0000	0.0000	1.216	0.000
3	0.0090	0.00170	0.0100	0.1600	0.0800	0.0500	0.1600	90.0	20.0	3.1200	50.00	900.0	-1	-1	0.00	0.0000	0.0000	1.216	0.000
4	0.0090	0.00170	0.0100	0.1600	0.0800	0.0500	0.1600	90.0	20.0	3.0200	50.00	900.0	-1	-1	0.00	0.0000	0.0000	1.216	0.000

F L O W R E S U L T S A T C H O K E P O I N T (W = 0.03146 LB/SEC ITERATIONS = 25)

STN NO.	KNIFE NO.	AREA (IN**2)	TEMP (DEG R)	WRT/PTA	WRT/PSA	4FL/D	KFACT	LOSS TYPE	PT (PSIA)	PS (PSIA)	MN	KFACT METHOD	PARM	AMUL	ADDER	XKUNC	MOD AREA (IN**2)
																	0.125
1		0.094	900.00	0.2158	0.2249				35.000	33.586	0.247						0.125
2	1	0.094	900.00	0.2177	0.2270	0.000	0.217	CONTR	34.698	33.270	0.249	Q	0.189	0.860	0.000	0.252	0.125
3	1	0.094	900.00	0.2266	0.2372	0.000	0.973	LHOLE	33.331	31.839	0.260	Q	1.111	1.000	0.003	0.969	0.125
4	1	0.094	900.00	0.2372	0.2531	0.000	1.000	EXPND	31.839	29.837	0.310	PT-PS	0.000	1.000	0.000	1.000	0.125
5	2	0.091	900.00	0.2703	0.2891	0.000	0.276	CONTR	31.299	29.257	0.316	Q	0.189	0.860	0.000	0.321	0.112
6	2	0.091	900.00	0.2872	0.3103	0.000	0.929	LHOLE	29.449	27.255	0.339	Q	1.111	1.000	0.004	0.925	0.112
7	2	0.091	900.00	0.3103	0.3429	0.000	1.000	EXPND	27.255	24.667	0.386	PT-PS	0.000	1.000	0.000	1.000	0.112
8	3	0.088	900.00	0.3306	0.3682	0.000	0.341	CONTR	26.404	23.709	0.401	Q	0.189	0.860	0.000	0.397	0.108
9	3	0.088	900.00	0.3604	0.4118	0.000	0.843	LHOLE	24.220	21.197	0.447	Q	1.111	1.000	0.004	0.840	0.108
10	3	0.088	900.00	0.4118	0.5080	0.000	1.000	EXPND	21.197	17.182	0.564	PT-PS	0.000	1.000	0.000	1.000	0.108
11	4	0.086	900.00	0.4619	0.6078	0.000	0.451	CONTR	19.523	14.835	0.647	Q	0.189	0.860	0.000	0.525	0.105
12	4	0.086	900.00	0.5265	0.9833	0.000	0.567	LHOLE	17.127	9.170	1.000	Q	1.111	1.000	0.004	0.563	0.105
13	4	0.086	900.00	0.9833		0.000	1.000	EXPND	9.170			PT-PS	0.000	1.000	0.000	1.000	0.105

F L O W C U R V E WHERE PR = PT UP / PT DOWN AND PHI = W * SQRT(TIN) / (PT UP * AREF) (WHERE AREF= 0.090)

I	1	2	3	4	5	6	7	8	9	10	11	12	13	14
1./PR**2	0.00000	0.01005	0.04774	0.10763	0.18440	0.27332	0.37008	0.47068	0.57013	0.66397	0.74923	0.82473	0.89696	0.93135
PHI**2	0.00000	0.00109	0.00519	0.01167	0.01989	0.02925	0.03921	0.04930	0.05906	0.06814	0.07620	0.08297	0.08823	0.09002
R/G * PHI**2	0.00000	0.00181	0.00860	0.01934	0.03297	0.04849	0.06501	0.08173	0.09792	0.11297	0.12633	0.13755	0.14628	0.14925

K N I F E -- T O -- K N I F E S E A L D E S I G N M O D E L

Straight Labyrinth Seal Optimization
Data set #4

LMAX 0.500000 HMAX 0.250000 PRATIO 1.07900 TYPE STRAI DIRECTION ISRCHP 0 IPASSP 0 IWPRNT 0

INITIAL VALUES TO BEGIN OPTIMIZATION

SPECIFIC HEAT RATIO (GAMMA)	=	1.3600	
MOLECULAR WEIGHT	=	28.9700	
MAX NUMBER OF KNIVES	=	6	
SEAL TYPE	=	STRAIGHT	
FLOW DIRECTION	=		
SEAL LENGTH (2-D SEAL)	=	0.0000	(INCHES)
AVG. KNIFE DIAMETER (3-D SEAL)	=	2.6000	(INCHES)
FLOW DIVERGENCE ANGLE (ALPHA)	=	0.0000	(DEGREES)
INLET TOTAL PRESSURE	=	35.0000	(PSIA)

K N I F E G E O M E T R Y D A T A

KNIFE NO.	CL (IN)	KR (IN)	KT (IN)	KP (IN)	KH (IN)	SH (IN)	DTC (IN)	THETA (DEG)	BETA (DEG)	DIA (IN)	ROUGH (RMS)	TEMP (DEGR)
1	0.0080	0.00170	0.0100	0.1000	0.1020	0.0000	0.0000	90.0	20.0	2.6000	0.00	900.0
2	0.0080	0.00170	0.0100	0.1000	0.1020	0.0000	0.0000	90.0	20.0	2.6000	0.00	900.0
3	0.0080	0.00170	0.0100	0.1000	0.1020	0.0000	0.0000	90.0	20.0	2.6000	0.00	900.0
4	0.0080	0.00170	0.0100	0.1000	0.1020	0.0000	0.0000	90.0	20.0	2.6000	0.00	900.0
5	0.0080	0.00170	0.0100	0.1000	0.1020	0.0000	0.0000	90.0	20.0	2.6000	0.00	900.0
6	0.0080	0.00170	0.0100	0.1000	0.1020	0.0000	0.0000	90.0	20.0	2.6000	0.00	900.0

OPTIMIZATION STEP FOR STRAIGHT SEAL WITH NO. KNIVES = 6

RANGES AVAILABLE FROM EMPIRICAL DATA

	MIN	INITIAL	MAX	
1	0.900000E-02	0.100000E-01	0.200000E-01	KT
2	0.350000	0.960400E-01	0.980000E-01	KP
3	1.00000	1.00000	1.00000	KH/KP
4	0.100000E-01	0.000000E+00	1.00000	SH
5	45.0000	89.0000	90.0000	KTHETA
6	30.0000	30.0000	30.0000	ROUGH
7	0.100000E-02		3.30000	KT/CL
8	0.540000		4.00000	(KP-KT)/KH/CL

N O R M A L C O N V E R G E N C E

RESULTS FOR CONVERGED VARIABLE VALUES

NUMBER OF KNIVES	=	6	
SEAL TYPE	=	STRAIGHT	
FLOW DIRECTION	=	STLD	
SEAL LENGTH (2-D SEAL)	=	0.0000	(INCHES)
AVG. KNIFE DIAMETER (3-D SEAL)	=	2.6000	(INCHES)
INLET TOTAL PRESSURE	=	35.0000	(PSIA)
AREA NORMALIZING FACTOR	=	1.0000	

K N I F E G E O M E T R Y D A T A

KNIFE NO.	CL (IN)	KR (IN)	KT (IN)	KP (IN)	KH (IN)	SH (IN)	DTC (IN)	THETA (DEG)	BETA (DEG)	DIA (IN)	ROUGH (RMS)	TEMP (DEGR)	KCCO	KECO	4FL/D	DEL C (IN)	DEL E (IN)	AREA MULT	ALPHA (DEG)
1	0.0080	0.00170	0.0090	0.0960	0.0960	0.0000	0.0000	45.0	20.0	2.6000	30.00	900.0	-1	1	0.00	0.0000	0.0055	1.000	
2	0.0080	0.00170	0.0090	0.0960	0.0960	0.0000	0.0000	45.0	20.0	2.6000	30.00	900.0	1	1	0.00	0.0055	0.0055	1.000	3.608
3	0.0080	0.00170	0.0090	0.0960	0.0960	0.0000	0.0000	45.0	20.0	2.6000	30.00	900.0	1	1	0.00	0.0055	0.0055	1.000	3.608
4	0.0080	0.00170	0.0090	0.0960	0.0960	0.0000	0.0000	45.0	20.0	2.6000	30.00	900.0	1	1	0.00	0.0055	0.0055	1.000	3.608
5	0.0080	0.00170	0.0090	0.0960	0.0960	0.0000	0.0000	45.0	20.0	2.6000	30.00	900.0	1	1	0.00	0.0055	0.0055	1.000	3.608
6	0.0080	0.00170	0.0090	0.0960	0.0960	0.0000	0.0000	45.0	20.0	2.6000	30.00	900.0	1	-1	0.00	0.0055	0.0000	1.000	3.608

FLOW 0.856995E-02 PRESSURE RATIO 1.07900 DESIRED PR 1.07900

F L O W R E S U L T S A T S P E C I F I E D F L O W R A T E (W = 0.00857 LB/SEC ITERATIONS = 45)

STN NO.	KNIFE NO.	AREA (IN**2)	TEMP (DEG R)	WRT/PTA	WRT/PSA	4FL/D	KFACT	LOSS TYPE	PT (PSIA)	PS (PSIA)	MN	KFACT METHOD	PARM	AMUL	ADDER	XKUNC	MOD AREA (IN**2)
1		0.066	900.00	0.1121	0.1133				35.000	34.631	0.125						0.066
2	1	0.066	900.00	0.1132	0.1144	0.000	0.914	CONTR	34.664	34.292	0.126	Q	0.213	1.000	0.798	0.116	0.066
3	1	0.066	900.00	0.1137	0.1149	0.000	0.415	LHOLE	34.510	34.136	0.127	Q	1.126	0.407	0.000	1.021	0.066
4	1	0.066	900.00	0.1139	0.1151	0.000	0.166	EXPND	34.448	34.074	0.127	PT-PS	0.000	0.166	0.000	1.000	0.066
5	2	0.066	900.00	0.1143	0.1156	0.000	0.372	CONTR	34.309	33.933	0.127	Q	0.213	0.407	0.798	0.117	0.066
6	2	0.066	900.00	0.1147	0.1159	0.000	0.265	LHOLE	34.210	33.833	0.128	Q	1.126	0.260	0.000	1.021	0.066
7	2	0.066	900.00	0.1149	0.1162	0.000	0.166	EXPND	34.148	33.770	0.128	PT-PS	0.000	0.166	0.000	1.000	0.066
8	3	0.066	900.00	0.1153	0.1166	0.000	0.373	CONTR	34.007	33.628	0.129	Q	0.213	0.407	0.798	0.118	0.066
9	3	0.066	900.00	0.1157	0.1170	0.000	0.265	LHOLE	33.907	33.526	0.129	Q	1.126	0.260	0.000	1.020	0.066
10	3	0.066	900.00	0.1159	0.1172	0.000	0.166	EXPND	33.844	33.463	0.129	PT-PS	0.000	0.166	0.000	1.000	0.066
11	4	0.066	900.00	0.1164	0.1177	0.000	0.373	CONTR	33.702	33.319	0.130	Q	0.213	0.407	0.798	0.119	0.066
12	4	0.066	900.00	0.1167	0.1181	0.000	0.265	LHOLE	33.601	33.217	0.130	Q	1.126	0.260	0.000	1.019	0.066
13	4	0.066	900.00	0.1170	0.1183	0.000	0.166	EXPND	33.538	33.153	0.130	PT-PS	0.000	0.166	0.000	1.000	0.066
14	5	0.066	900.00	0.1175	0.1188	0.000	0.374	CONTR	33.395	33.008	0.131	Q	0.213	0.407	0.798	0.120	0.066
15	5	0.066	900.00	0.1178	0.1192	0.000	0.264	LHOLE	33.293	32.905	0.131	Q	1.126	0.260	0.000	1.019	0.066
16	5	0.066	900.00	0.1180	0.1194	0.000	0.166	EXPND	33.228	32.840	0.132	PT-PS	0.000	0.166	0.000	1.000	0.066
17	6	0.066	900.00	0.1186	0.1200	0.000	0.374	CONTR	33.084	32.693	0.132	Q	0.213	0.407	0.798	0.121	0.066
18	6	0.066	900.00	0.1195	0.1209	0.000	0.650	LHOLE	32.831	32.437	0.133	Q	1.126	0.638	0.000	1.018	0.066
19	6	0.066	900.00	0.1209		0.000	1.000	EXPND	32.437			PT-PS	0.000	1.000	0.000	1.000	0.066

PARAMETER VALUES AND DERIVATIVES FOR STRAIGHT SEAL 6 KNIVES MIN FLOW 0.856995E-02

	MIN	OPTIMUM	MAX	DEL W/DEL X
* KT	0.900000E-02	0.900896E-02	0.200000E-01	436.632
KP	0.350000	0.960400E-01	0.980000E-01	0.000000E+00
KH/KP	1.00000	1.00000	1.00000	0.000000E+00
SH	0.100000E-01	0.000000E+00	1.00000	0.000000E+00
* KTHETA	45.0000	45.0444	90.0000	0.317253
ROUGH	30.0000	30.0000	30.0000	0.000000E+00

CONSTRAINTS	MIN	VALUE	MAX
KT/CL	0.100000E-02	1.12612	3.30000
(KP-KT)/KH	0.540000	0.906196	4.00000

* INDICATES BINDING CONSTRAINTS

Straight Labyrinth Seal Optimization
Data set #4

CLEARANCE	0.800000E-02
KNIFE RADIUS	0.170000E-02
DIST TO CONTACT	0.000000E+00
BETA	20.0000
PRESSURE RATIO	1.07900
PRESSURE IN	35.0000
TEMPERATURE	900.000
MAX SEAL LENGTH	0.500000
MAX SEAL HEIGHT	0.250000

SUMMARY OF MINIMUM FLOW FOR VARIOUS SEAL CONFIGURATIONS

TYPE	DIR	NO. KNIVES	KT	KP	KH	SH	KTHETA	ROUGH	SEAL LENGTH	SEAL HEIGHT	MIN FLOW	
STRAIGHT		6	0.00900896	0.096040	0.096040		45.0444	30.00	0.48921		0.0085700	----OPTIMUM

REPORT DOCUMENTATION PAGE

Form Approved
OMB No. 0704-0188

1. AGENCY USE ONLY (*Leave blank*)	2. REPORT DATE	3. REPORT TYPE AND DATES COVERED
	October 2004	Final Contractor Report

4. TITLE AND SUBTITLE

Numerical, Analytical, Experimental Study of Fluid Dynamic Forces in Seals
Volume 5—Description of Seal Dynamics Code DYSEAL and Labyrinth Seals Code KTK

5. FUNDING NUMBERS

WBS–22–5000–0013
NAS3–25644

6. AUTHOR(S)

Wilbur Shapiro, Raymond Chupp, Glenn Holle, and Thomas Scott

7. PERFORMING ORGANIZATION NAME(S) AND ADDRESS(ES)

Mechanical Technology, Inc. (MTI)
968 Albany-Shaker Road
Latham, New York 12110

8. PERFORMING ORGANIZATION REPORT NUMBER

E–14708–5

9. SPONSORING/MONITORING AGENCY NAME(S) AND ADDRESS(ES)

National Aeronautics and Space Administration
Washington, DC 20546–0001

10. SPONSORING/MONITORING AGENCY REPORT NUMBER

NASA CR—2004-213199-VOL5
(Corrected Copy)

11. SUPPLEMENTARY NOTES

This corrected copy supercedes the original report. Wilbur Shapiro, Mechanical Technology, Inc., Latham, New York 12110; Raymond Chupp, Glenn Holle, and Thomas Scott, Allison Engine Company, Indianapolis, Indiana 46206. Project Manager, Anita D. Liang, Aeronautics Directorate, NASA Glenn Research Center, organization code 2200, 216–977–7439. Responsible person, Robert C. Hendricks, Research and Technology Directorate, NASA Glenn Research Center, organization code 5000, 216–977–7507.

12a. DISTRIBUTION/AVAILABILITY STATEMENT

Unclassified - Unlimited
Subject Categories: 07, 20, and 34 Distribution: Nonstandard

Available electronically at http://gltrs.grc.nasa.gov

This publication is available from the NASA Center for AeroSpace Information, 301–621–0390.

12b. DISTRIBUTION CODE

13. ABSTRACT ***(Maximum 200 words)***

The objectives of the program were to develop computational fluid dynamics (CFD) codes and simpler industrial codes for analyzing and designing advanced seals for air-breathing and space propulsion engines. The CFD code SCISEAL is capable of producing full three-dimensional flow field information for a variety of cylindrical configurations. An implicit multidomain capability allow the division of complex flow domains to allow optimum use of computational cells. SCISEAL also has the unique capability to produce cross-coupled stiffness and damping coefficients for rotordynamic computations. The industrial codes consist of a series of separate stand-alone modules designed for expeditious parametric analyses and optimization of a wide variety of cylindrical and face seals. Coupled through a Knowledge-Based System (KBS) that provides a user-friendly Graphical User Interface (GUI), the industrial codes are PC based using an OS/2 operating system. These codes were designed to treat film seals where a clearance exists between the rotating and stationary components. Leakage is inhibited by surface roughness, small but stiff clearance films, and viscous pumping devices. The codes have demonstrated to be a valuable resource for seal development of future air-breathing and space propulsion engines.

14. SUBJECT TERMS

CFD seal code; Industrial seal codes; User-friendly seal codes; Fluid-film seal codes; Clearance seal codes; Seals; Dynamics; Design; Computational analysis; Fluid forces

15. NUMBER OF PAGES

123

16. PRICE CODE

17. SECURITY CLASSIFICATION OF REPORT	18. SECURITY CLASSIFICATION OF THIS PAGE	19. SECURITY CLASSIFICATION OF ABSTRACT	20. LIMITATION OF ABSTRACT
Unclassified	Unclassified	Unclassified	